NOVEL SENSOR DESIGN FOR DETECTION OF DANGEROUS CONTAMINATED MARINE BIOTOXINS

A Thesis submitted in fulfilment of the

requirements for the Degree of

Master of Engineering

in

INFORMATION AND TELECOMMUNICATION ENGINEERING

By

MOHD SYAIFUDIN BIN ABDUL RAHMAN

SCHOOL OF ENGINEERING AND ADVANCED TECHNOLOGY

MASSEY UNIVERSITY

PALMERSTON NORTH

NEW ZEALAND

March 2009

To my parents:

Abdul Rahman Bin Daud

and

Mariah Binti Abdul Rahman

Abstract

Planar electromagnetic sensing system has been used as one of the NDT methods to evaluate the material properties i.e., to evaluate near-surface properties such as conductivity, permeability and dielectric properties. The applications of planar electromagnetic sensors will depend on both the characteristic of the sensor type chosen and also the characteristic of material under test. Conventional planar interdigital sensors and novel planar interdigital sensors have been designed, fabricated and tested for detection of dangerous marine biotoxins in seafood. Our main objective is to sense the presence of dangerous contaminated acid in mussels and other seafoods. Initial studies were conducted with three peptide derivatives namely Sarcosine, Proline and Hydroxylproline. These three chemicals are structurally closely related to our target molecule (domoic acid). The initial results have shown that all sensors respond very well to the chemicals and it is possible to discriminate the different chemicals from the output of the sensor. Novel interdigital sensors have shown better sensitivity measurement compared to conventional interdigital sensors. The novel interdigital sensors were then being tested with three seafood products. Results from the analysis have shown that novel interdigital sensor with configuration #1 (Sensor_1) has better sensitivity compared to other sensors. Sensor_1 has been chosen for experiment using proline and mussels. The changes in sensor sensitivity were analysed with mussels before and after adding the proline. The presence of proline on the mussel surface and also injected proline to the mussel samples were clearly detected by Sensor_1. Further experiment was conducted with small amount of domoic acid (0.5 µg to 5.0 µg) injected to a mussel and it was found that Sensor_1 was able to detect small amount of domoic acid (1.0 µg) injected into the mussel sample. Sensor_1 was able to detect approximately 12.6 µg/g of domoic acid in mussel meat. Three threshold levels of particular sample thickness have been established for detection of domoic acid. The first prototype of a low cost sensing system known as SIT (Seafood Inspection Tool) has been developed. The outcomes from the experiments provide chances of opportunity for further research in developing a low cost miniature type of sensors for reliable sensing system for commercial use.

Acknowledgements

First of all I would like to thank God, for giving me the strength and time to complete this research work. I am indebted to Associate Professor Dr. Subhas Mukhopadhyay, my research supervisor for his passionate interest in the subject and supervising my research work. I thank him for providing valuable advice, expert guidance and the friendly way that he teaches.

I would like to express my gratitude to my families, friends and colleagues who have helped and giving advice during the experiments and the preparation of the thesis. In particular I would like to thank my wife, Nina for her continual support during my studies at Massey University. I would like to thank Malaysian Agricultural Research and Development Institute (MARDI) for providing me the financial support to pursue my studies.

Special thanks to Dr. Krishanthi Jayasundera from the Institute of Fundamental Science, Massey University for her help and guidance related to chemistry and marine biotoxins. I would like to thank Dr. Gourab Sen Gupta for his help and guidance on microcontroller programming. I would like to acknowledge Mr. Nathan Eichler for his help on the software part of the embedded system. I also would like to acknowledge the help of Mr. Ken Mercer, Mr. Collin Plaw and Mr. Bruce Collins for their help on technical matters and invaluable comments to improve the experimental works in the laboratory.

And finally I would like to thank my beloved parents for their unconditional love and support. Thank you for all the sacrifices you made to give me a better chance in life.

Contents

List of Figures

List of Tables

Chapter 1

Introduction

1.1 Introduction to Sensor

Sensor is a device that measures a physical quantity and converts it into an electrical signal which can be read by an observer or by an instrument [1]. Sensors are a type of transducers, which means that they change one form of energy into another. For this reason, sensors can be classified according to the type of energy transfer that they detect. For example, a thermocouple converts temperature to an output as electrical signal (voltage) which can be read by a voltmeter.

Sensor technology is being used in all sectors of industry and can give a product an added value that makes it competitive. During the past two decades, there has been an unprecedented growth in the number of products and services, which utilise information gained by monitoring and measuring using different types of sensors. The development of sensors to meet the need is referred to as sensor technology and is applicable in a very broad domain including the environment, medicine, commerce and industry [2]. Non-military world market for sensors has grown at an average annual rate of 4.5% between 1998 and 2008 [3].

Figure 1.1 shows the market sector most heavily impacted by sensors. The market sector which has most heavily impacted by sensors is in the health care sector with 20%. It is also shown that the sensors have impact on food processing sector (12%) and the environment sector (11%). Some impact is on markets such as agriculture (8%), chemical engineering (8%), domestic and other appliances (7%), security and defence (7%), transport (6%), and energy (6%). Less impact is made in sectors such as construction/housing (3%), wood and textile (3%), IT/communication (4%), and metal and plastic processing (5%) [2].

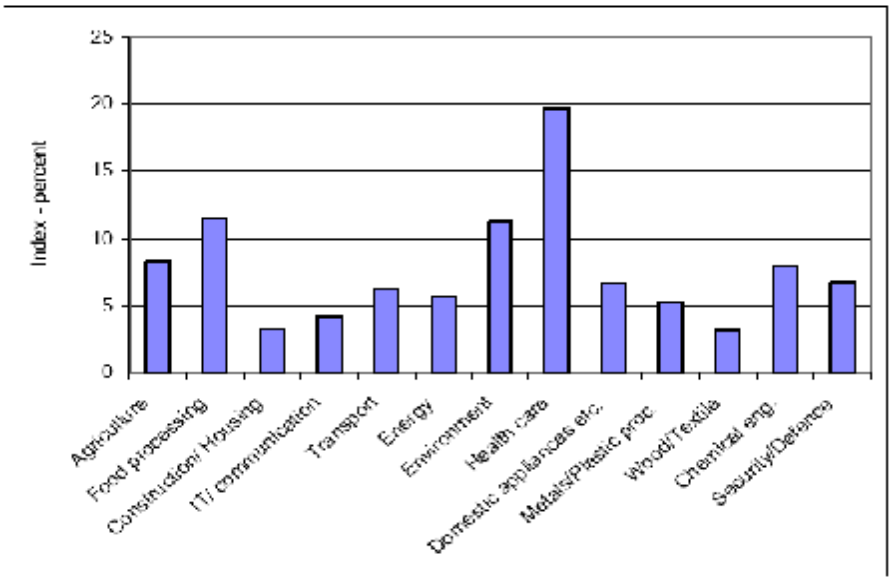

Figure 1.1: Market impact of all sensor types by industries [2]

1.2 Sensors and Non-destructive Testing (NDT)

Non-destructive testing (NDT) or sometimes also referred as non-destructive evaluation (NDE) is defined as non-invasive techniques to determine the integrity of a material, component or structure or quantitatively measure some characteristics of an object. In other words, NDT does inspect or measure without doing any harm or damage of the system. NDT has been applied in many different branches of industry. With the increasing demand for highly reliable and high performance inspection techniques, during manufacturing, production and use of a system or structure, the demand for the employment of suitable NDT techniques is increasing.

There are different NDT techniques available with different characteristics. The following are the most commonly used NDT techniques: Visual, Liquid Penetrant, Magnetic, Ultrasonic, Acoustic, Radiography, Eddy current and X-ray. The type of technique to be used entirely depends on the specific application. Some of the NDT or NDE methods are used for;

a. Flaw detection and evaluation
b. Leak detection
c. Location determination
d. Dimensional measurements

e. Structure and micro-structure characterization
f. Estimation of mechanical and physical properties
g. Stress (strain) and dynamic response measurements
h. Material sorting and chemical composition determination

The use of NDT is even more indispensable in the case of structures that have to work in severe operating environments. There are NDT applications at almost any stage in the production or the life cycle of a component. Some of the most important areas are:

i. Power stations – nuclear and conventional power plants [4].
ii. Metal industry – steel producers, steam and pressure vessel construction for the inspection of cracks, defects, and any other flaws and their characterization, fatigue estimation, quality assurance, wall thickness and coating thickness testing, determination of hardness etc [5-9].
iii. Petrochemical industry [10].
iv. Transportation – railways [11].
v. Food industry - Quality assurance of food products.
vi. Medical sciences.
vii. Civil engineering - inspection of concrete structures, bridges, infrastructure due to aging problem.
viii. Aircraft - fatigue estimation in aircraft surface and other parts.
ix. Pipe inspection - Inspection of pipes and piping systems in industrial plants.
x. Others.

1.3 Planar Electromagnetic Sensors

Planar electromagnetic sensing system has been used as one of the NDT methods to evaluate the material properties. Planar electromagnetic sensors have been used for the evaluation of near-surface properties such as conductivity, permeability and dielectric properties. The applications of planar electromagnetic sensors will depend on both the characteristic of the sensor type chosen and also the characteristic of material under test.

1.3.1 Background of Planar Electromagnetic Sensors Research Works at Massey University

Planar electromagnetic sensor research works were conducted under the School of Engineering and Advanced Technology (SEAT). Three types of sensors; meander, mesh and interdigital configurations have been fabricated and tested for various applications. All developed sensors were planar type and have a very simple structure. The operating principle of these sensors is based on the interaction of the electromagnetic field generated by the sensors with the neighbouring material under test (MUT) [12]. Applications of these three sensors depend on their characteristic and also the characteristic of the material under test. The characteristic and the experimental results of these type of sensor has been reported in [12, 13].

1.3.2 Planar Meander and Mesh Sensors

Planar meander and mesh sensors consist of two coils: one coil is known as the exciting coil and the other coil is known as the sensing coil [12, 13]. The exciting coil carries alternating current and generates a high frequency electromagnetic field penetrates in to the system under test. The induced electromagnetic field in the testing system will generate eddy currents on the system under test, given that the material under test is of conducting or magnetic type. Due to the flow of eddy current the induced field in the testing system will modify the generated field, and the resultant field will be detected by the pick-up coil or sensing coil, which is placed above the exciting coil. The representation of the mesh and meander type sensors are shown in figure 1.2.

Planar meander and mesh type sensors has been used for assessment and inspection of the surface properties of any conducting and magnetic materials [14, 15]. The sensor can be either of a meander type or of a mesh type depending on its applications. The use of planar meander-type magnetic sensors has already been reported for the inspection of the printed circuit boards (PCBs) [16] and also for the evaluation of the near-surface material properties (e.g., conductivity, permeability, thickness, liftoff, existence of cracks, defects, etc.) [17]. The mesh type of sensor has been used to replace the meander in order to detect cracks in a metal [14, 15, 18, 19]. This is because the meander type has disadvantages on which the performance of the sensor is not independent of the alignment of the cracks or non-homogeneity of the material structure (in the process of evaluating material integrity), with respect to the sensor configuration. In this case for the mesh type sensor, the eddy currents take a more circular pattern thus eliminating the geometry/alignment effects encountered in meander type sensors, with the material under test.

The structural configuration of the planar type sensor is shown in figure 1.3. The exciting coil and the sensing coil are separated by a polyimide film of 50μm thickness. In order to improve the directivity of flux flow a magnetic plate of NiZn is placed on top of the sensing coil. The size of the sensor depends on the number of pitches used in that. The optimum pitch size depends on the application [19, 20].

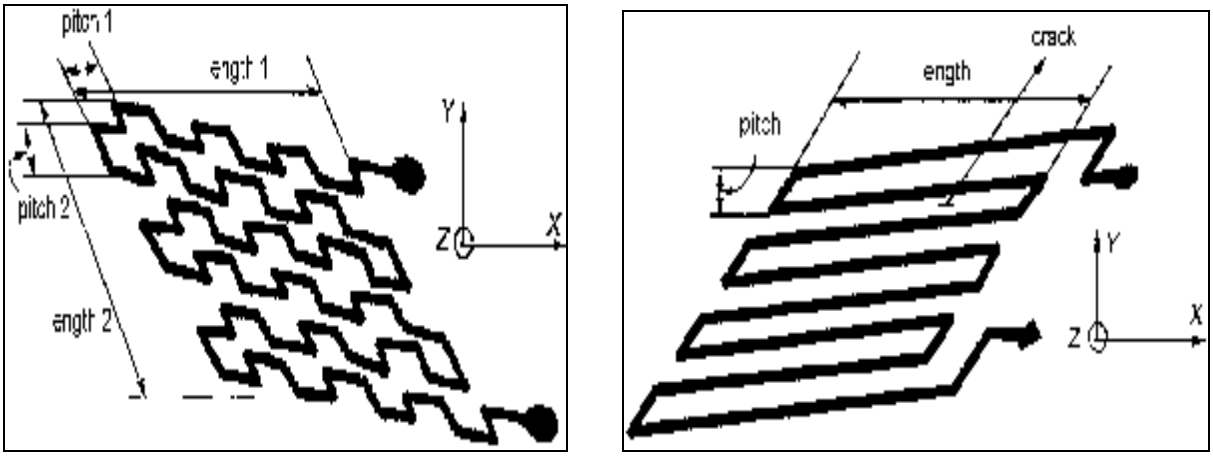

(a) Configuration of mesh-type sensor. (b) Configuration of meander-type sensor.

Figure 1.2: Configuration of planar electromagnetic sensors; (a) Mesh-type sensor and (b) Meander-type sensor.[12]

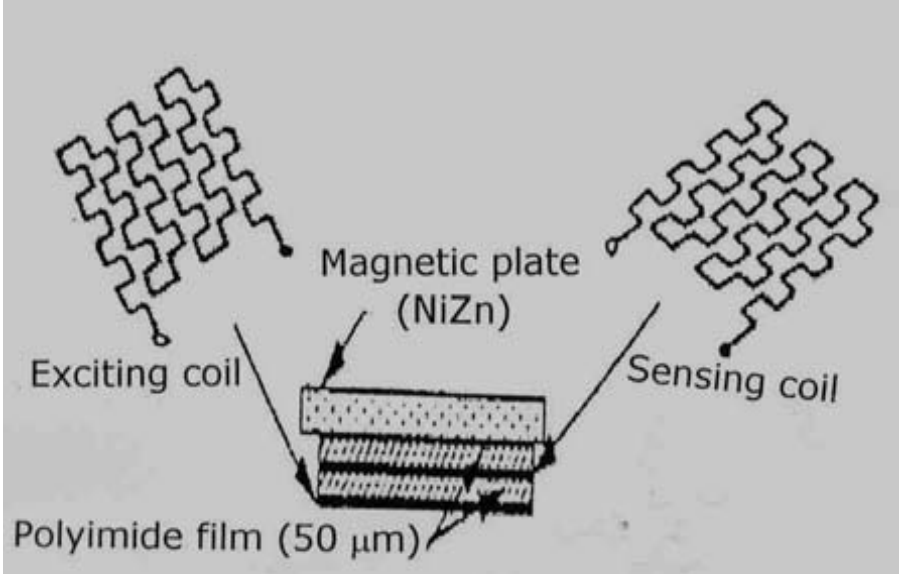

Figure 1.3: Structure of the sensor [12].

1.3.3 Planar Interdigital Sensor

Planar interdigital sensor is based on the interdigital electrode structures which have been widely used in photosensitive detectors [21-24], surface acoustic wave (SAW) [25-29], humidity sensors [30-33], sensors for chemicals and gasses [34-39], measurement of electrolyte conductivity (EC) [40], determination of components contained in aqueous solutions [41], determination of moisture, fiber and titanium dioxide in paper pulp [42, 43], for the complex permittivity characterization of materials [44], measuring tablet hardness and coating thickness (pharmaceutical products) [45], the detection of small amount of magnetic beads over the surface of microsensors [46].

Currently, the numbers of research works in developing planar interdigital sensors are increasing. Planar interdigital sensors have been used for estimation of properties of dielectric material such as milk, saxophone reeds, meat and leather [47-54] . Evaluation of diffusion-driven material property profiles using three-wavelength interdigital sensor has been reported by Mamishev et. al. [55]. Interdigital type of microimpedance biosensor has been developed for bacterial detection and foodborne bioterrorism agents [56, 57]. The dielectric behaviour of nematic liquid crystals was studied with interdigital capacitors [58]. Design and applications of interdigital capacitive sensors were discussed in [59].

Detail discussions on development of planar interdigital sensor will be discussed in chapter 4 of the thesis. The theoretical and the analysis of fabricated novel planar interdigital sensor have been reported in chapter 5.

1.3.4 Applications of Planar Electromagnetic Sensors

Planar electromagnetic sensors have been used in various applications. The examples given are related to the research works conducted by undergraduate students and post-graduate students of Massey University.

i. Estimation of fat content in pork meat

The electromagnetic interaction of planar interdigital sensors with pork belly cuts has been investigated [54]. Three interdigital sensors of varying periodicity were fabricated and tested on six pork belly pieces. The interdigital sensors used for experimentation has one sided access to the meat under test (MUT). Electric field lines pass through the MUT, and the measured capacitance between the two electrodes will depend on the material dielectric properties and material geometry. The interdigital sensors were driven by a sine wave with a peak-to-peak voltage of 10 V. The measurements were made at frequencies in the range from 5 kHz to 1 MHz.

The pork belly pieces had skin on top and muscle at the bottom, where the personal view of top and bottom is contradictory. The pork bellies were around 20-30 mm thick. Glad wrap was placed on top of the sensor to prevent direct contact with the pork meat. This is done to keep up the high standards of hygiene required when testing meat. The pieces of pork were placed on the sensor according to four different orientations**.** Each of the six pieces of pork was tested for all four orientations at the same frequency range mentioned above. The driving signal for the sensors were provided by the Agilent 33120A waveform generator and the Agilent 54622D mixed signal oscilloscope, analyzed the input voltage, output current and the phase. The experimental setup is shown in figure 1.4. The results were analyzed to determine the relationship between the reactive impedance values with the fat content of the pork belly. The fat content was estimated by mathematical analysis and then was compared to the results obtained by the chemical analysis. Results from the experiments have shown that

planar interdigital sensors can be used to determine the fat content of pork meat in a non-destructive and non-invasive way.

Figure 1.4: Experimental setup to determine fat content in pork meat.

ii. Inspection of quality of saxophone reeds

Two types of planar electromagnetic sensors have been used to evaluate the quality of saxophone reeds [52]. The mesh type sensor with network analyser was used in the experiment as shown in figure 1.5 and figure 1.6 respectively. Mesh-type planar sensors were evaluated and found to be very effective at a high operating frequency (500 MHz). However, the system is expensive as it requires the use of high-end costly equipment (i.e. network analyser). A low-cost solution employing interdigital planar sensors has been proposed and evaluated as shown in figure 1.7. The initial results for quality inspection of saxophone reeds were very promising. There was a measurable difference shown by the sensor between "good" and "bad" reeds. Therefore, the planar electromagnetic sensor can be one of the options to evaluate the quality of saxophone reeds.

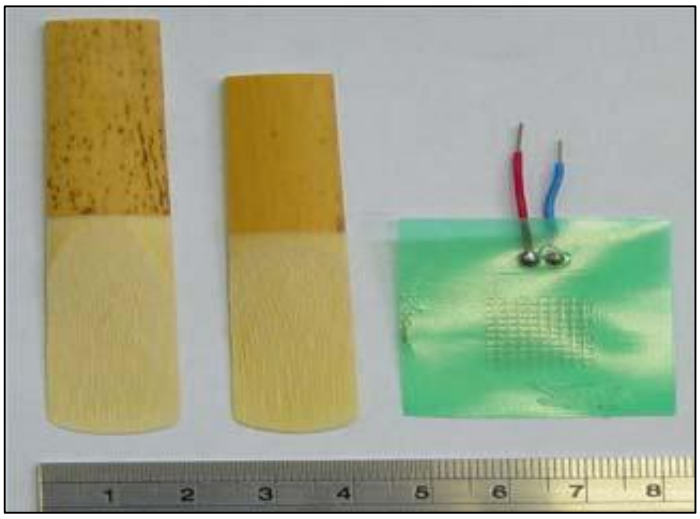

Figure 1.5: Sensor and different sections of a tenor and alto saxophone reeds.

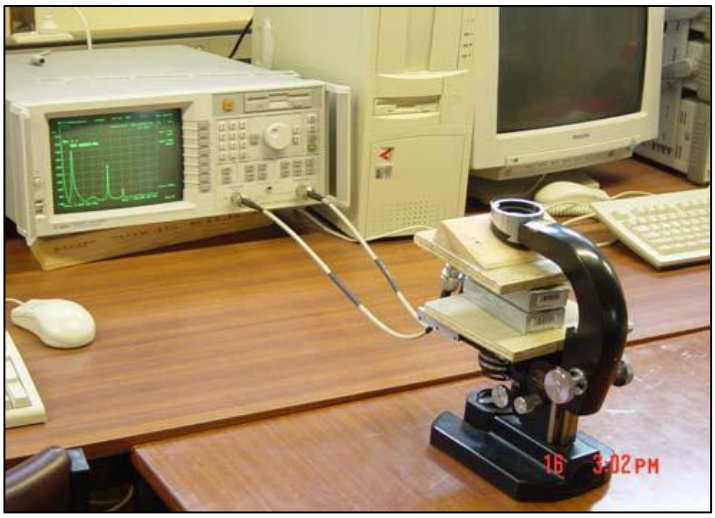

Figure 1.6: Sensor, modified microscope, low-loss cables, and network analyzer used to test the reeds.

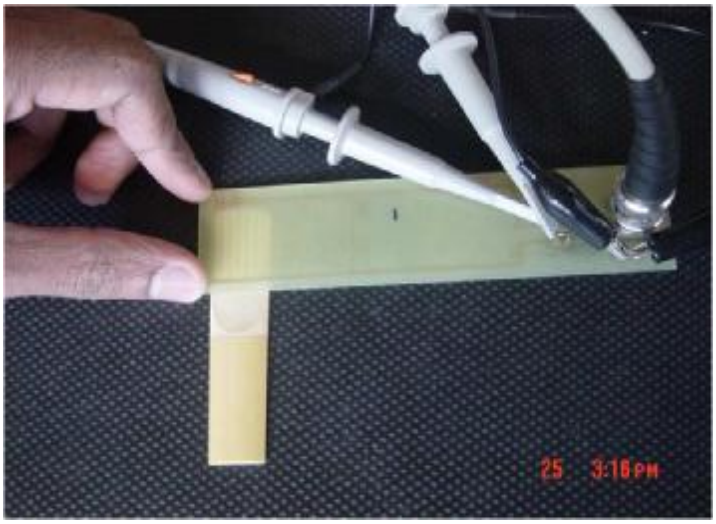

Figure 1.7: Experiment setup using the interdigital sensor.

iii. Quality improvement of leather tanning process using a novel sensor

Novel interdigital based sensing system has been developed for quality improvement of leather tanning process [47, 60]. The developed sensing system was able to measure looseness in the sheepskin; to alter the tanning process in order to produce better quality leather. The sensor has the planar interdigital structure and the consecutive fingers are connected to positive and negative electrodes respectively. The proximity depth of electric field can be adjusted by varying the distance between two electrodes of opposite polarity. The measured reactive impedance of the sensor depends on the material dielectric properties as well as on the electrode and material geometry. From the measurement, the effective permittivity of the sensor is calculated which is related to the quality of leather. It is possible to predict some information of skin quality during various stages of leather processing. This is very useful for optimizing the process of leather manufacture to achieve the desired qualities for the finished product. Experimental setup to access the quality of leather is shown in figure 1.8.

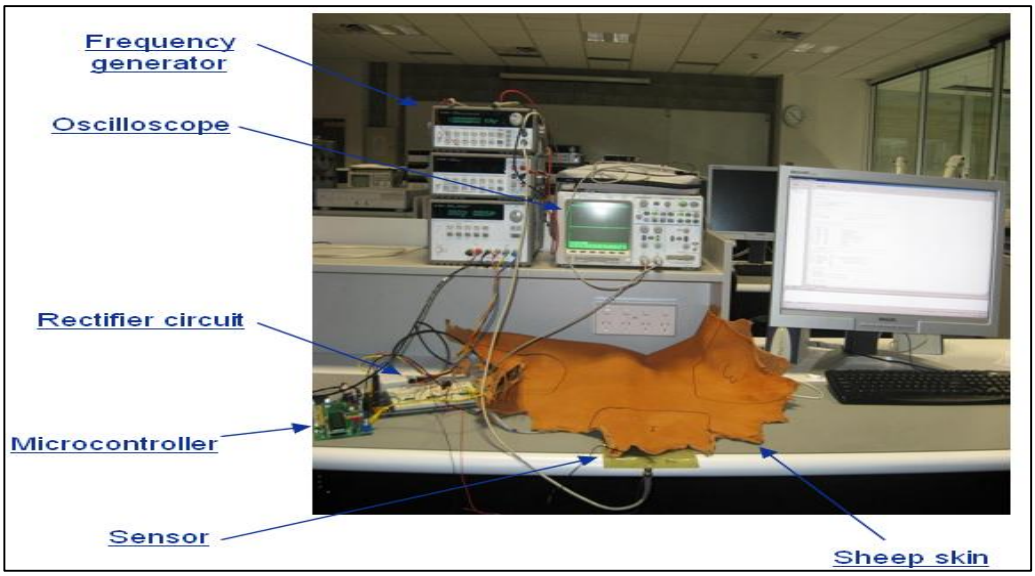

Figure 1.8: Experimental setup to access the quality of leather

iv. Inspect quality of currency coins

Planar electromagnetic sensors can be used to inspect quality of currency coins [61]. The mesh type of sensor was used in the experiment. Figure 1.9 shows the experimental set-up based on a network analyzer for coin testing. The response of the network analyzer for different types of coins has been observed for a frequency range of 300 kHz to 1.3 GHz. It was observed that the network analyzer give different response (in the transmission mode) for a few coins made of different countries. It can be said that different types of coins have produced different profiles. The developed system can successfully differentiate coins from different countries.

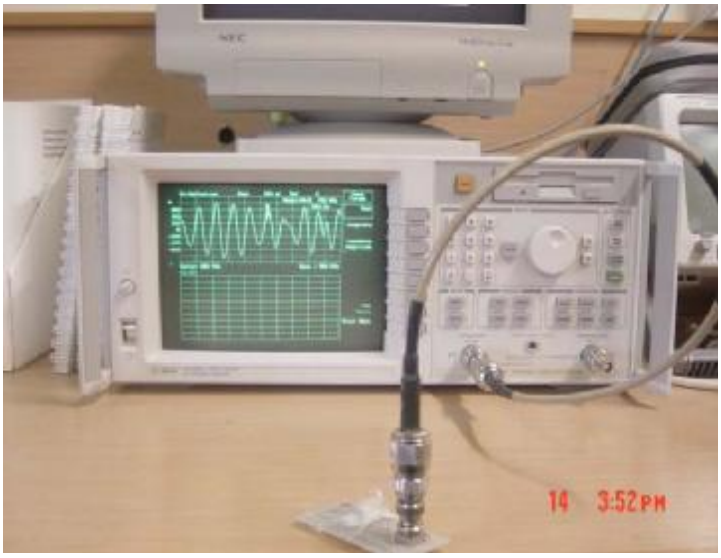

Figure 1.9: Experimental setup using mesh type sensor and a network analyzer

v. Quality monitoring of dairy products

The possibility of employing planar type electromagnetic sensors for estimation of properties of dielectric materials such as milk, butter, cheese, yogurt etc. has also been investigated for the purpose of composition analysis of dairy products [53]. The experimental results have shown that there were variations of impedance with frequency for different dairy products. The effects of dielectric materials such as milk, butter, cheese, curds, and yogurts on the transfer impedance of planar electromagnetic sensors have been investigated. It was observed that the dielectric materials have a great influence to make appreciable change in the transfer impedance. The experimental results have shown that the sensor has the potential to be used

to determine composition of dairy products. The transfer impedance can be used to determine the quality of the product through an appropriate computation technique.

1.4 Organization of the Thesis

This thesis is organized into nine chapters. Chapter 1 provides the introduction to sensor technology in particular planar electromagnetic sensors and their applications. Background of previous research works at Massey University was also included in this chapter. Chapter 2 describes the seafood poisoning caused by marine biotoxins. Shellfish toxins are highlighted in this chapter and the main focus is on Amnesic Shellfish Poisoning (ASP) which is related to domoic acid. Chapter 3 of the thesis describes the existing methods of seafood inspection. Some issues of the existing methods are discussed which gives us the motivation to develop a reliable low cost sensing system as one of the tools for seafood inspection. In Chapter 4, the development of planar interdigital sensors is explained in details. This includes the sensor design and fabrication process of the conventional and novel sensors. Chapter 5 talks on the theoretical and field analysis of the developed sensors. The circuit analysis and the modelling using COMSOL Multiphysics are described in this chapter. The experimental setup, measurement method and experimental procedures are described in Chapter 6 which includes the experiments conducted for the initial studies of three chemicals, experiments with seafood products, experiments of proline with mussels and experiments of domoic acid with mussels. Results and discussion from the experiments conducted are also discussed in details in Chapter 6. Chapter 7 describes the development of low cost sensing system for seafood inspection. This chapter will highlight details on the embedded system developed called Seafood Inspection Tool or SIT. Chapter 8 describes the conclusion of the research works and finally Chapter 9 provides some information for the future research work.

Chapter 2

Introduction to Seafood Poisoning

2.1 Seafood Poisoning

Seafood plays an important role in human diet and also a source of top-quality protein [62-64]. But eating seafood also can cause illnesses from seafood poisoning. Illness from seafood poisoning were caused by dangerous contaminated chemicals or marine biotoxins [65-67]. Seafood contaminated by marine biotoxins apparently look, smells or tastes normal but after human or animals consume a sufficient amount of contaminated seafood, they may suffer a variety of gastrointestinal and neurological illnesses [66].

Shellfish toxins (phycotoxins) and ciguatoxins are the most dangerous marine biotoxins [65]. The toxins accumulate in the digestive glands of the shellfish without causing any toxic effect on it. Shellfish toxins can cause paralytic shellfish poisoning (PSP), diarrhoeic shellfish poisoning (DSP), amnesic shellfish poisoning (ASP), neurotoxic shellfish poisoning (NSP) and azaspiracid shellfish poisoning (AZP), while ciguatoxins can cause ciguatera fish poisoning (CFP) [65, 68].

Figure 2.1 shows the global increase of marine algal toxin incidence. Encircled areas indicate where outbreaks have occurred or toxin has been detected at levels sufficient to impact human or environmental health [68]. The incidence of seafood poisoning caused by the shellfish toxins is increasing. Table 2.1 shows the main marine toxins, their source organisms, infected organisms, and countries where their presence has been revealed. Brief information of shellfish toxins will be discussed in this chapter. Their main structural characteristic and toxic effects will be described as being reported in [65, 67-70]. Only ASP will be discussed in details since the main goal of the research work for the thesis is related to it.

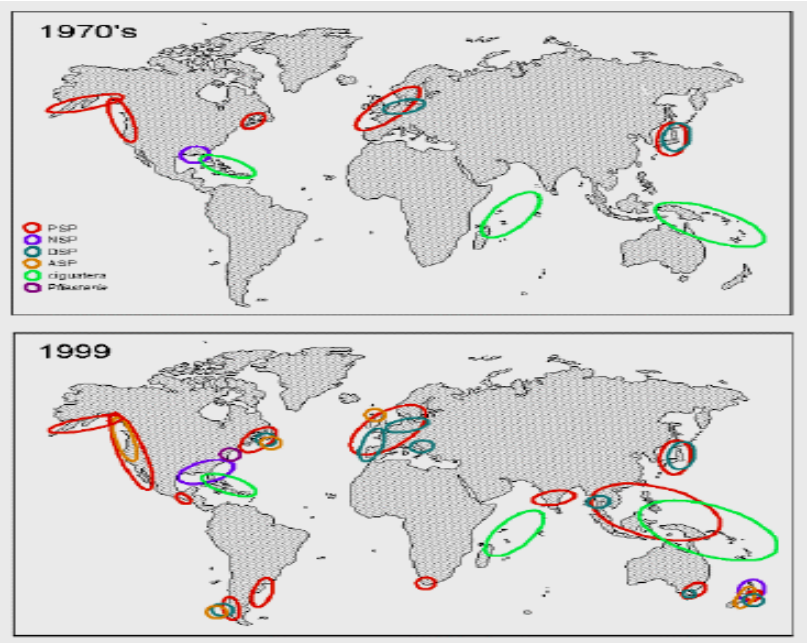

Figure 2.1: Global increase of marine algal toxins incidence [68]

Table 2.1: Main marine toxins, their source organisms, and infected organisms and countries where their presence has been revealed*

Toxin	Source organisms	Infected organisms	Countries
DSP	*Dinophysis acuminata*, *D. acuta*, *D. caudata*, *D. fortii*, *D. hastata*, *D. mitra*, *D. norvegica*, *D. rotundata*, *D. sacculus*, *D. tripos*, *Gonyaulax polyhedra*, *Phalacroma rotundatum*, *Protoceratium reticulatum*, *Protoperidinium oceanicum*, *P. pellucidum*, *Prorocentrum arenarium*, *Prorocentrum belizeanum*, *Prorocentrum concavum* (or *Prorocentrum maculosum*), *Prorocentrum lima*, *Prorocentrum redfieldi*	Clams, mussels, oysters, scallops	Europe: Belgium, Croatia, Denmark, France, Germany, Greece, Ireland, Italy, The Netherlands, Norway, Portugal, Spain, Sweden, United, Kingdom; Africa: South Africa North America: Canada, USA Central and South America: Argentina, Brazil, Chile, Mexico, Uruguay; Asia: China, India, Japan, The Philippines, The Russian Federation; Oceania: Australia, New Zealand
PSP	*Alexandrium andersonii*, *A. catenella*, *A. cohorticula*, *A. fraterculus*, *A. fundyense*, *A. minutum* (or *A. excavata*), *A. tamarensis*, *Aphanazomenon flos-aquae*, *Gymnodinium catenatum*, *Pyrodinium bahamense*, *Spondylus butler*, *Zosimous acnus*	Clams, crabs, cockles, cods, copepods, gastropods, herrings, lobsters, mackerels, mussels, ormers, oysters, puffer fishes, salmons, scallops, starfishes, whales, whelks	Europe: Denmark, France, Germany, Ireland, Italy, The Netherlands, Norway, Portugal, Spain, Sweden, United Kingdom; Africa: Morocco, South Africa, Tunisia; North America: Canada, USA; Central and South America: Argentina, Brazil, Chile, Guatemala, Mexico, Trinidad y Tobago, Uruguay, Venezuela; Asia: China (also Hong Kong and Taiwan), India, Japan, Malaysia, The Philippines, Thailand, Timor-Leste; Oceania: Australia, New Zealand
ASP	*Alsidium corallinum*, *Amphora coffaeformis*, *Chondria armata*, *C. baileyana*, *Nitzschia navis-varingica*, *Pseudo-nitzschia australis*, *Pseudo-nitzschia fraudulenta*, *Pseudo-nitzschia multiseries*, *Pseudo-nitzschia multistriata*, *Pseudo-nitzschia pseudodelicatissima*, *Pseudo-nitzschia pungens*, *Pseudo-nitzschia seriata*, *Pseudo-nitzschia turgidula*	Anchovies, clams, crabs, gastropods, lobsters, mackerels, mussels, oysters, scallops	Europe: Belgium, Denmark, France, Ireland, Italy, The Netherlands, Norway, Portugal, Spain, United Kingdom; North America: Canada, USA; Central and South America: Argentina, Chile, Mexico; Asia: Japan; Oceania: Australia, New Zealand
NSP	*Chattonella antiqua*, *Chattonella marina*, *Fibrocapsa japonica*, *Gymnodinium breve* (or *Ptychodiscus breve*), *Heterosigma akashiwo*, *Raphidophyceae*	Clams, mullets, mussels, oysters, tunas, whelks	Europe: France, Germany, Greece, The Netherlands, Portugal, The Russian Federation, Spain, United Kingdom; Africa: South Africa; North America: Canada, USA; Central and South America: Brazil, Mexico; Asia: China (also Hong Kong), Japan, Korea, Malaysia; Oceania: Australia, New Zealand

AZP	*Protoceratum crassipes*, *Protoperidinium*	Mussels, oysters	Europe: Ireland, Norway, Portugal, United Kingdom
CFP	*Gambierdiscus toxicus*, *Gymnodinium sangieneum*, *G. polyedra*, *Ostreopsis lenticularis*, *Prorocentrum concavum*, *Prorocentrum mexicanum*, *Prorocentrum rhathytum*	Amberjacks, barracudas, bonefishes, carrangs, Chinamanfishes, crabs, emperors, groupers, hogfishes, jacks, javelin fishes, mackerels, marine snails, moray eels, mullets, parrotfishes, porgys, shrimps, snappers, swordfishes, surgeon fishes, triggerfishes, tunas, wrasses	Europe: France, Germany, Italy, The Netherlands; Africa: Madagascar; North America: Canada, USA; Central and South America: Anguilla (United Kingdom), The Bahamas, Chile, Cuba, Dominican Republic, Guadeloupe (France), Haiti, Jamaica, Martinique (France), Mexico, Puerto Rico (USA), Saint Barthelemy (France), Saint Martin (France – The Netherlands), Saint Vincent (United Kingdom), Venezuela, Virgin Islands (USA); Asia: China, Fiji, French Polynesia (France), New Caledonia (France), Israel, La Reunion (France), several South Pacific Islands; Oceania: Australia, New Zealand, Tonga

*See Ref. [65] for specific references.

2.2 Paralytic Shellfish Poisoning (PSP) Toxins

Paralytic shellfish poisoning is caused by the consumption of molluscan shellfish contaminated with a suite of heterocyclic guanidines collectively called saxitoxins (STXs). Due to their world-wide incidence, PSP toxins pose the serious threat to public health and cause an immeasurable economic damage. They are water-soluble and thermo-stable tetrahydropurine compounds, which can be further divided into four groups: carbamate, N-sulfo-carbamoly, decarbamoyl and deoxydecarbamoyl. Among them, the carbamate saxitoxin (STX) is the most toxic.

Human affected by the PSP will have symptoms like neurological, the gastrointestinal ones (nausea, vomiting and diarrhoea) being less than usual. These symptoms appear between 15 min – 10 hour after contaminated shellfish ingestion, starting with slight tingling, numbness in mouth and extremities, prickly sensation in fingertips and toes, lips and skin burning, dizziness, floating sensation, headache, ataxia, and fever. However, it is often reported a noticeable calm and serenity in intoxicated patients. However, people who are affected with severe poisoning which is characterised by general muscular incoordination, dysmetria and respiratory distress can lead to death within 2-25 hours. These toxins block the sodium channels, affecting the propagation of the action potential. Only symptomatic treatment exists, based on adequate ventilation and gastric lavage when no vomiting has occurred spontaneously.

2.3 Diarrhoeic Shellfish Poisoning (DSP) Toxins

DSP toxins are a group of thermostable polyether and lipophilic compounds, which includes okadaic acid (OA) and its acidic derivaties named dynophysistoxins (DTXs). The first incidence of DSP occurred in Japan in the late 1970s. The main symptom of human intoxication is diarrhoea, although other effects are also relevant, such as nausea, vomiting and abdominal pain. Human will experience the symptom in a period of 30 min to a few hours after consumption of contaminated shellfish. Patients can show gastrointestinal disorders up to 3 - 4 days, afterwards being completely recovered. Hospitalisation is not required to the patients who got DSP and there is no cases of human deaths have been reported.

2.4 Neurotoxic Shellfish Poisoning (NSP) Toxins

Brevetoxins (PbTxs) is the main group of NSP toxins. Intoxications by brevetoxins will show effects after 30 min – 3 hour after their ingestion. Symptom of NSP includes nausea, tingling and numbness of the perioral area, loss of motor control and severe muscular ache.

2.5 Azaspiracid Shellfish Poisoning (AZP) Toxins

AZP was detected for the first time in 1995 among consumers in the Netherlands after eating blue mussels from Ireland. The symptoms were similar to those of diarrhoeic shellfish poisoning (DSP), but the concentration of the DSP toxins was low. Subsequently, the AZP group was discovered.

2.6 Ciguatera Fish Poisoning (CFP) Toxins

Ciguatera Fish Poisoning (CFP) is a form of human poisoning resulting from the ingestion of some species of tropical marine fish, which have accumulated naturally occurring toxins through their diet. CFP is most prevalent in circumtropical regions with coral reef environments [71, 72]. Ciguatoxins is produced by microscopic sea plants (dinoflagellates). CFP are associated with consumption of contaminated reef fish such as barracuda, grouper, and snapper. Patients can suffer for weeks to months with debilitating neurologic symptoms, including profound weakness, temperature sensation changes, pain, and numbness in the extremities.

2.7 Amnesic Shellfish Poisoning (ASP) Toxins

In late 19th and early 20th century a large number of illnesses were linked with the consumption of raw oysters, claws and mussels. It was found that these illnesses were related to the ingestion of domoic acid-contaminated mussels which led to ASP [1-4]. ASP is characterized according to both gastrointestinal and neurological symptoms, including severe headache, confusion, and either temporary or permanent memory loss. As shown in figure 2.1, there was no incidence of ASP reported in 1970's but in 1999 the numbers of incidences increase rapidly. This is because most of the countries have implemented the extensive shellfish toxins monitoring programme.

2.7.1 Domoic Acid (DA)

Domoic acid (DA) is a naturally occurring toxin produced by microscopic algae, specifically the diatom species Pseudo-nitzschia [68, 73-75]. DA is a chemical that is produced by algae or plankton when it blooms. The incidence of Pseudo-nitzschia blooms is increasing world-wide, and toxic blooms have been reported in many localities [76]. DA is a water-soluble ticarboxylic amino acid that acts as an analog of the neurotransmitter glutamate and is a potent glutamate receptor agonist [68]. Shellfish ingest these algae, where the toxin concentrates and can accumulate this toxin without apparent ill effects [68, 69]. However, for marine mammals and humans, DA is an acid that acts as a neurotoxin. The toxin is not destroyed by cooking or freezing. Figure 2.2 shows the chemical structure of domoic acid.

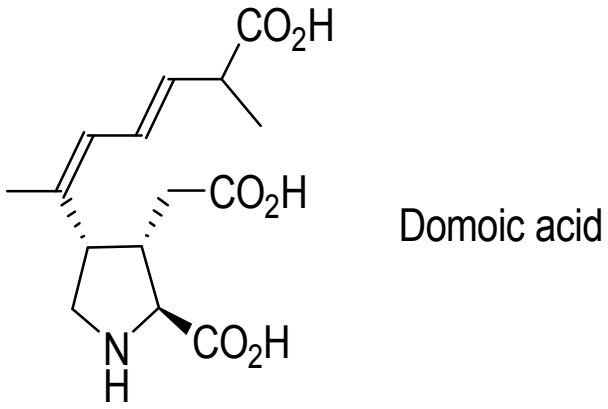

Figure 2.2: Chemical structure of Domoic Acid

The presence of DA in shellfish has been reported in various regions of the world [65, 68]. There have been numerous reports of toxicity in a variety of wildlife species indicating that DA moves up the food chain in marine ecosystems. Studies have proven that certain amount of DA can cause health problems to animals and humans [77-82]. In 1987, DA was identified as the toxin responsible for an outbreak of illness in Prince Edward Island, Canada [83, 84]. It was caused by eating blue mussels. Effects on both the gastrointestinal tract and the nervous system were observed. It was reported that 107 patients (all adult) met the case definition [85]. Dose-related symptoms included nausea, vomiting, abdominal cramps, diarrhoea, headache, memory loss and convulsions and several deaths were attributed to the toxin. As a result of the episode of human illness in Canada, most countries have set a regulatory guideline of 20 μg/g of DA in shellfish meat.

DA was first identified in New Zealand in shellfish harvested during 1993 [86]. Shellfish are now routinely tested for DA in New Zealand under Marine Biotoxin Monitoring Programme, which tests samples from both commercial and recreational harvest sites from around 5650 km coastline. This extensive shellfish sampling and analysis program are conducted to protect consumers and to satisfy overseas market that New Zealand produce is safe and conforms to the regulatory limits.

2.8 Conclusion

In order to protect consumers from shellfish poisoning, most countries have set a regulatory guideline of 20 μg/g of DA in shellfish meat [65, 66]. All the products need to be tested for the toxin, which places a heavy workload on the laboratories and is extremely expensive to the industry. This has motivated us towards the development of a low cost sensing system which can detect the presence of DA and their related analogs without much difficulty. The technology can be used as an alternative tool for preliminary screening of DA in a sample. If the sample is found suspicious, expensive analytical method should be used to provide accurate determination and quantification of contaminated samples. The developed sensing system should be reliable, easy to use, robust and cost effective.

Chapter 3

Existing Methodology of Seafood Inspection

3.1 Introduction

This chapter will discuss the different methodologies exist for seafood inspection. As being mentioned in the previous chapter, there is a requirement for monitoring of shellfish to ensure consumer safety. Most countries have established shellfish monitoring programs and regulatory maximum permitted levels (MPL) for human exposure have been set worldwide [87-90]. The toxicity of the shellfish toxins (phycotoxins) is summarised in table 3.1 which has been reported by Ian Garthwaite [69]. Details of this information can be referred to [68, 70, 87, 91-93].

The classical method of monitoring toxicity is by using mouse bioassay, in which an extract of shellfish is injected into mice. If the mice die, the shellfish are toxic [94]. Modern analytical techniques, such as HPLC, LC-MS, immunoassay, cellular bioassays, and molecular probes, have increasing role to play in both the monitoring process and in the identification of the environmental conditions and organisms responsible for toxin production [69]. An emerging technology as biosensor in the future should be able to deal with complicated matrices and sometimes toxin mixtures [67].

The works done in the report is only concentrating on detection of DA in shellfish. Therefore only a few existing methods related to the detection of DA have been reviewed. The existing method of DA detection is based on using chromatography technique, surface plasmon resonance (SPR), and immunoassay technique using enzyme-linked Immunosorbent assay (ELISA). This chapter will highlight these three existing methods which have been widely used to detect the contaminated shellfish with domoic acid.

Table 3.1: Toxin properties: areas of common occurrence, toxicity, and regulatory action levels [69]

Toxin	**Most common geographical areas**	LD_{50} **(i.p. mouse µg/kg)**	**MPL (µg/100 g flesh)**	**MPL (mouse units)**
ASP (Domoic acid)	Canada, Northern USA, North Sea	120	2000	Sensitivity very low
PSP (Saxitoxins)	North East USA, Asia, South America, Europe	10	80 [a]	400
NSP (Brevetoxins)	Florida, Mexico, New Zealand	200	80 [b]	20
DSP (Okadaic acid)	Japan, Europe	200	16 [c] or 20	5
CTX (Ciguatoxin)	Tropical areas – reef fish	0.25 – 0.9	3.5 (fish flesh)	Sensitivity too low

[a] As 'saxitoxin equivalents

[b] MPL assuming 1MU = 4 µg PbTx-2 (personal communication Professor T. Yasumoto)

[c] MPL (Europe) (personal communication M.L. Fernandez, EU Reference Laboratory, Vigo, Spain)

3.2 Chromatography technique

Chromatographic techniques have been widely used for the detection of shellfish toxins. These techniques allow separation, highly selective identification and sensitive quantification of the different toxins present into a sample. Liquid chromatography (LC) is a separation technique in which the mobile phase is a liquid. Liquid chromatography can be carried out either in a column or a plane. Present day liquid chromatography that generally utilizes very small packing particles and a relatively high pressure is referred to as high performance liquid chromatography (HPLC) [95].

In the HPLC technique, the sample is forced through a column that is packed with irregularly or spherically shaped particles or a porous monolithic layer (stationary phase) by a liquid (mobile phase) at high pressure. HPLC is historically divided into two different sub-classes based on the polarity of the mobile and stationary phases. Technique in which the stationary phase is more polar than the mobile phase (e.g. toluene as the mobile phase, silica as the stationary phase) is called normal phase liquid chromatography (NPLC) and the opposite (e.g. water-methanol mixture as the mobile phase and C18 = octadecylsilyl as the stationary phase) is called reversed phase liquid chromatography (RPLC). Ironically the "normal phase" has fewer applications and RPLC is therefore used considerably more [95].

Overview of different chromatographic techniques for marine toxins detection have been reported by Quilliam [96]. LC has been used as Association of Analytical Communities (AOAC) official method for DA in mussels [97]. Identification of DA in mussels using LC technique has been reported in [74, 98, 99]. A new sensitive determination method of DA using HPLC has been reported in [73, 78, 100, 101]. The very recent application of toxin analysis is using high-performance liquid chromatography coupled with mass spectrometer, HPLC-MS. LC-MS is reviewed by Quilliam, who is also developing procedures for the multiple determination of toxins in shellfish [102, 103]. Table 3.2 shows the chromatographic detection procedures for Amnesic Shellfish Poisoning (ASP) [69].

Although chromatographic technique is one of the best methods for the detection of DA but they require expensive equipments, trained personnel, and sophisticated method of sampling preparation, laborious and also time-consuming. The lack of standards is also a serious difficulty, since non-certified or unknown toxins cannot be evaluated [67]. Other related problems that may appear during analysis are peak spreading, poor resolution and need of continuous calibration.

Table 3.2: Chromatographic detection procedures for ASP

Toxin class	**Detection method**	**Derivation**	**Detection limit in shellfish***	**Reference and comments**
ASP	UV 242 nm	None	400 ng/g	[104, 105]
(domoic acid)		SAX cleanup	20 – 30 ng/g	
	Fluorescence	FMOC	(15 pg/ml)	[106]
	LC - MS		10 ng/g	[102]

* Detection limit of instrumental method is given (pg/injection) where limit in shellfish following extraction is not given by author and unknown.

See Ref. [69] for specific and other shellfish toxins.

3.3 Surface Plasmon Resonance (SPR)

Surface Plasmon Resonance (SPR) is a powerful technique to measure biomolecular interactions in real-time in a label free environment. While one of the interactants is immobilized to the sensor surface, the other are free in solution and passed over the surface. Association and dissociation is measured in arbitrary units and displayed in a graph called the sensorgram. SPR-based instruments use an optical method to measure the refractive index near a sensor surface (within ~ 200 nm to the surface). SPR instruments comprise three essential units integrated in one system: optical unit, liquid handling unit and the sensor surface. The features of the sensor chip have a vital influence on the quality of the interaction measurement. The sensor chip forms a physical barrier between the optical unit (dry section) and the flow cell (wet section) [107].

SPR has been widely used as detection technique in bio-sensing system. Application of SPR-based biosensor has been used to detect DA in shellfish [67]. A rapid and sensitive immuno-based screening method was reported to detect DA present in extracts of shellfish species using a surface plasmon resonance-based optical biosensor [108]. An immunosensor based on surface plasmon resonance (SPR) was used for the detection of DA [109]. A portable SPR biosensor has been used to detect domoic acid in clam extracts [110]. The detection method based on SPR is suitable for laboratory analysis and not suitable for in-situ monitoring since the samples need to be prepared accordingly, analysis may take longer time and the equipment (SPR) is expensive.

3.4 Enzyme-linked Immunosorbent Assay (ELISA)

Immunoassay techniques are based on the affinity recognition between antibodies and antigens, and the most commonly found format is the enzyme-linked immunosorbent assay (ELISA) [67]. Immunoassay are developed using antibodies which recognize specific toxin structures. The choice of antibodies is crucial for determining the usefulness of the assay [69]. Enzymes are used as labels to detect the interaction between polyclonal or monoclonal antibodies and toxins. There is a compromise between highly specific antibodies, able to detect a specific toxin, and less specific antibodies, able to detect all the members of a toxic family. Hence, cross-reactivity may be an advantage or a limitation depending on the purpose [67].

ELISA is relatively cheap and can be used to handle large number of samples. Research of using ELISA to determine DA has been reported in [75, 111-114]. ELISA method normally can be used to detect only one particular toxin. Only one research work reported by Garthwaite et.al [113], which integrates ELISA for screening of DSP, PSP, ASP and NSP toxins. To develop the ELISA strip and to prepare the samples will need to follow some laboratory procedures and tedious work. Also there is no guarantee that the ELISA strip will respond very well to all samples.

3.5 Conclusion

Looking at the issues and complexity of the existing methods, where samples have to be prepared accordingly to certain laboratory procedures, required expensive equipments, needs trained personnel and time-consuming, we have designed and fabricated novel planar interdigital sensor based sensing system with the purpose of an easy detection of molecules for DA. The developed sensing system is easy to be used for the purpose of sampling inspection and can provide fast analysis of DA within shellfish meat for in-situ monitoring. Further analysis of contaminated chemicals (DA) in the seafood can be done in the laboratory using expensive techniques. The developed sensing system should be reliable and cost effective.

Chapter 4

Development of Planar Interdigital Sensor

4.1 Introduction to Planar Interdigital Sensors

Chapter 4 will highlight and discuss the operating principle of interdigital sensor and the design consideration for conventional interdigital sensors and also novel planar interdigital sensors. The operating principle of planar interdigital sensor basically follows the rule of two parallel plate capacitors, where electrodes open up to provide a one sided access to the material under test (MUT) [59]. The electric field lines of parallel plate capacitor and an interdigital sensor are shown in figure 4.1 (a) and (b). The electric field lines generated by the sensor penetrate into the MUT and will change the impedance of the sensor. The sensor behaves as a capacitor in which the capacitive reactance becomes a function of system properties. Therefore by measuring the capacitive reactance of the sensor the system properties can be evaluated.

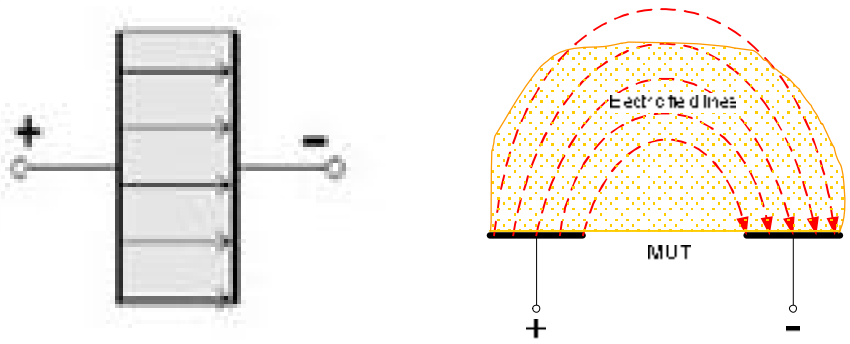

(a) (b)

Figure 4.1: Electric field lines of (a) Parallel plate capacitors (b) Planar interdigital sensor

Since the electrodes of an interdigital sensor are coplanar, therefore the measured capacitance will have a very low signal-to-noise ratio. In order to get a strong signal, the electrode pattern of the interdigital sensor can be repeated many times. The term "interdigital" refer to a digit-like or finger-like periodic pattern of parallel in-plane electrodes, used to build up the capacitance associated with the electric fields that penetrate into a material sample [59]. The conventional interdigital sensor is shown in figure 4.2. AC voltage source will be applied as an excitation voltage between the positive terminal and the negative terminal. An

electric field is formed from positive terminal to negative terminal. Mamishev et.al. [59] also stated that for a semi-infinite homogeneous medium placed on the surface of the sensor, the periodic variation of the electric potential along the X-axis creates an exponentially decaying electric field along the Z-axis, which penetrates the medium. Figure 4.3 illustrates Mamishev statement.

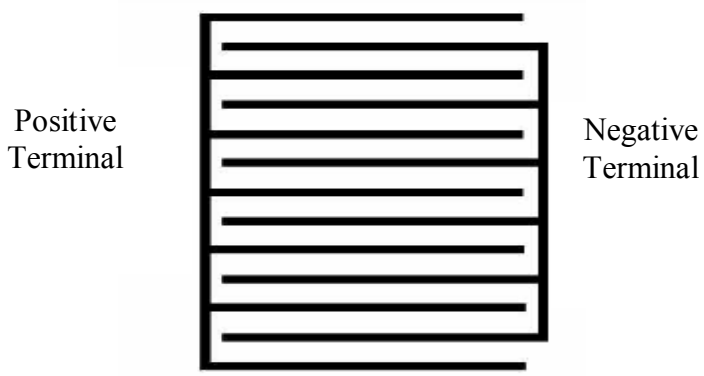

Figure 4.2: Configuration of conventional planar interdigital sensor

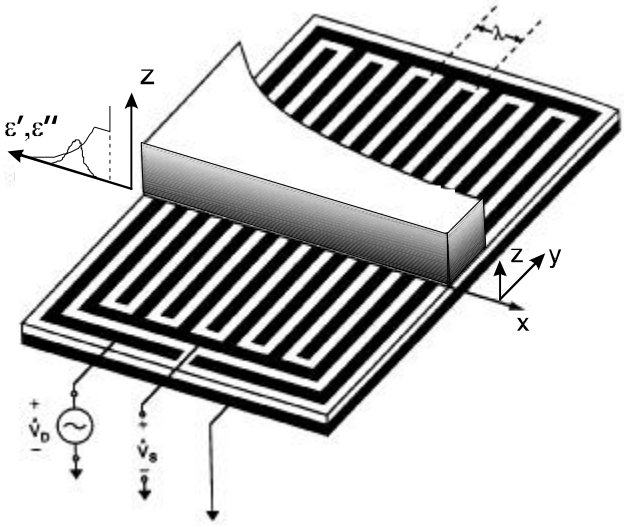

Figure 4.3: Fringing electric field of interdigital sensor [59]

Figure 4.4 shows the side view of the interdigital sensor showing how electric field was formed between positive and negative electrodes. It is shown clearly in figure 4.4 that the penetration depths of the electric field lines vary for different pitch length. The pitch length of the interdigital sensors is the distance between two consecutive electrodes. Also in figure 4.4, there are three pitch length (l_1, l_2 *and* l_3) showing the different penetration depths with respect to the pitch length of the sensor. The penetration depth can be increased by increasing the

pitch length, but the electric field strength generated at the neighbouring electrodes will be weak.

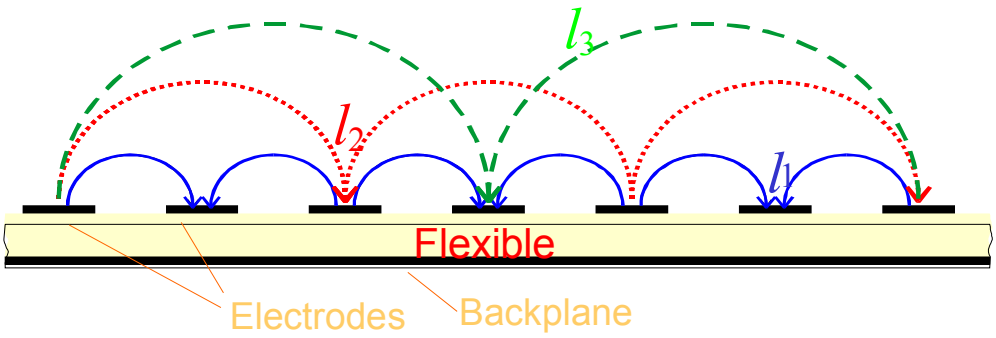

Figure 4.4: Electric field formed between positive and negative electrodes for different pitch lengths, (l_1, l_2 *and* l_3) [59]

Planar interdigital sensors can be used for different sensing application. Figure 4.5 illustrates on the sensing possibilities of planar interdigital sensors. These sensing possibilities for various characteristic of samples have given us the opportunity to design and fabricate a miniature type of planar interdigital sensor to detect the contaminated seafood with dangerous chemical.

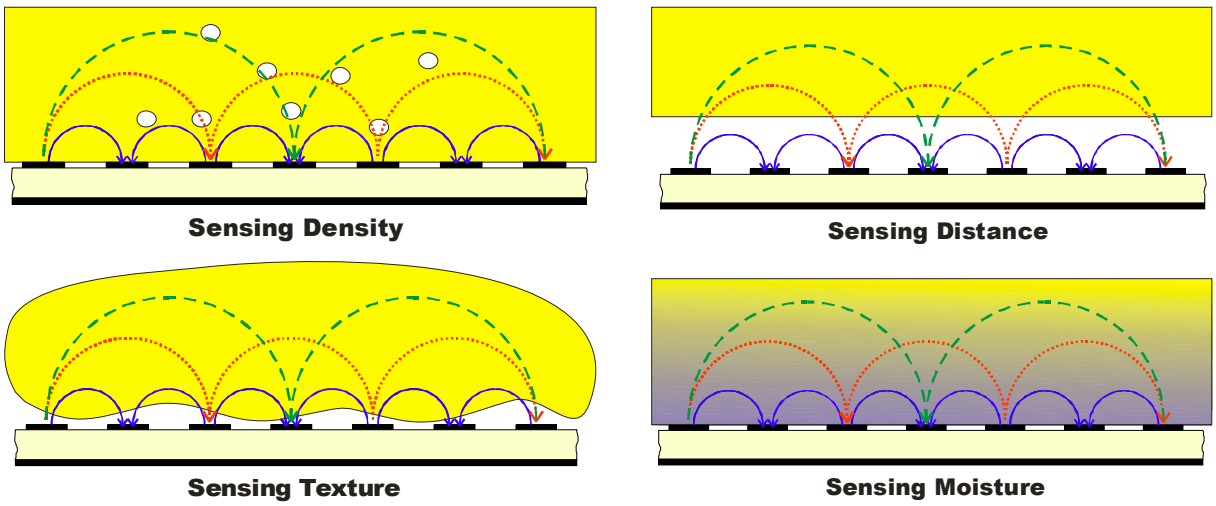

Figure 4.5: Sensing possibilities to detect various characteristic of samples [59]

4.2 Sensor Design and Fabrication

4.2.1 Design and Fabrication Process

All sensors were design using Altium Designer 6 software. Altium Designer 6.0 is a single, unified application that incorporates all technologies and capabilities necessary for unified electronic product development. The fabrication process of the sensors was done in Massey Mechatronics Laboratory. The final design of each sensor from the Altium Designer was printed in negative on a white paper and then was transferred into a special film.

The conducting layers of the board are typically made of thin copper foil. The insulating layers (dielectric) are typically laminated together with epoxy resin pre-impregnated. The film together with the board was exposed to the UV light. This process will impress and burn the desired sensor design onto the board. The printed circuit was developed. The printed circuit board was immersed into a special chemical for etching process to remove the unwanted copper, leaving only the desired copper trace. The sensor was cut to a desired design to make it suitable for testing.

4.2.2 Conventional Interdigital Sensors

Initial part of the research works were involving designed and fabricated of three conventional planar interdigital sensors. The initial goal is to understand how conventional interdigital sensor works and respond to materials. All three sensors were designed with different configurations, so that the difference of their response can be evaluated. Each sensor was designed to have same effective area of 5.00 mm by 5.00 mm but with different pitch lengths of 0.25 mm, 0.51 mm and 1.02 mm. The negative and positive electrodes have the same length of 4.75 mm and width of 0.25 mm. Figure 4.6 shows the representation of conventional interdigital sensor with configuration #1 (Din_10mil) and figure 4.7 shows the representation of conventional interdigital sensor with configuration #2 (Din_20mil) and configuration #3 (Din_40mil). Figure 4.8 shows the fabricated conventional interdigital sensors.

Table 4.1: Conventional interdigital sensor parameters

Sensor	Sensing area, (mm^2)	Pitch length, (mm)	Number of electrodes	
			Positive	Negative
Din_10mil	25	0.25	5	6
Din_20mil	25	0.51	4	4
Din_40mil	25	1.02	2	3

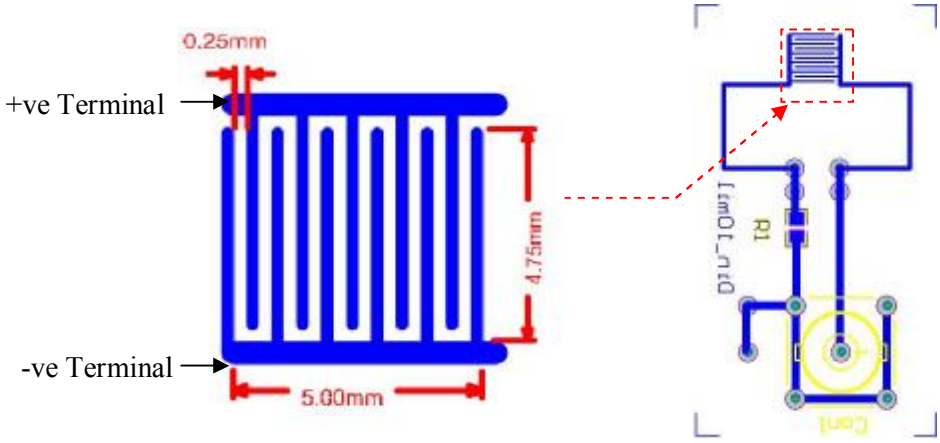

Figure 4.6: Representation of conventional interdigital sensor with configuration #1

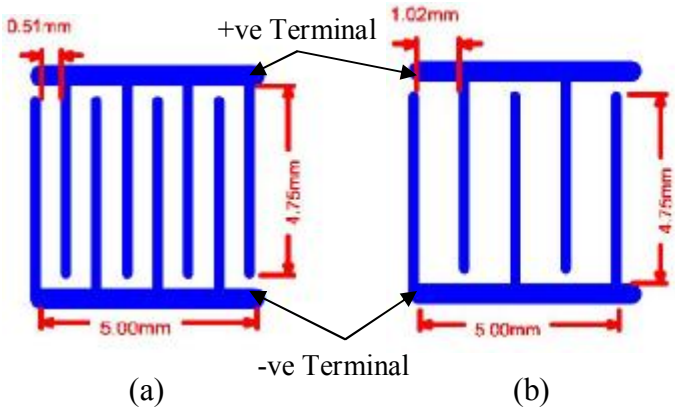

Figure 4.7: Conventional sensor with (a) Configuration #2 and (b) Configuration #3

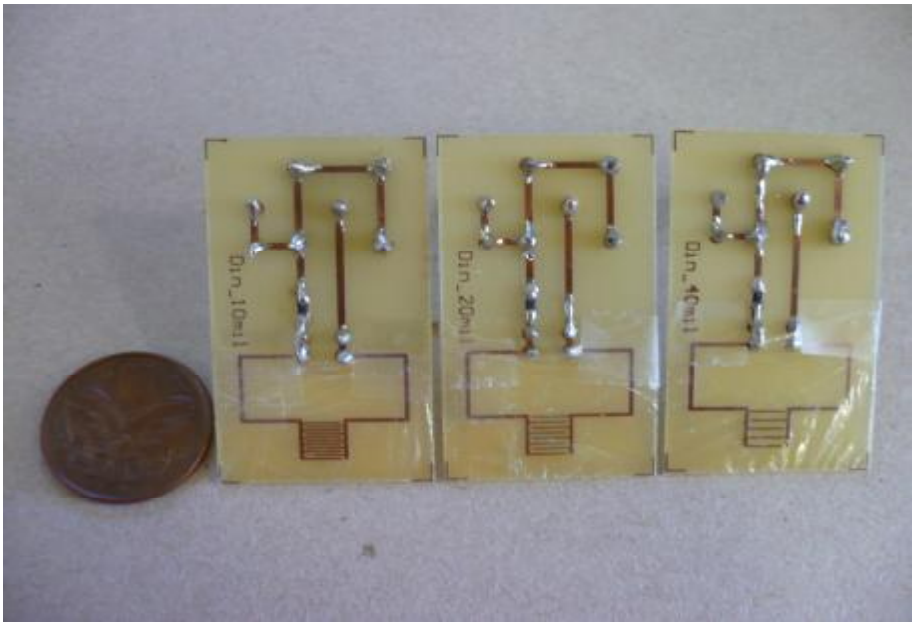

Figure 4.8: The fabricated conventional interdigital sensors compared to 20¢ New Zealand coin

4.2.3 Novel Planar Interdigital Sensors

Three types of novel interdigital sensors have been designed and fabricated. It is novel as we report this type of sensor at the first time. Each sensor has the same effective area of 4.75 mm by 5.00 mm and having pitch of 0.25 mm (5 mil). The positive and negative electrodes have the same length and width of 4.75 mm and 0.125 mm respectively. This is the smallest design that we can fabricate in our laboratory. As for this research work, we have used these 5 mil sensors design.

All sensors were designed to have equal numbers of electrodes. The only parameter changing in the sensor design is the *d*, spacing between two adjacent positive and negative electrodes between which the electric field-lines exist. Sensor_1 was designed to have two positive electrodes at each end separated by eleven negative electrodes. Sensor_2 and Sensor_3 were designed with the same dimensions but with different configurations. Sensor_2 has five negative electrodes between two positive electrodes and have the same pitch like Sensor_1. Sensor_3 has three negative electrodes between two positive electrodes. Figure 4.9 shows the representation of sensor configuration #1 (Sensor_1). Figure 4.10 shows sensor configuration #2 (Sensor_2) and sensor configuration #3 (Sensor_3). The fabricated novel interdigital sensors are shown in figure 4.11.

Table 4.2: Novel interdigital sensor parameters

Sensor	Sensing area, (mm^2)	Pitch length, (mm)	Number of electrodes	
			Positive	Negative
Din_10mil	23.75	0.125	2	11
Din_20mil	23.75	0.125	3	10
Din_40mil	23.75	0.125	4	9

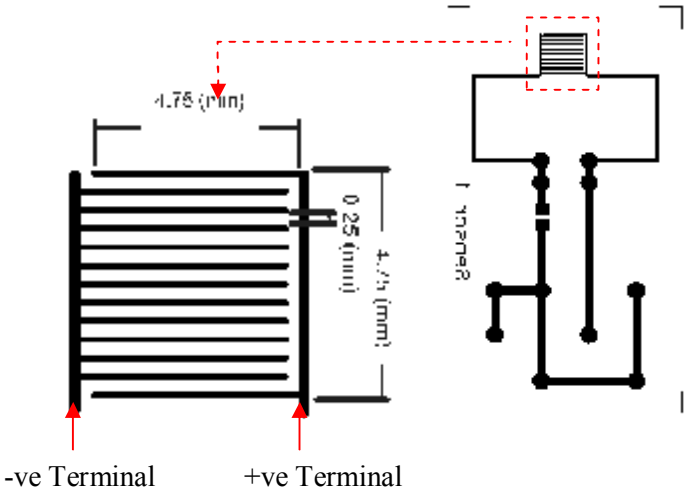

Figure 4.9: Representation of Sensor_1 configuration

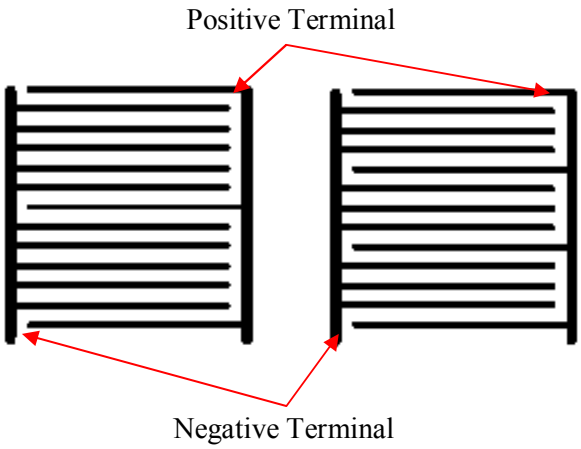

Figure 4.10: Sensor_2 and Sensor_3 with different configurations

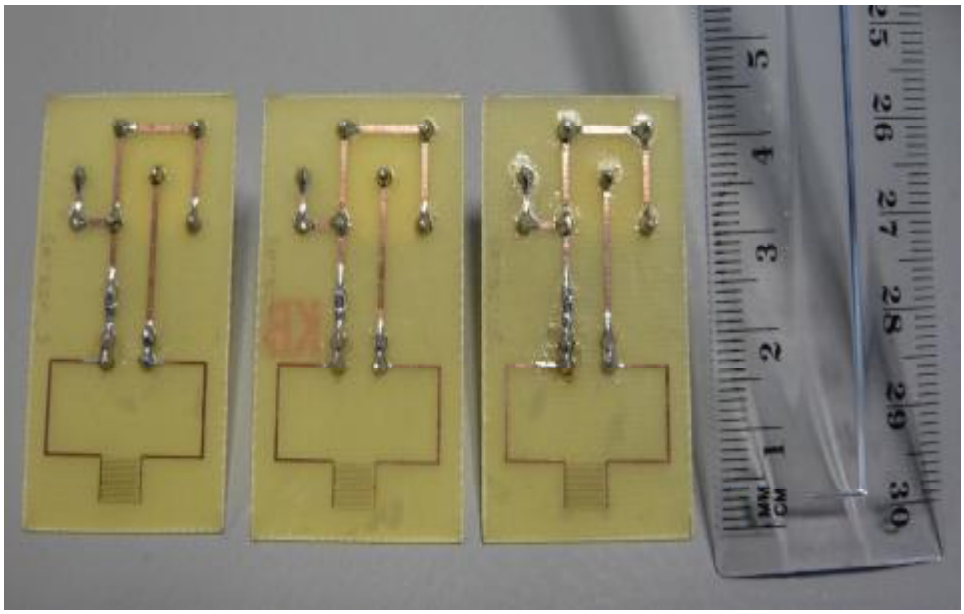

Figure 4.11: The fabricated novel interdigital sensors

4.3 Conclusions

The operating principles and the characteristic of planar interdigital sensors have been discussed in details. Three types of conventional interdigital sensors and three types of novel interdigital sensors have been designed and fabricated. The Altium Designer 6 software was used to design the sensors and all sensors were fabricated in Massey laboratory. The novel interdigital sensors were designed to have optimum number of negative electrodes which to increase the sensor sensitivity. The novel interdigital sensors were designed to have the same effective area but different in sensor configurations.

Chapter 5

Theoretical and Field Analysis

5.1 Introduction

Theory and analysis of fabricated sensors will be discussed in this chapter. As being mentioned in Chapter 4 of the thesis, planar interdigital sensor follows the same operating principle of two parallel plate capacitors. Figure 5.1 shows the representation of the equivalent circuit diagram for the interdigital sensor. An excitation dc voltage source (ac signal) was applied to the sensor (V_{in}). The electric field will be created by the sensor in the system under test. The voltage (sensing voltage, V_s) across the series resistance (R_s) is observed, to measure the current (I_s) flowing to the sensor. The selection of R_s value depends on the measured current flow (I_s) and the phase different between excitation signal and sensing signal measured from the oscilloscope. The chosen R_s should produce a good sensing voltage (V_s) as well as to give better phase different which is close to 90°, so that the real part of the circuit can be neglected.

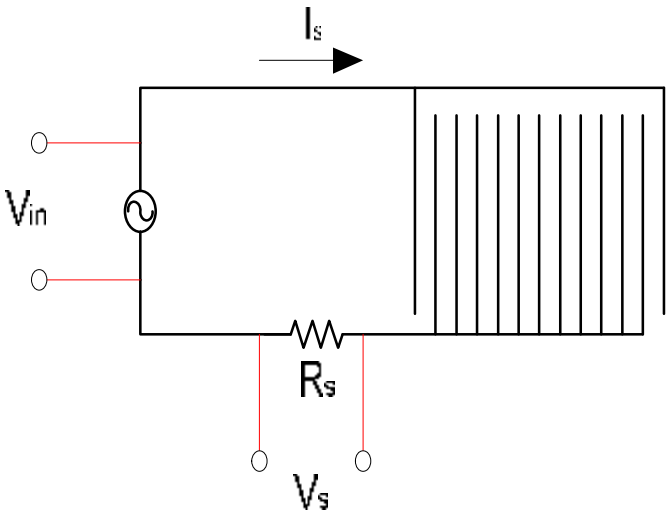

Figure 5.1: Equivalent circuit diagram of interdigital sensor

The experimental set up as shown in figure 5.2 was used to carry out to get the measurement data of excitation and sensing parameters, impedance and capacitance value from each sensor. Agilent function wave generator was used to generate an excitation voltage 10 Vpp (voltage peak to peak) with frequency of 10 kHz. The operating frequency of 10 kHz was chosen for the experiments because it produced a good sensor output voltage (Vs) and also the frequency of 10 kHz can be easily generated by a microcontroller for a low cost sensing system (see Chapter 7 for details). Agilent signal oscilloscope was used to observe the waveforms and to measure the phase different between excitation signal and sensing signal. Measurement data of excitation and sensing parameters, impedance and capacitance value from each sensor were calculated. The capacitance of parallel plate capacitor can be calculated from (1).

$$C = \frac{\varepsilon_0 \varepsilon_r A}{d} \tag{1}$$

where

C = capacitance in farads, F

ε_0 = the permittivity of free space (ε_0 = 8.854x10-12 F/m)

ε_r = the relative static permittivity or dielectric constant (vacuum = 1)

A = effective area, square meters

d = effective spacing, meters

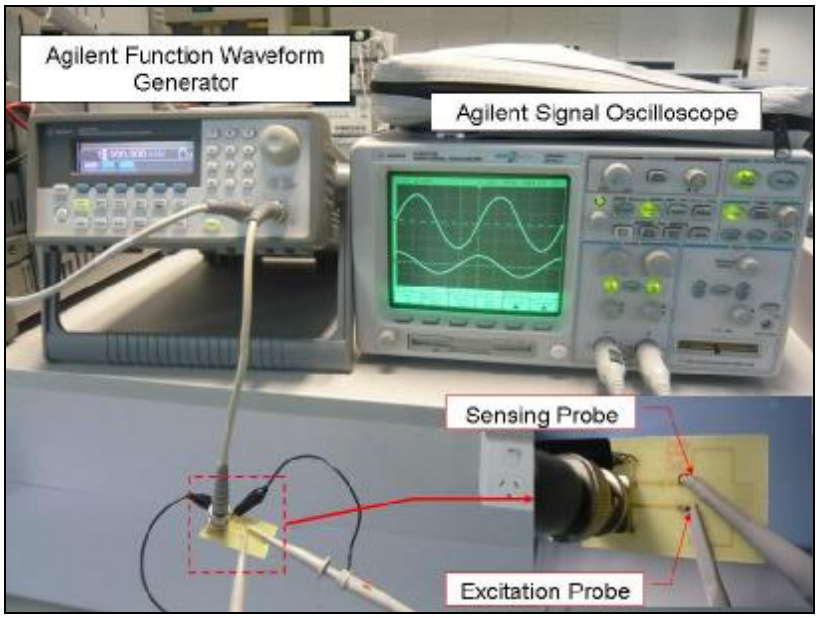

Figure 5.2: Experiment setup for sensor analysis

The sensor impedance can be calculated by;

$$Z = \frac{V_{in}}{I_s} = \frac{V_{in}}{V_s / R_s}$$

$$Z = \frac{V_{in}}{V_s} * R_s \qquad (2)$$

V_{in} : Voltage across the sensor

V_s : Voltage across the series of resistor, *Rs*

I_s : The current flowing through the sensor

Both the magnitude and the phase of the sensor impedance are measured. The real part (*R*) and the imaginary part (capacitive reactance, Xc) is given by;

$$R = Z\cos\theta \qquad (3)$$

$$X_c = Z\sin\theta \qquad (4)$$

Since the phase angle, θ measured was close to 90°, so the real part of the sensor impedance (*R-Rs*), is very small compared to the imaginary part (capacitive reactance). The real part has not been considered for estimation of system properties. Moreover, the change of real part with sample is really negligible. Therefore, for interdigital sensor only capacitive reactance will be measured to evaluate the system properties. Capacitive reactance varies with frequency. As the frequency applied to the capacitor increase, its reactance decreases and as the frequency decrease its reactance increases. This is because the electrons in the form of an electrical charge on the capacitor electrodes, pass from one electrode to the other more rapidly with respect to the varying frequency. As the frequency increases, the capacitor passes more charge across the electrodes in a given time resulting in a greater current flow through the capacitor appearing as if the internal resistance of the capacitor has decreased. Therefore, a capacitor connected in an AC circuit can be said to be "Frequency Dependant". The characteristic of impedance for interdigital sensor is shown in figure 5.3.

Capacitive Reactance has the electrical symbol "Xc" and has units measured in Ohms the same as resistance, (R). It is calculated using the following formula:

$$X_C = \frac{1}{2\pi fC} \tag{5}$$

From equation (5) the effective capacitance can be calculated by;

$$C = \frac{1}{2\pi fX_c} \tag{6}$$

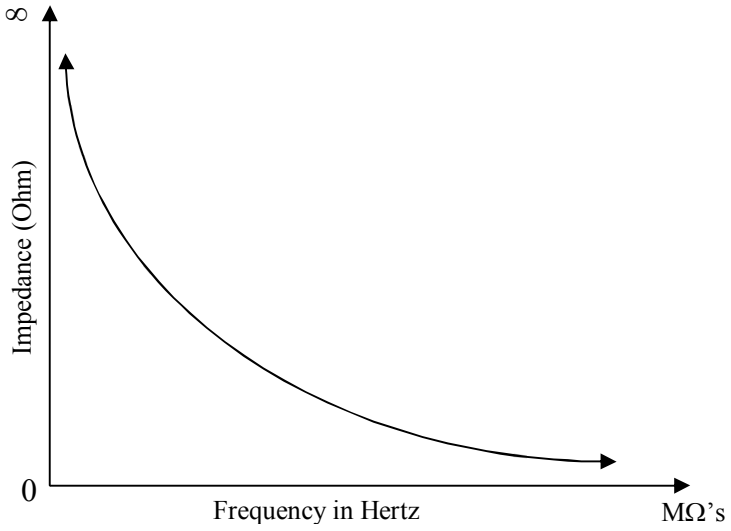

Figure 5.3: Impedance characteristic of interdigital sensor

5.2 Analysis of Conventional Sensors

5.2.1 The Equivalent Circuit for Conventional Sensors

The equivalent circuit for conventional interdigital sensor is shown in figure 5.4 (a), (b) and (c). Equation (1) can be used to analyse the capacitance within each sensor geometry. The conventional sensors design have different area, *A* and *d*, spacing. Their total capacitance (C_{eq}) is given by;

$$C_{eq} = C_1 + C_2 + ... + C_n \tag{7}$$

where, $C_1 = C_2 = C_3 = ...C_n$

Since in the design parameter *A* and *d* are different, therefore equation (6) only valid for each sensor configuration. This is because the value of C_1 for sensor configuration #1 is not the same as C_1 for sensor configuration #2 and configuration #3.

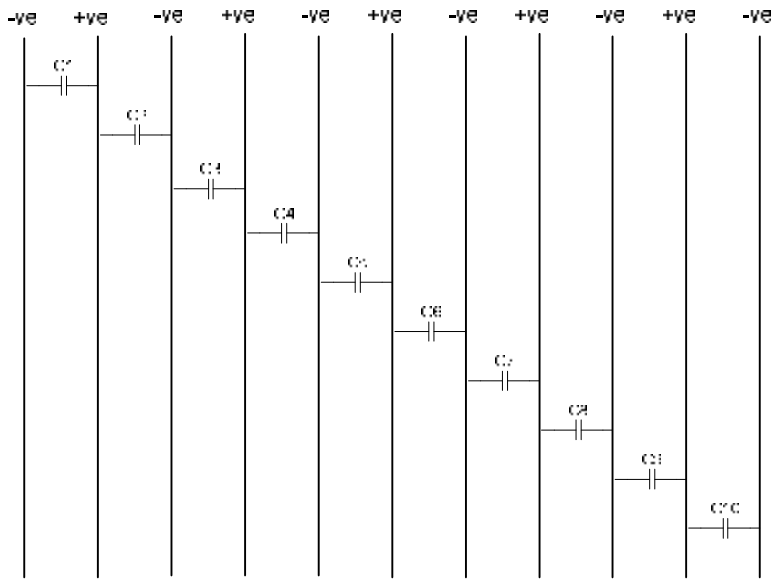

(a)

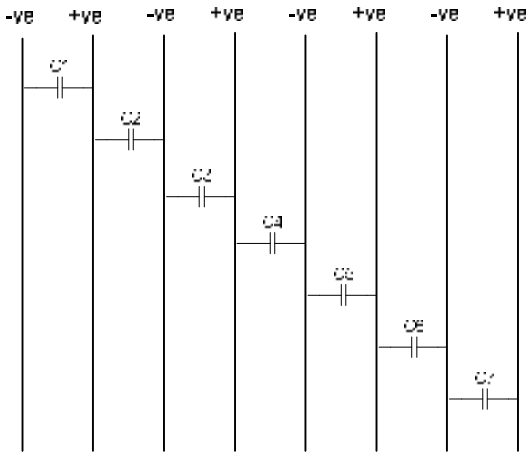

(b)

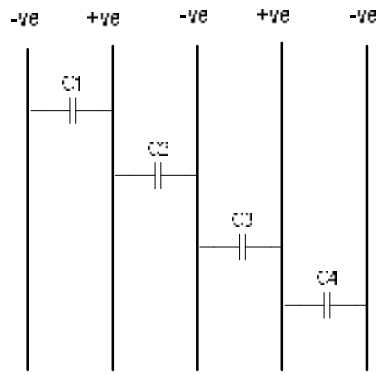

(c)

Figure 5.4: Equivalent circuit of conventional interdigital sensor (a) configuration #1 (b) configuration #2 and (c) configuration #3

5.2.2 Circuit Analysis

All sensors were connected with a series surface mount resistor to measure the current through the sensor. An excitation voltage of 10 Vpp with 10 kHz was applied to the circuit. A series of surface mount resistor of 47 kΩ was placed. Although the sensing voltage was reasonably high (about 350 mV), but the phase difference observed from the oscilloscope was 75°. This resistor was then replaced with 82 kΩ. The phase different was 81° which is close to 90°. The value of resistor of 82 kΩ was selected for the conventional interdigital sensors. Figure 5.5, 5.6 and 5.7 shows the signal waveforms of excitation voltage and sensing voltage available for all sensors. Table 5.1 shows all parameters calculated from the circuit analysis.

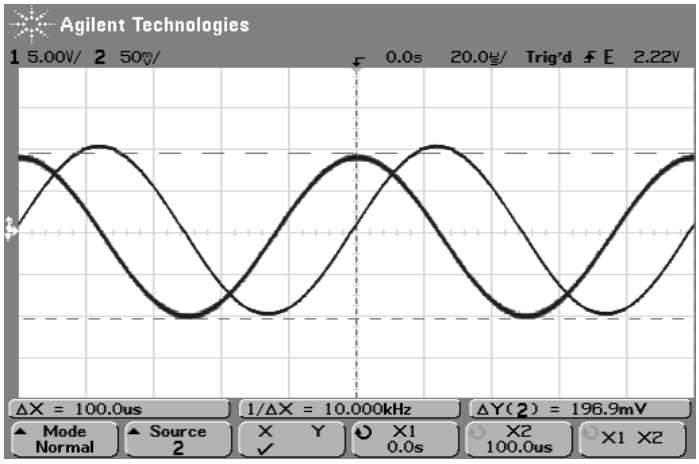

Figure 5.5: Signal waveform of sensor with configuration #1 (Din_10mil)

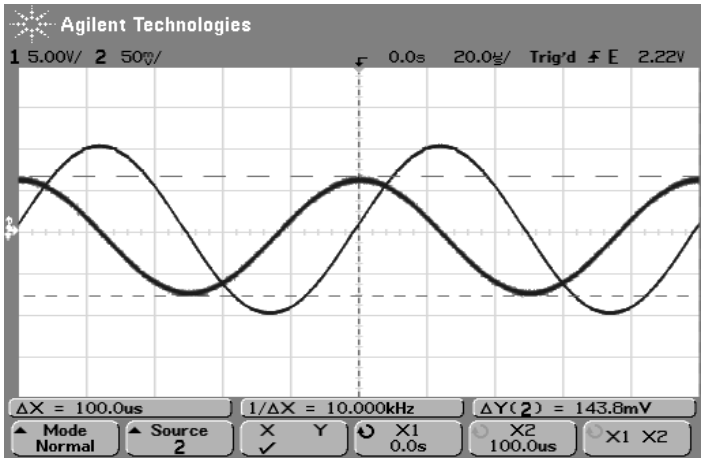

Figure 5.6: Signal waveform of sensor with configuration #2 (Din_20mil)

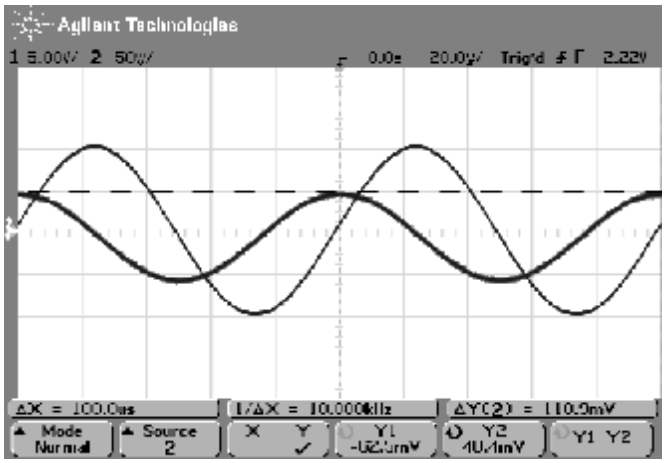

Figure 5.7: Signal waveform of sensor with configuration #3 (Din_40mil)

Table 5.1: Relationship between excitation voltage, sensing voltage, current, impedance and capacitance for each conventional sensor

Sensor Type	Excitation Parameters		Sensing Parameters			Impedance (MΩ)	Capacitance (pF)
	V_{in} (V)	Freq (kHz)	V_S (mV)	Phase Angle	I_S (mA)		
Din_10mil	10.0	10.0	196.9	81.0	2.401	4.165	3.821
Din_20mil	10.0	10.0	143.8	81.0	1.754	5.702	2.791
Din_40mil	10.0	10.0	110.9	81.0	1.352	7.394	2.152

The impedance characteristic of the fabricated conventional sensors was observed by varying the frequency from 200 Hz – 30 kHz. The impedance characteristic for conventional interdigital sensor is shown in figure 5.8. The phase difference of conventional sensors was also observed. It is shown from figure 5.9 that at the frequency of 10 kHz, all three

conventional sensors have better phase difference of 81°. Which was good as it was close to 90° phase difference.

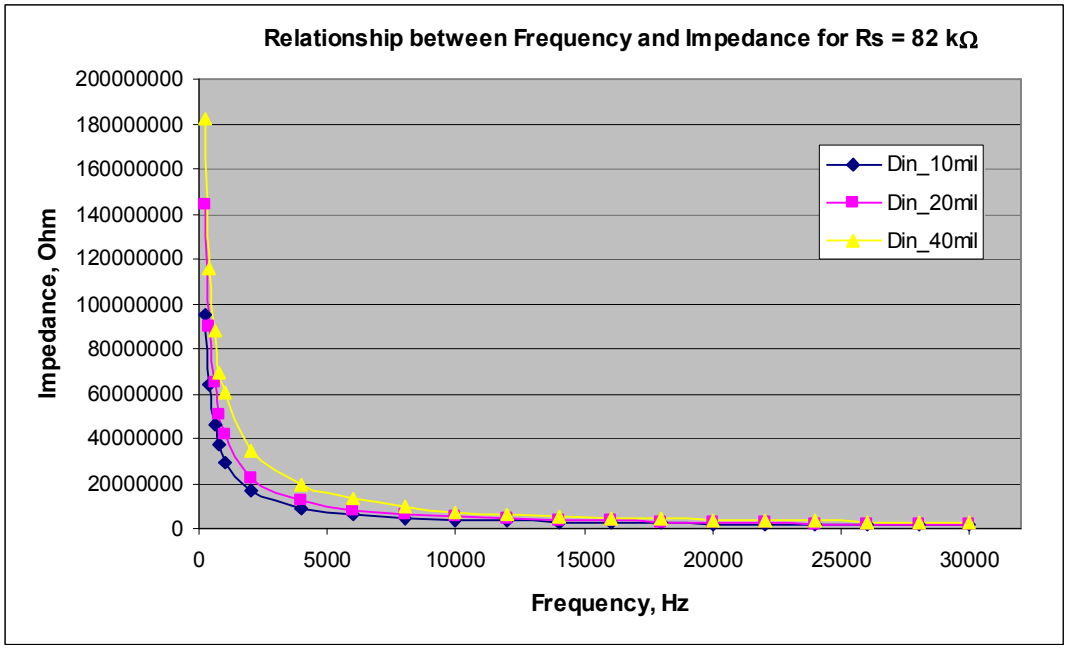

Figure 5.8: Impedance characteristic of conventional interdigital sensor

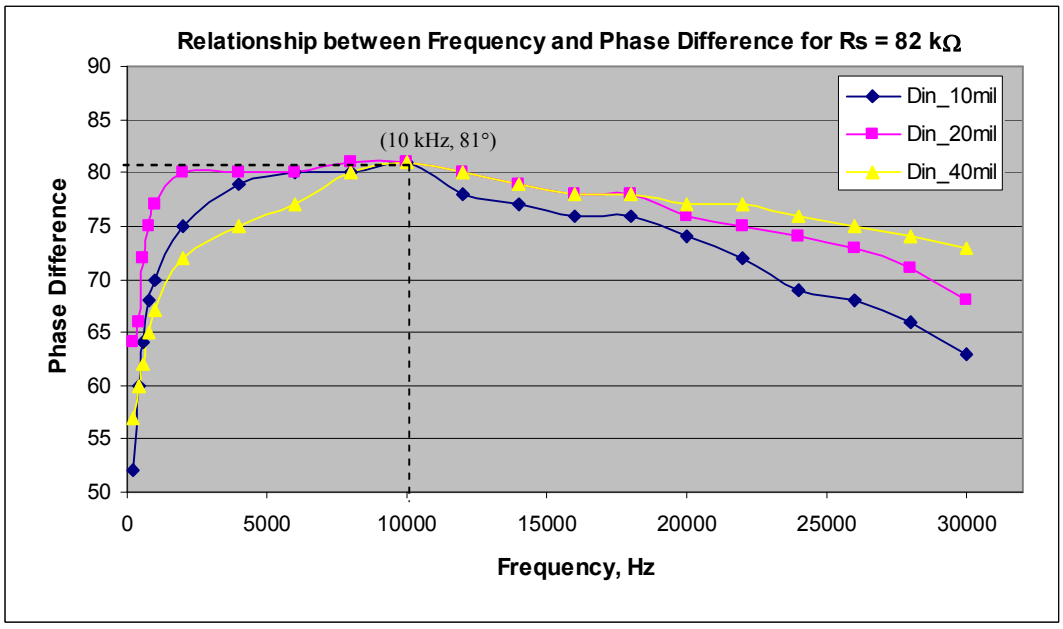

Figure 5.9: Phase difference characteristic of conventional interdigital sensor

Conventional interdigital sensor with configuration #3 is better than configuration #1 and configuration #2. This is because it has higher capacitive reactance value that will give better sensing performance. In term of electric field strength, the sensor with configuration #3 has greater penetration depth since the pitch length is wider. But in the design, it has big air gap between positive and negative electrodes which will increase the fluctuation of voltage air for calibration. This will affect the sensor performance for rapid analysis. The sensor will have better performance if we can increase the number negative electrodes in between the positive electrodes. This is how the novel interdigital sensors were designed and fabricated.

5.3 Analysis for Novel Interdigital Sensors

5.3.1 The Equivalent Circuit for Novel Sensors

The equation (1) can be used to calculate the capacitance of a planar type capacitor by introducing two factors, one for change of distance, 'd' and another for change of area, 'A'. It is important during the sensor design stage, to estimate the equivalent capacitance within each sensor geometry. The equivalent representation for each sensor geometry is shown in figure 5.10 (a), (b) and (c). Each sensor was analysed for the optimum number of negative electrodes within sensor geometry. Since the sensors have the same area and electrodes spacing, therefore it is easy to evaluate the capacitance through each sensor geometry.

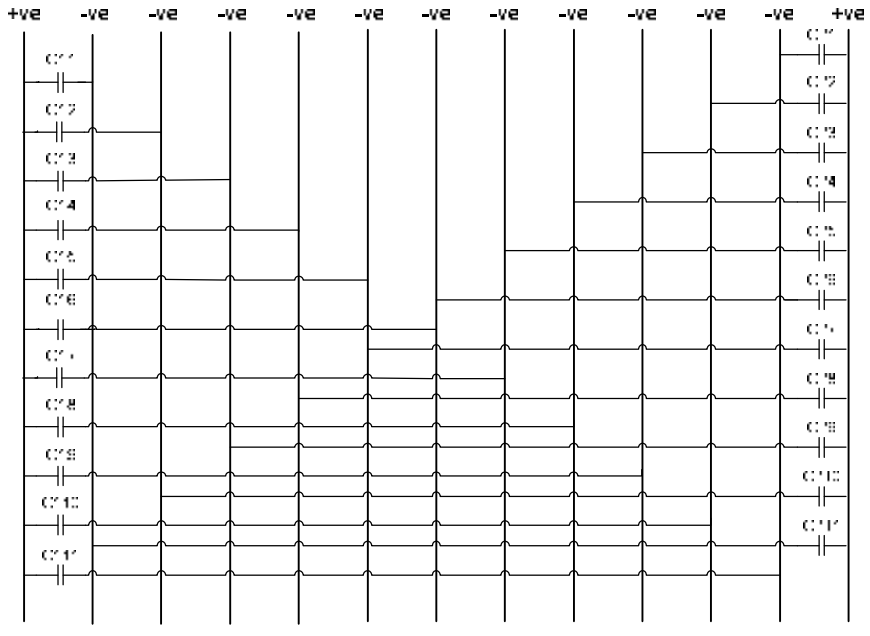

(a)

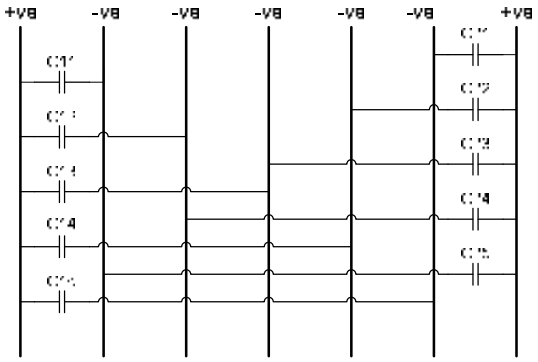

(b)

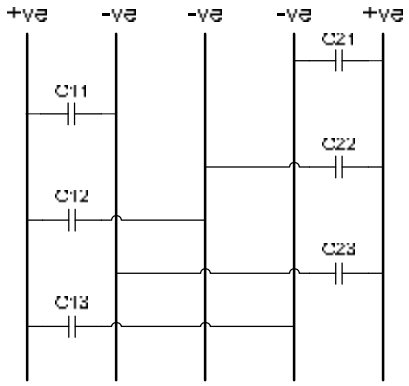

(c)

Figure 5.10: The equivalent representation of different sensors; (a) Sensor_1 with electrodes configuration 1-11-1 (b) Sensor_2 with electrodes configuration 1-5-1-5-1 and (c) Sensor_3 with electrodes configuration 1-3-1-3-1-3-1

The capacitance is a function of distance between positive and negative electrodes. So, we can write

$$C_{12} = \frac{1}{2}C_{11}; \ldots C_{1n} = \frac{1}{n}C_{11}$$

$$\text{and } C_{22} = \frac{1}{2}C_{21}; \ldots C_{2n} = \frac{1}{n}C_{21} \tag{8}$$

where; $C_{11} = C_{21}$

The capacitance C_{11} of figure 5.10(a) will have different value of C_{11} in figures 5.10(b) and 5.10(c) respectively. The estimated capacitance within each sensor geometry as a function of distance is shown in figure 5.11. It is seen that Sensor_1 has better uniformity of equivalent capacitance compare to Sensor_2 and Sensor_3. This uniformity is very important for achieving largest sensitivity of measurement.

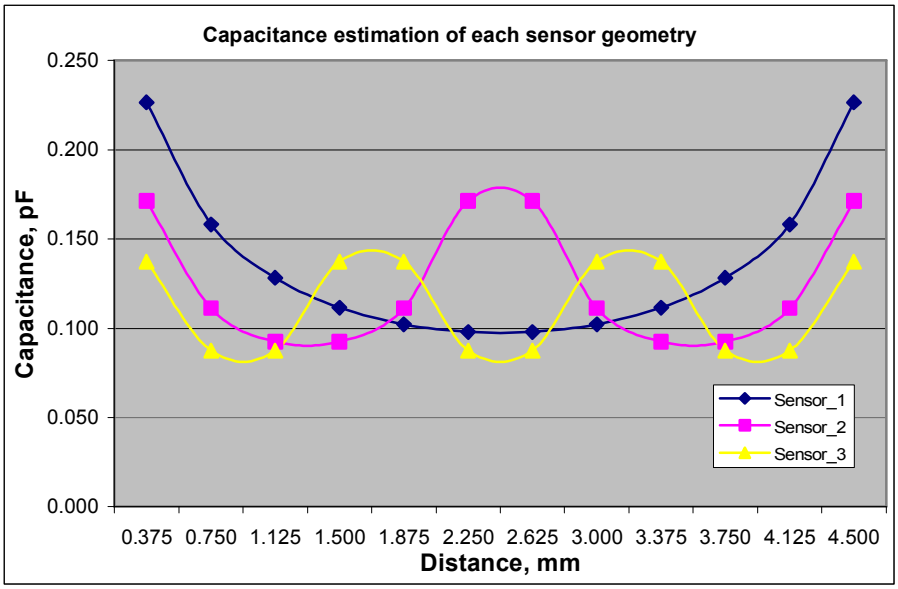

Figure 5.11: Variation of equivalent capacitance within each sensor geometry

5.3.2 Circuit Analysis

Sensor was connected in series surface mounted resistor to measure the current through the sensor. The initial resistor value selected was 82 kΩ. But this resistor value did not produce good phase different which is close to 90°. The final value of the resistor selected for the novel interdigital sensor was 120 kΩ with a phase difference of 83°. Figure 5.12, 5.13 and 5.14 shows the signal waveforms of excitation voltage and sensing voltage available for all sensors. Table 5.2 shows all parameters calculated from the circuit analysis.

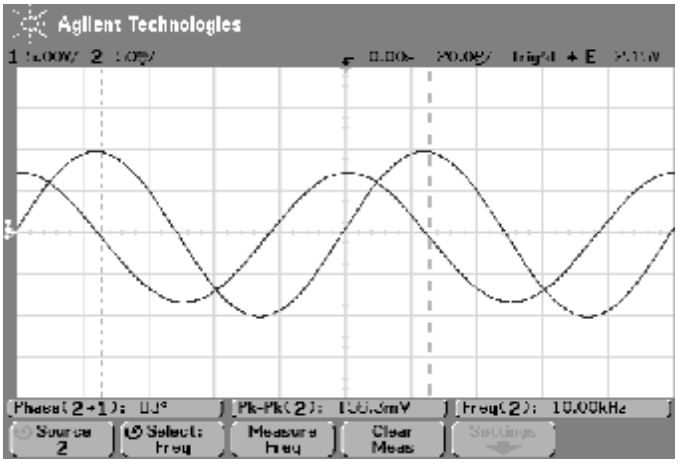

Figure 5.12: The signal waveform of Sensor_1

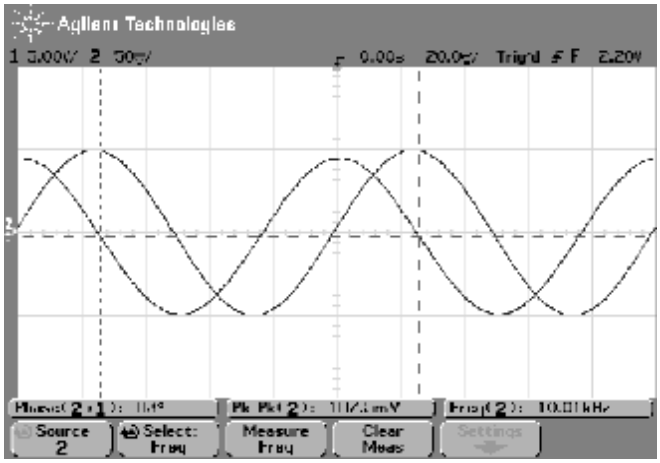

Figure 5.13: Signal waveform of Sensor_2

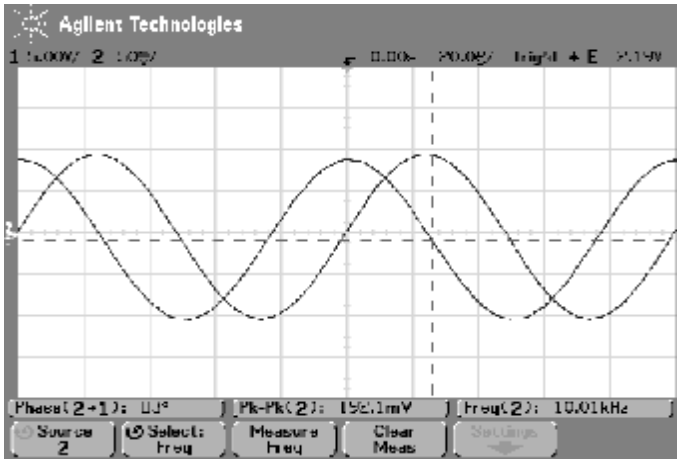

Figure 5.14: Signal waveform of Sensor_3

Table 5.2: Relationship between excitation voltage, sensing voltage, current, impedance and capacitance for novel sensors

Sensor Type	Excitation Parameters		Sensing Parameters			Impedance (MΩ)	Capacitance (pF)
	V_{in} (V)	Freq (kHz)	V_S (mV)	Phase Angle	I_S (mA)		
Sensor_1	10.0	10.0	156.3	83.0	1.303	7.678	2.072
Sensor_2	10.0	10.0	187.5	83.0	1.563	6.400	2.486
Sensor_3	10.0	10.0	192.1	83.0	1.601	6.247	2.547

The impedance characteristic of the fabricated novel interdigital sensors was observed by varying the frequency from 200 Hz – 30 kHz. The impedance characteristic for novel interdigital sensor is shown in figure 5.15. The phase difference of novel sensors was also observed. It is shown from figure 5.16 that at the frequency of 10 kHz, all three novel sensors have the same phase difference of 83° (close to 90° phase difference). Although it is shown that Sensor_2 and Sensor_3 have better phase difference at the frequency between 2 kHz – 8 kHz, but the frequency of 10 kHz was chosen as it gave the same phase difference (83°) with better voltage output (Vs).

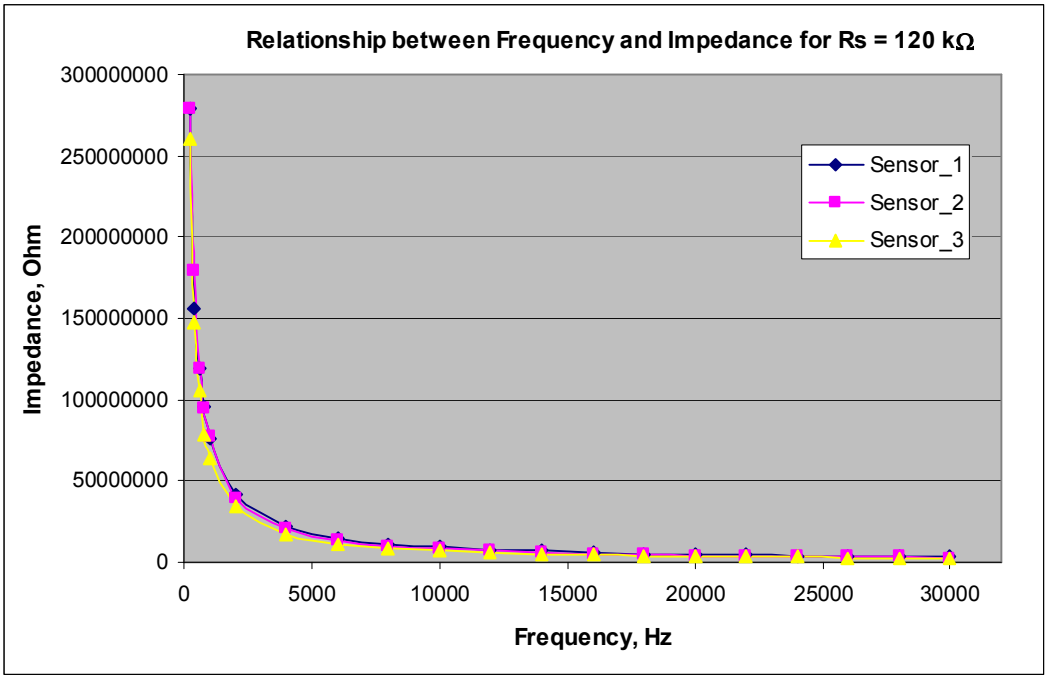

Figure 5.15: Impedance characteristic of novel interdigital sensor

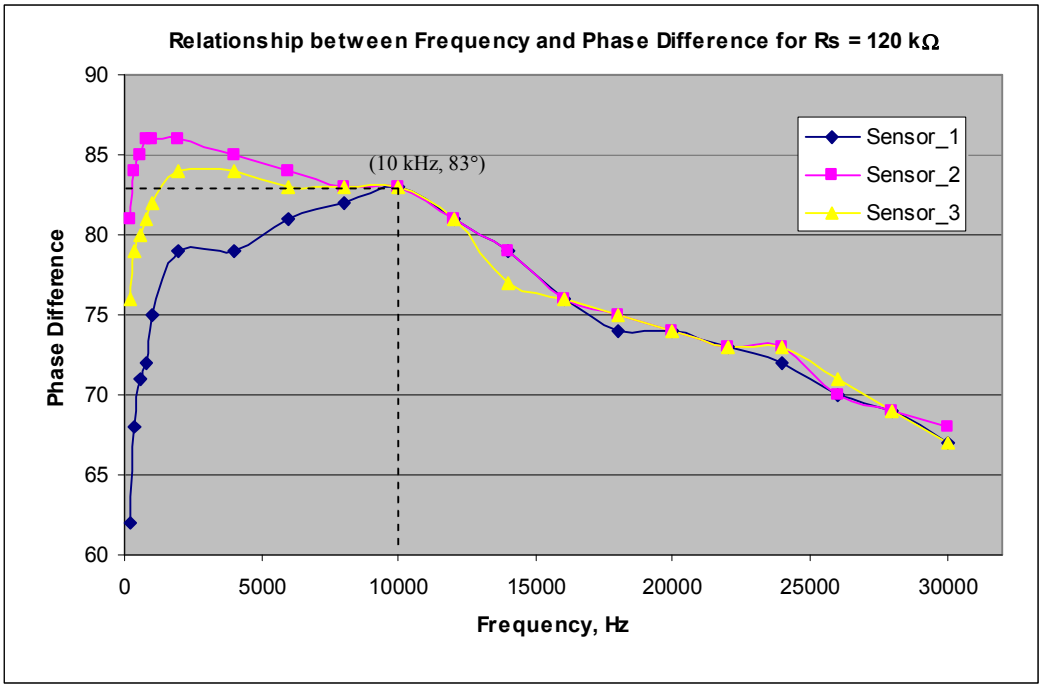

Figure 5.16: Phase difference characteristic of conventional interdigital sensor

Results from the circuit analysis have shown that novel interdigital sensors have better performance compared to the conventional interdigital sensors. Among these novel interdigital sensors, Sensor_1 will have largest sensitivity measurement since has better uniformity of equivalent capacitance within sensor geometry.

5.4 Modelling using COMSOL Multiphysics

The COMSOL Multiphysics® (formerly FEMLAB) is a finite element analysis and solver software package for various physics and engineering applications, especially coupled phenomena, or multiphysics. The software simulation environment facilitates all steps in the modelling process - defining your geometry, specifying your physics, meshing, solving and then post-processing your results. All sensors were modelled using this software to observe and to simulate the sensor performance. This simulation results is very important to design a better sensor with excellent sensing performance.

All sensors were modelled to analyse the distribution of electric field. The purpose of doing modelling is to get the simulation results of electric field distributions, electric field intensity and the estimation of capacitance for each sensor and their sensitivity. All figures for sensors modelling are in xyz axis and yz axis. The xyz axis will show clearly the arrangement

of positive electrodes (red) and negatives electrodes (blue) in the sensors design with electric field distribution between them. The yz axis will show the magnitude of electric field strength from positive electrodes to negative electrodes. The capacitance of the sensor can be calculated by;

$$C = \frac{2W_e}{V_0^2} \tag{9}$$

where W_e is the stored electrical energy and V_0 is the applied voltage.

The value for electrical energy density, W_e can be obtained from the simulation. Variation of electric field intensity with respect to depth can be analysed for each sensor designed. Electric field intensity is a measurement of electric field, norm (V/m) along the z-axis. The cross-section line data were set starting from coordinate X_0=2.75 mm, Y_0= 0 mm, Z_0= 0.125 mm and X_1=2.75 mm, Y_1=4.75 mm, Z_1=0.125 mm. The coordinate of Z_0 and Z_1 were replaced from 0.125 mm to 3.50 mm. Figure 5.17 shows how the measurement of electric field intensity can be modelled using COMSOL Multiphysics.

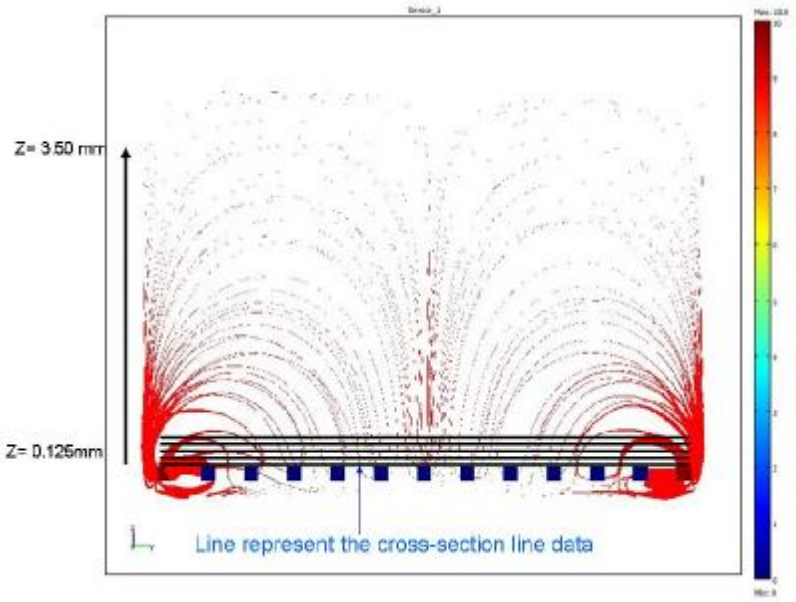

Figure 5.17: Measurement of electric field intensity

5.4.1 Modelling for Conventional Sensors

All three conventional sensors were modelled and analysed using COMSOL. Figure 5.18, 5.19 and 5.20 shows the simulation results of each conventional sensor. Sensor with configuration #1 has higher magnitude of electric field strength at neighbouring electrodes since it has more numbers of positive electrodes and shorter wavelength (λ), but lower in penetration depth. As for sensor with configuration #2 and configuration #3 have better penetration depth but lower in magnitude of electric field distribution at neighbouring electrodes. It is seemed that sensor with configuration #3 has better penetration depth compared to sensor of configuration #2.The average electric field intensity of conventional sensors is shown in figure 5.21. Table 5.3 shows the calculated capacitance value of each sensor measured from the simulation.

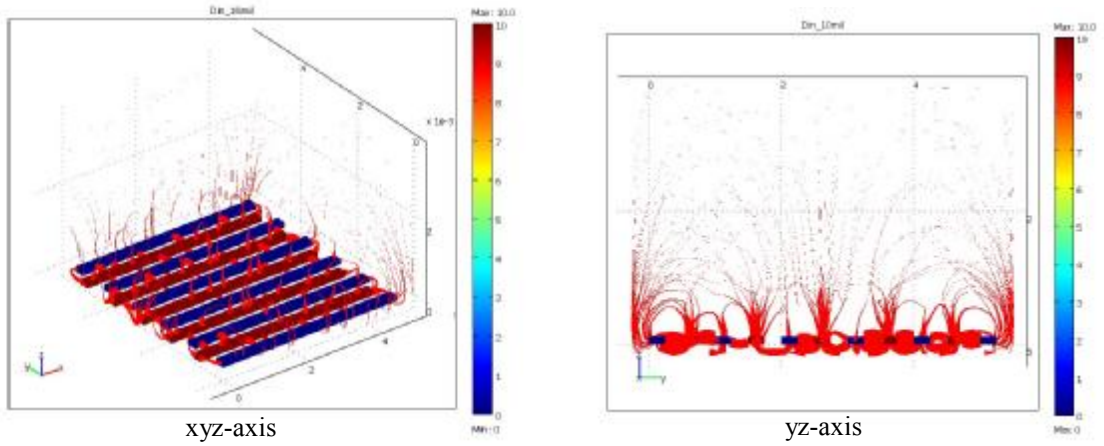

xyz-axis yz-axis

Figure 5.18: Electric field distribution of sensor configuration #1 (Din_10mil)

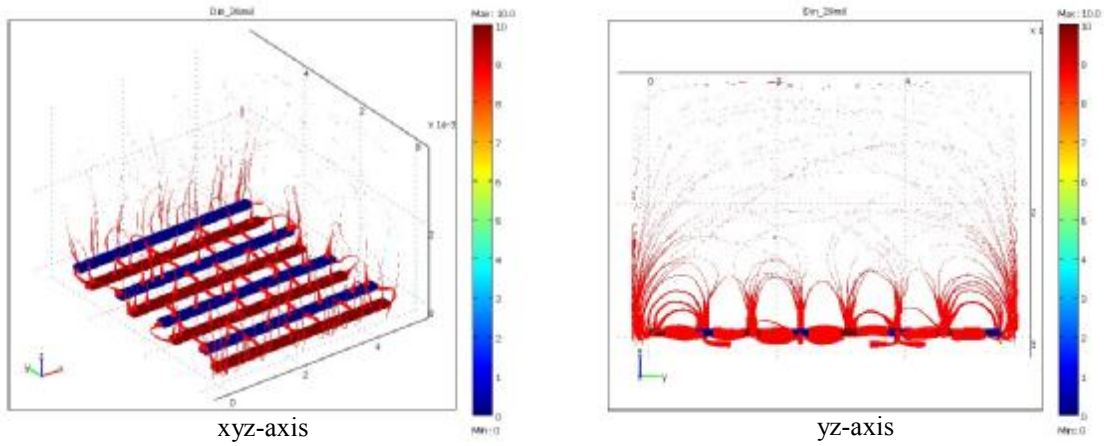

xyz-axis yz-axis

Figure 5.19: Electric field distribution of sensor configuration #2 (Din_20mil)

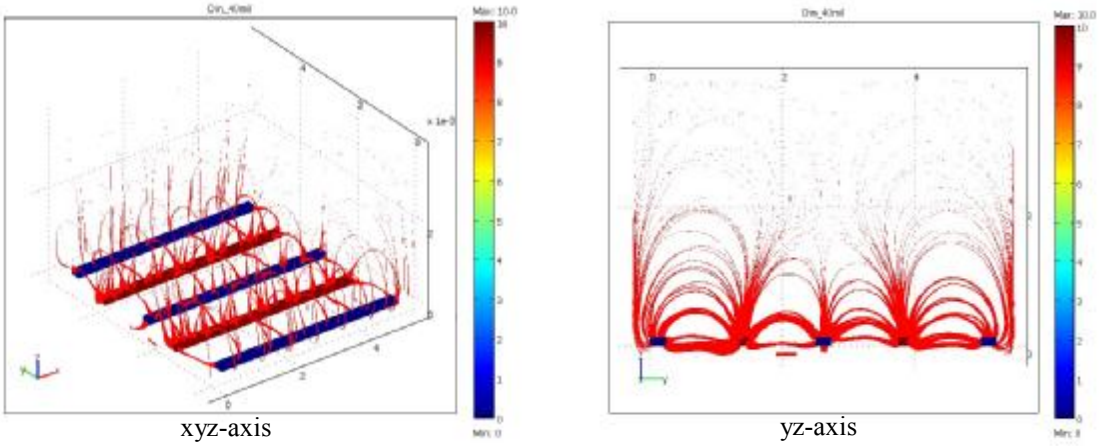

xyz-axis yz-axis

Figure 5.20: Electric field distribution of sensor configuration #3 (Din_40mil)

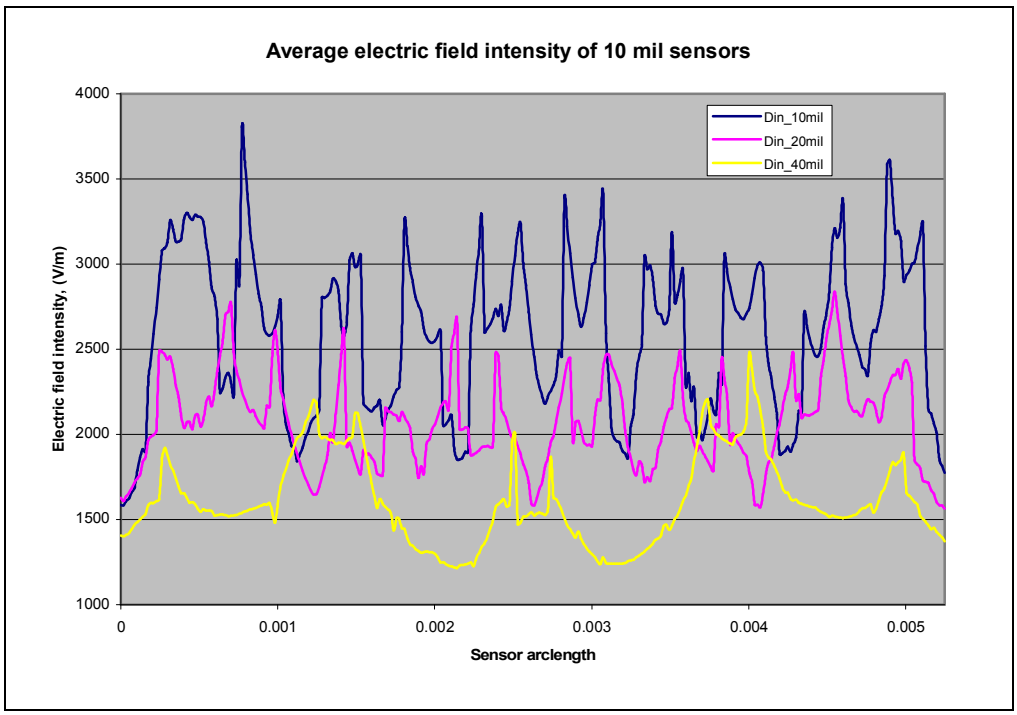

Figure 5.21: Electric field intensity of conventional sensors

Table 5.3: Capacitance calculated from the modelling using COMSOL for conventional sensors

Sensor Type	Simulation Parameters			Calculated Parameters
	V_0 (V)	Freq (kHz)	Electrical energy density (J)	Capacitance (pF)
Din_10mil	10.0	10.0	$3.2253x10^{-11}$	0.645
Din_20mil	10.0	10.0	$1.4684x10^{-11}$	0.294
Din_40mil	10.0	10.0	$5.7848x10^{-12}$	0.116

Results from the simulation have shown that sensor with configuration #3 has better penetration depth with uniform distribution of electric field strength. It is shown from the table that sensor with configuration #3 will generate higher capacitive reactance compare to other conventional sensors. It is seemed that sensor with configuration #3 has better sensitivity measurement for the conventional interdigital sensors. Therefore, results from the modelling have shown that conventional sensor with configuration #3 will has better sensing performance compare to sensor with configuration #1 and configuration # 2.

5.4.2 Modelling for Novel Sensors

All three novels sensors were modelling using the actual size (in mm). Result from the simulation is very important to support the analysis carried out from the circuit analysis. Simulation results for novel sensors are shown in figure 5.22, figure 5.23 and figure 5.24. As for Sensor_1 (figure 5.22), the magnitude of electric field strength is stronger at neighbouring electrodes but as it goes to the middle it becomes weak. The same things were observed from simulation result for Sensor_2 (figure 5.23) and Sensor_3 (figure 5.24) but with different electric field distribution pattern. The electric field strength becomes weak as the level of z-axis increases. This can be referred to the discussion on the sensor's pitch length and the penetration depth.

The electric field distribution for Sensor_1 is uniformly distributed compare to Sensor_2 and Sensor_3. This is because Sensor_1 has more number of negative electrodes in between positive electrodes. The average of electric field intensity is shown in figure 5.25. Sensor_1 has uniform average electric field intensity compared to other sensors. This uniformity will contribute to the better sensor sensitivity. Table 5.4 shows the calculated capacitance value of each sensor measured from the simulation. It was observed that the capacitance value obtained from the modelling is about 1/10 of the value obtained from the circuit analysis. This is because during the modelling, the voltage source (excitation voltage) used is a dc signal where else for the circuit analysis the voltage source used is an ac signal. From the table, Sensor_1 has higher capacitive reactance value compare to other sensors. This indicates that Sensor_1 will have better sensitivity measurement compared to Sensor_2 and Sensor_3. Results of modelling using COMSOL have shown that Sensor_1 will have better sensing performance for the novel interdigital sensors designed.

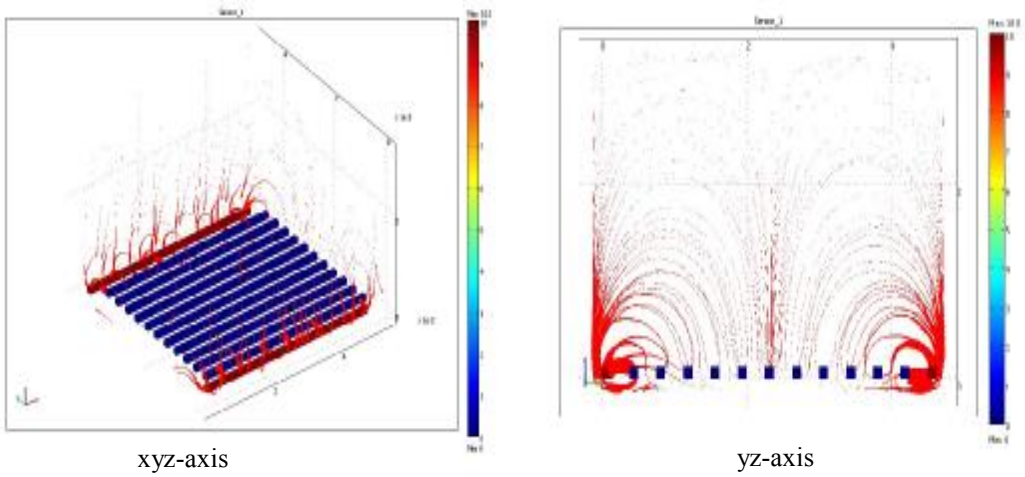

xyz-axis yz-axis

Figure 5.22: Electric field distribution of Sensor_1

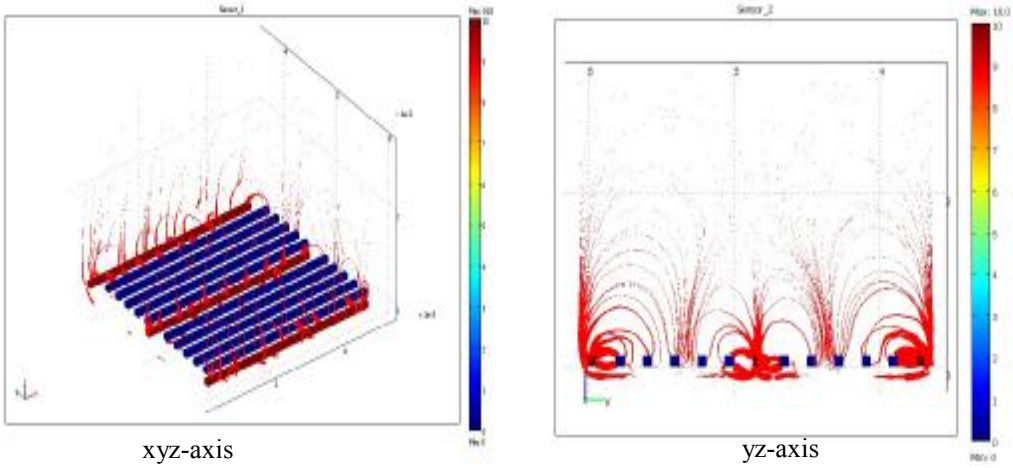

xyz-axis yz-axis

Figure 5.23: Electric field distribution of Sensor_2

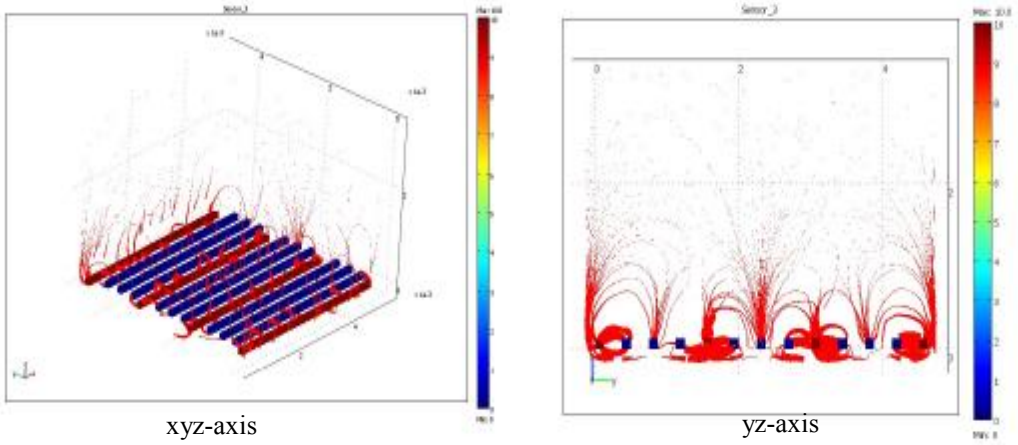

xyz-axis yz-axis

Figure 5.24: Electric field distribution of Sensor_3

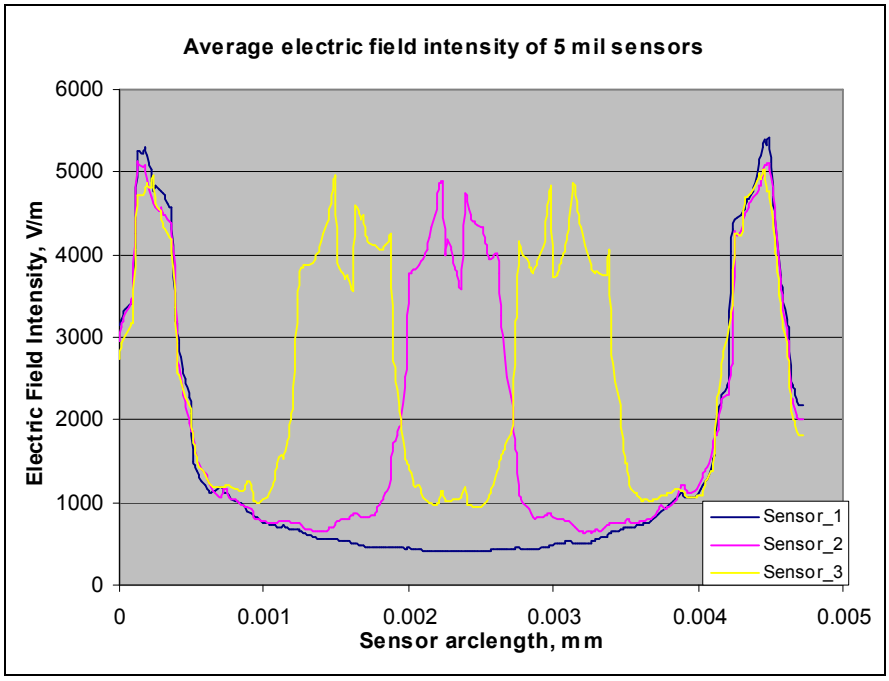

Figure 5.25: Electric field intensity of novel sensor

Table 5.4: Capacitance calculated from the modelling using COMSOL for novel sensors

Sensor Type	Simulation Parameters			Calculated Parameters
	V_0 (V)	Freq (kHz)	Electrical energy density (J)	Capacitance (pF)
Sensor_1	10.0	10.0	$7.5016x10^{-12}$	0.150
Sensor_2	10.0	10.0	$1.3823x10^{-12}$	0.276
Sensor_3	10.0	10.0	$1.9891x10^{-11}$	0.398

5.5 Conclusion

Theoretical and field analysis has been discussed in this chapter. An excitation voltage (V_{in}) of 10 Vpp with operating frequency of 10 kHz were chosen for the experiments. These values were chosen as they produced a good sensing voltage (V_s) for a selected series of surface mounted resistor (R_s). It was observed from the circuit analysis and simulation results, the novel interdigital sensors will have better sensitivity measurement compared to conventional sensors. It is also shown from the analysis that the optimum number of negative electrodes will contribute to better sensing performance. This is because from the analysis, the number of negative electrode can be used to minimise the air gap between positive electrodes as well as giving a good penetration depth, better uniformity in term of capacitance estimation, electric field distribution and average electric field intensity. The novel sensors were designed to have these characteristics. Both results from the circuit analysis and modelling using COMSOL Multiphysics have shown that Sensor_1 will have better sensitivity measurement compared to other novel sensors.

Chapter 6

Experimental Results and Discussions

6.1 Introduction

Chapter 6 will discuss on the experimental setup, measurement method, experimental procedures, experimental results and discussions which will include the experiments conducted for the initial studies using three chemicals, experiments with seafood products, experiments of proline with mussels and experiments of DA with mussels. This chapter also explains how samples were prepared for the experiments. The fabricated conventional interdigital sensors and novel interdigital sensors were tested to observe and to analyse their performance.

6.2 Experimental Setup and Measurement Method

The experimental set up as shown in figure 6.1 was constructed. A frequency of 10 kHz with 10 Vpp (voltage peak-to-peak) was applied to the sensor using Agilent Function Waveform Generator. DC power supply was used to supply voltage for microcontroller and signal rectification circuit. Signal rectification circuit was used to rectify and amplified the alternating signal from the sensor's output. Oscilloscope was used to observe the excitation voltage as well as to measure the output dc signal (from the sensor). The microcontroller was used to convert the analog value (mV) to the digital value using Analog to Digital Converter (ADC).

The signal output from the sensor is small and alternating. A full wave signal rectification circuit shown in figure 6.2 has been used to rectify and amplify this alternating signal. Two Low Power Quad Operational Amplifier, LM324 were used in the circuit. A full-wave rectifier will convert the signal waveform to one constant polarity (+ve and –ve) at its output. The amplified signal will pass through a low pass filter (smoothing filter) with cut off frequency of 13 Hz to get a good dc signal. This dc signal is fed to the analog input of microcontroller to obtain digital value. All measurements from the sensor output (dc signal) and also the digital value obtained from microcontroller were recorded. Detail discussions on

the signal rectification circuit design and analysis have been reported in Chapter 7 of the thesis.

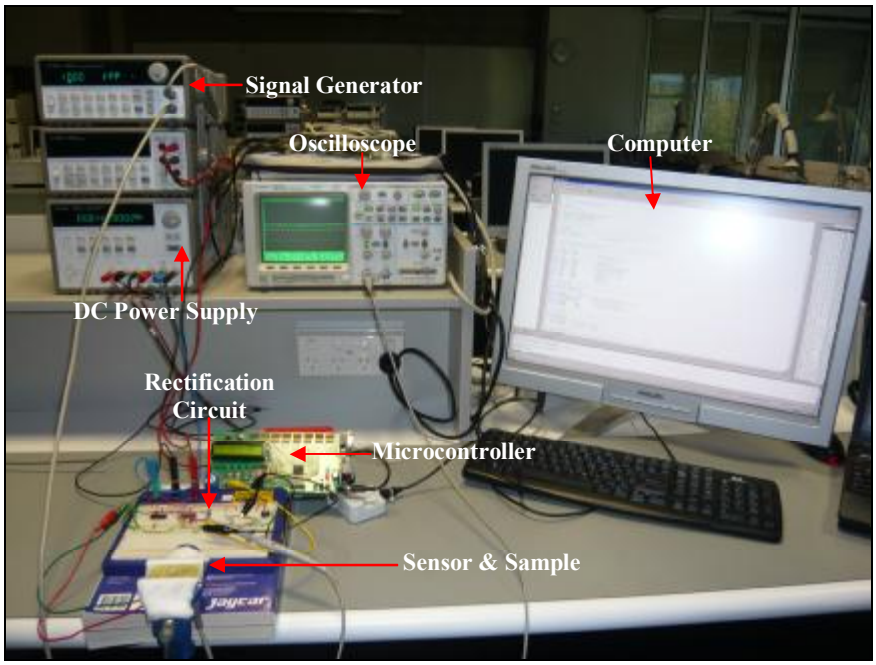

Figure 6.1: The experimental set-up

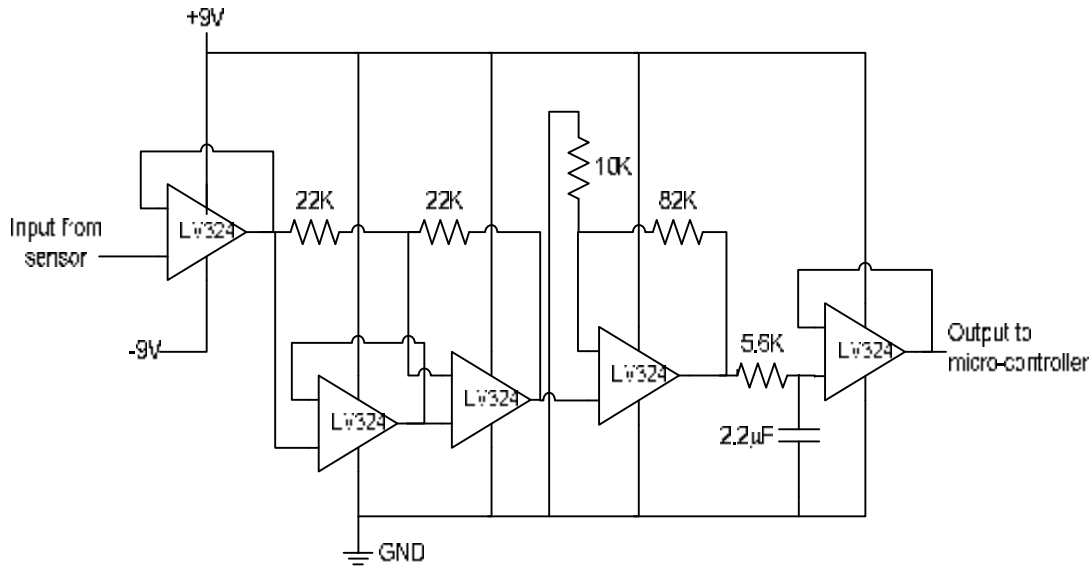

Figure 6.2: Full wave signal rectification circuit

Measurement data of air (V_{Air}) or sensor measurement without samples for calibration was first collected. The samples for measurement were then put on the sensor and the output voltage (V_{Out}) from the rectification circuit and digital value from microcontroller were recorded. The sensitivity can be calculated by;

$$Sensitivity = \frac{(V_{Out} - V_{Air})}{V_{Air}} * 100\% \quad (10)$$

6.3 Initial Studies with Chemical Samples

The initial studies were conducted to analyse the fabricated sensors with three different chemicals. The initial goal is to evaluate which of these sensors give a good response and could discriminate well between three different chemical samples. Three peptide derivatives namely sarcosine, proline and hydroxylproline were used for the initial studies, which are structurally and closely related to the target molecule, domoic acid (DA). N-methyl glycine represents the simplest structure. The proline molecule is arguably the most important amino acid in peptide conformation, containing the basic structural similarity to the DA. The hydroxyproline containing hydroxyl group at 4-position represents the susbtituent at C4, which is particularly crucial for the binding.

Figure 6.3 shows the chemical structure of the three chemical samples used for the initial studies. Figure 6.4 shows the chemical sample prepared for the experiments. These three chemical samples were chosen for the initial studies because their prices are cheaper compared to the domoic acid. Therefore, the experiments can be repeated many times to analyse the fabricated sensors. Table 6.1 shows the prices of each chemical in the market.

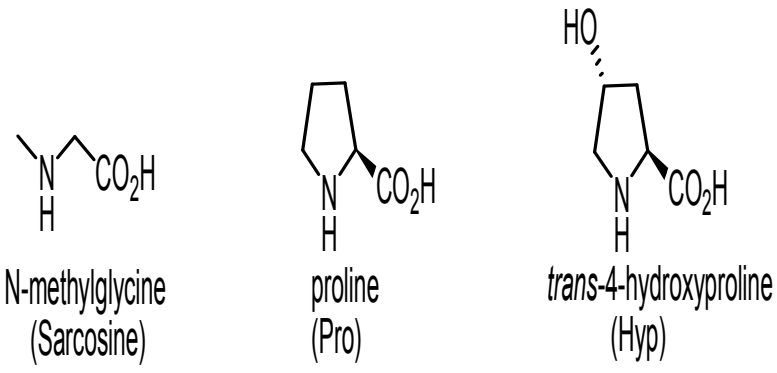

Figure 6.3: Sarcosine, Proline and Hydroxyproline molecules used for initial studies

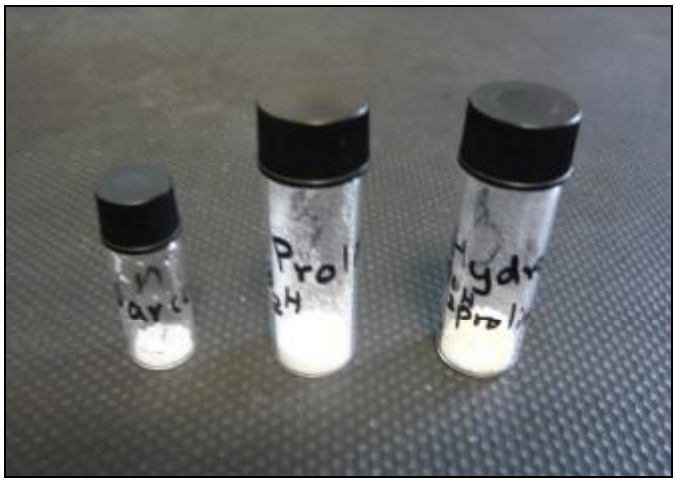

Figure 6.4: Three chemical samples prepared for the experiments

Table 6.1: Prices of different chemicals in the market

No.	Chemicals	Quantity	Price (USD)
1	Sarcosine	100 g	$ 53.30
2	L-Proline	100 g	$ 100.00
3	Hyroxy Proline	25 g	$ 102.80
4	Domoic Acid	1 mg	$ 508.00
5	Kaimic Acid	10 mg	$ 54.80

A small amount of samples of sarcosine, proline and hydroxyproline (1.4 mg) were used for the experiment. Each chemical were placed on the effective area of the sensor as shown in figure 6.5. The electrodes were separated from the sample with the help of glad-wrap. The experimental setup is shown in figure 6.1.

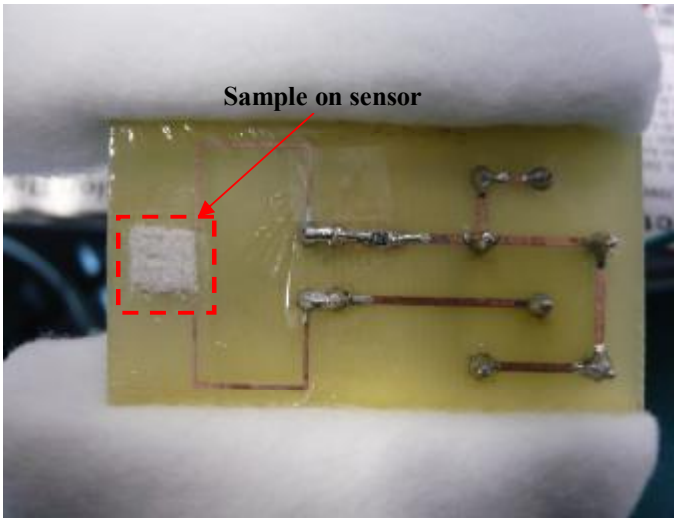

Figure 6.5: The sample on the sensor of measurement

6.3.1 Experimental Results with Conventional Sensors

All three fabricated conventional sensors were successfully tested with three chemical samples. Result in table 6.2 shows the comparative values of output voltage from three conventional sensors. The sensor sensitivity is the main parameter to show which of the conventional sensors has better sensing performance. Figure 6.6 shows the relationship between sensor sensitivity for different sensor configurations and figure 6.7 shows relationship between sensor sensitivity for different chemical samples.

It can be said that all sensors respond very well to the chemical samples. It is shown that conventional sensor with configuration #3 has better sensor sensitivity compared to the sensor with configuration #1 and #2. This is because sensor with configuration # 3 has better penetration depth and uniform distribution of electric field strength (see discussions for circuit analysis and modelling in Chapter 5). That is why conventional sensor with configuration #3 has better sensitivity measurement compared to other fabricated conventional sensors.

Table 6.2: Measurement data of conventional sensors

Samples	Sensor Configuration	Voltage (mV)	Sensitivity (with respect to air)
Air	Sensor #1	572.1	Nil
	Sensor #2	346.4	Nil
	Sensor #3	249.1	Nil
Sarcosine	Sensor #1	593.2	3.56
	Sensor #2	354.0	2.15
	Sensor #3	262.1	4.96
Proline	Sensor #1	586.1	2.39
	Sensor #2	350.7	1.23
	Sensor #3	258.3	3.56
Hydroxy	Sensor #1	583.1	1.87
	Sensor #2	349.9	1.00
	Sensor #3	255.2	2.31
Note: Sensor #1 is Din_10mil Sensor #2 is Din_20mil Sensor #3 is Din_40mil			

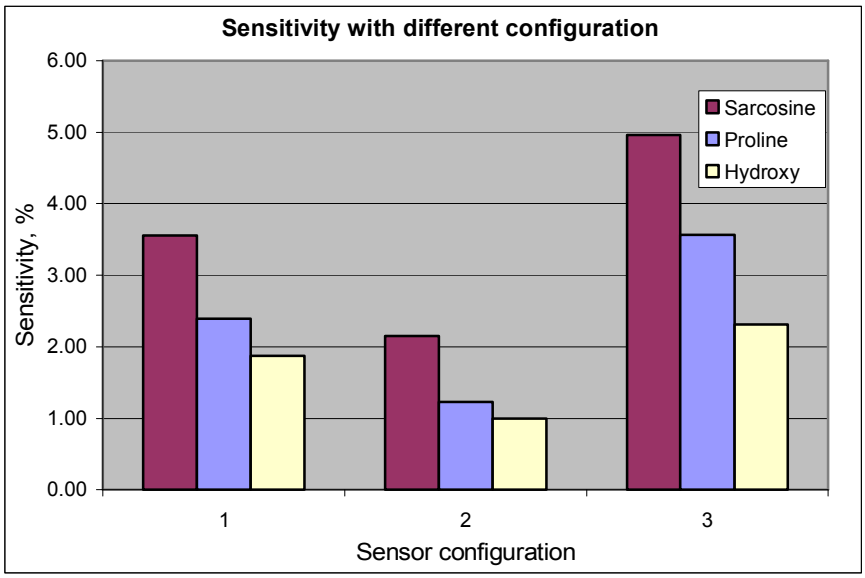

Figure 6.6: The relationship between sensitivity and sensor configuration

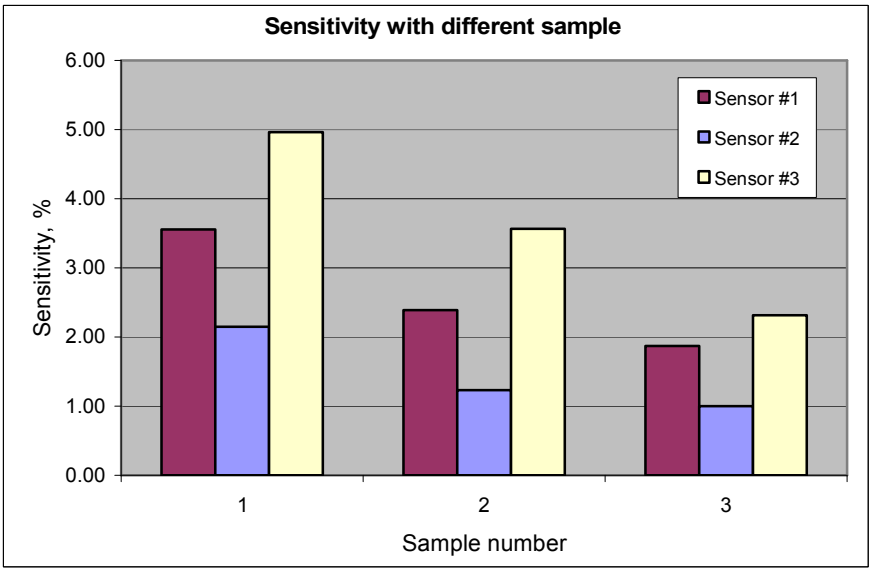

Figure 6.7: The relationship between sensitivity and chemical samples

6.3.2 Experimental Results with Novel Sensors

All fabricated novel interdigital were successfully tested with three chemical samples. Table 6.3 shows the comparative values of output voltage from three novel interdigital sensors. Figure 6.8 shows the comparison of sensor sensitivity with different sensor configuration and figure 6.9 shows the results of sensor sensitivity for different chemical samples. It can be said that all the sensors respond very well to the chemicals and it is possible to discriminate the different chemicals from the output of the sensor. Sensor_1 shows a good response and better sensitivity compared to Sensor_2 and Sensor_3. This is because Sensor_1 was designed to have greater penetration depth, better uniformity in term of capacitance estimation, electric field distribution and average electric field intensity (see Chapter 5). Therefore, Sensor_1 has better sensitivity measurement compared to Sensor_2 and Sensor_3.

Table 6.3: Measurement data of novel sensors

Samples	Sensor Configuration	Voltage (mV)	Sensitivity (with respect to air)
Air	Sensor_1	374.1	Nil
	Sensor_2	442.0	Nil
	Sensor _3	533.4	Nil
Sarcosine	Sensor_1	413.5	10.53
	Sensor_2	486.8	10.14
	Sensor _3	579.3	8.61
Proline	Sensor_1	401.2	7.24
	Sensor_2	473.0	7.01
	Sensor _3	573.1	7.44
Hydroxy	Sensor_1	384.3	2.73
	Sensor_2	457.8	3.57
	Sensor _3	561.5	5.27

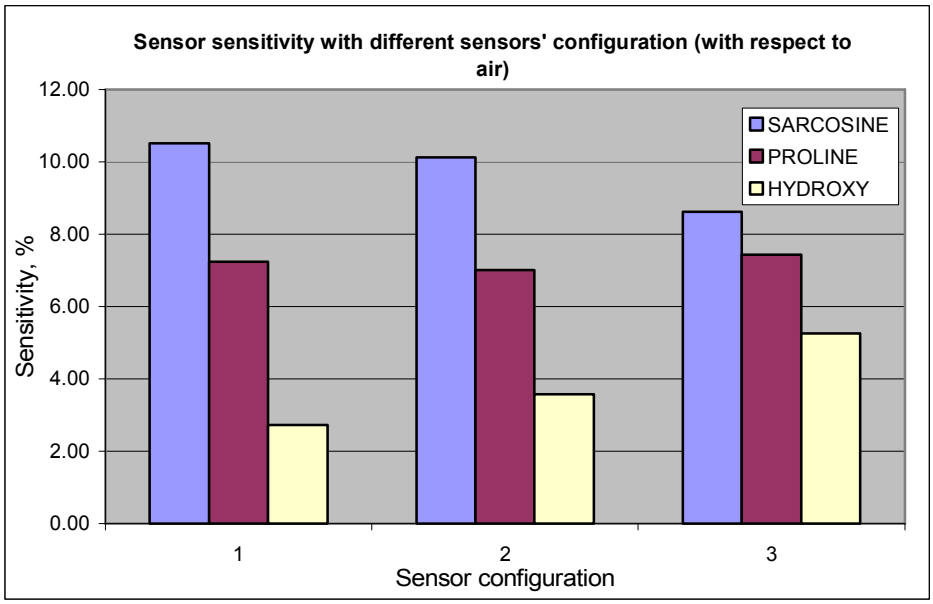

Figure 6.8: Comparison of sensors' sensitivity with different configurations

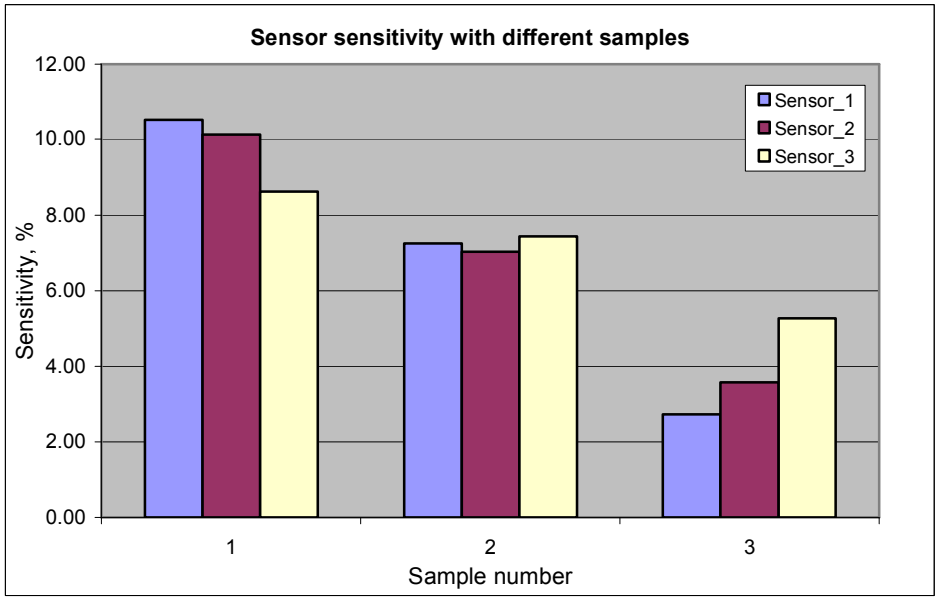

Figure 6.9: Comparison of sensors' sensitivity with different samples

Results from the initial studies have shown that novel interdigital sensors have better sensing performance compared to the conventional sensors. Results also proved that the discussions reported in Chapter 5 were true, which indicated that novel interdigital sensors have better response in order to access the chemical properties of a given sample. Therefore, novel interdigital sensors have been selected for further analysis.

6.4 Experiments with Seafood Products

Experiments were repeated to analyse the responds of the fabricated novel interdigital sensors with different seafood products. Three types of seafood products (10 samples of fish, 10 samples of squid and 10 samples of mussel) were prepared for the experiment. Each sample was cut about 4.75 mm by 4.75 mm (size of effective area of fabricated sensors). The same experiment setup shown in figure 6.1 was used. Data was collected and then analysed to choose the best novel interdigital sensor to be used for further analysis with proline and domoic acid (DA).

6.4.1 Experimental Results with Seafood Products

All novel interdigital sensors were successfully tested with samples of three seafood products. The experiments were conducted in the laboratory at a room temperature of 20.8 °C with humidity of 40%. The first experiment was to evaluate the fabricated novel interdigital sensors with fish samples. Figure 6.10 shows the samples prepared for the experiment. Table 6.4 shows the measurement data collected for Sensor_1 for fish samples. Table 6.5 shows the measurement data for Sensor_2 and Table 6.6 shows the measurement data for Sensor_3. Figure 6.11 shows the sensors' sensitivity for experiment with fish samples. Result of experiment with fish samples have shown that Sensor_1 has better sensitivity measurement compared to Sensor_2 and Sensor_3.

Figure 6.10: 10 samples of fish prepared for the experiment

Table 6.4: Measurement data of Sensor_1 for fish samples

Samples	Air		Sensor_1		
	Vout	ADC	Vout	ADC	Sensitivity
Fish_1	337.5	268	387.5	316	12.90323
Fish_2	337.5	268	393.8	320	14.2966
Fish_3	337.5	268	406.3	332	16.9333
Fish_4	337.5	268	400.0	325	15.625
Fish_5	337.5	268	406.3	332	16.9333
Fish_6	337.5	268	400.0	325	15.625
Fish_7	337.5	268	406.3	332	16.9333
Fish_8	337.5	268	387.5	316	12.90323
Fish_9	337.5	268	406.3	332	16.9333
Fish_10	337.5	268	400.0	326	15.625

Table 6.5: Measurement data of Sensor_2 for fish samples

Samples	Air		Sensor_2		
	Vout	ADC	Vout	ADC	Sensitivity
Fish_1	387.5	313	431.3	355	10.15534
Fish_2	387.5	313	437.5	358	11.42857
Fish_3	387.5	313	456.3	372	15.0778
Fish_4	387.5	313	450.0	366	13.88889
Fish_5	387.5	313	456.3	371	15.0778
Fish_6	387.5	313	450.0	369	13.88889
Fish_7	387.5	313	456.3	373	15.0778
Fish_8	387.5	313	431.3	355	10.15534
Fish_9	387.5	313	456.3	372	15.0778
Fish_10	387.5	313	450.0	364	13.88889

Table 6.6: Measurement data of Sensor_3 for fish samples

Samples	Air		Sensor_3		
	Vout	ADC	Vout	ADC	Sensitivity
Fish_1	481.3	393	525.0	430	8.32381
Fish_2	481.3	393	543.8	445	11.4932
Fish_3	481.3	393	556.3	455	13.48193
Fish_4	481.3	393	543.8	442	11.4932
Fish_5	481.3	393	556.3	456	13.48193
Fish_6	481.3	393	543.8	443	11.4932
Fish_7	481.3	393	556.3	455	13.48193
Fish_8	481.3	393	531.3	436	9.410879
Fish_9	481.3	393	556.3	456	13.48193
Fish_10	481.3	393	550.0	450	12.49091

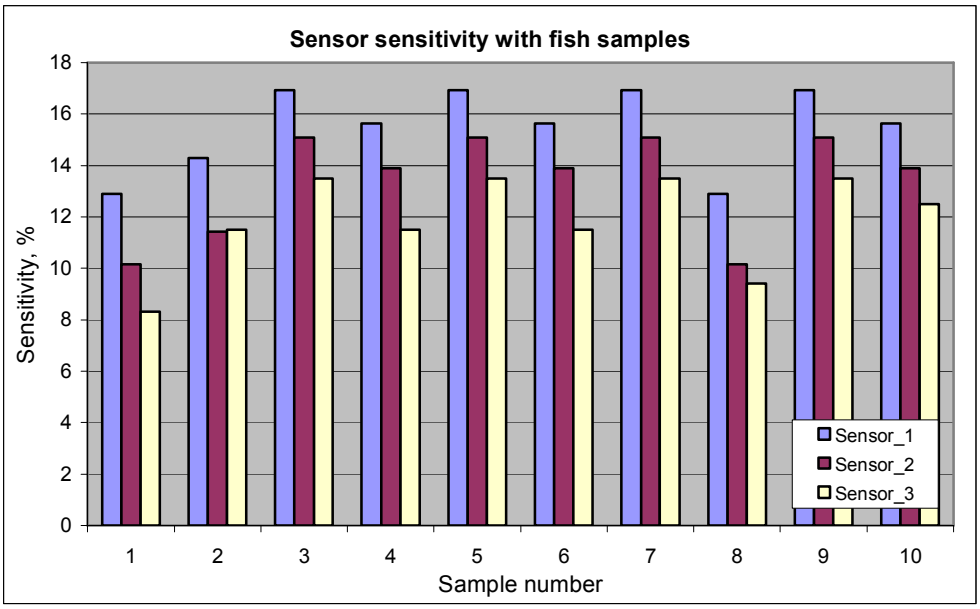

Figure 6.11: Comparison of sensors' sensitivity with fish samples

The second experiment was conducted to evaluate the response of novel interdigital sensors with mussel samples. Figure 6.12 shows the samples prepared for the experiment. Table 6.7 shows the measurement data of Sensor_1 for mussel samples. Table 6.8 shows data measurement of Sensor_2 and Table 6.9 for Sensor_3 respectively. Figure 6.13 shows the relationship between sensors' sensitivity with mussel samples. Again, it is shown that, Sensor_1 has better sensitivity measurement compared to other novel interdigital sensors.

Figure 6.12: 10 samples of mussel prepared for the experiment

Table 6.7: Measurement data of Sensor_1 for mussel samples

Samples	Air		Sensor_1		
	Vout	ADC	Vout	ADC	Sensitivity
Mussel_1	337.5	268	375.0	300	10.0000
Mussel_2	337.5	268	387.5	313	12.90323
Mussel_3	337.5	268	381.3	309	11.48702
Mussel_4	337.5	268	387.5	316	12.90323
Mussel_5	337.5	268	375.0	301	10.0000
Mussel_6	337.5	268	381.3	310	11.48702
Mussel_7	337.5	268	381.3	309	11.48702
Mussel_8	337.5	268	393.8	320	14.2966
Mussel_9	337.5	268	387.5	316	12.90323
Mussel_10	337.5	268	381.3	309	11.48702

Table 6.8: Measurement data of Sensor_2 for mussel samples

Samples	Air		Sensor_2		
	Vout	ADC	Vout	ADC	Sensitivity
Mussel_1	387.5	313	418.8	341	7.473734
Mussel_2	387.5	313	437.5	360	11.42857
Mussel_3	387.5	313	425.0	345	8.823529
Mussel_4	387.5	313	437.5	359	11.42857
Mussel_5	387.5	313	418.8	341	7.473734
Mussel_6	387.5	313	425.0	344	8.823529
Mussel_7	387.5	313	425.0	343	8.823529
Mussel_8	387.5	313	443.8	363	12.68589
Mussel_9	387.5	313	437.5	356	11.42857
Mussel_10	387.5	313	425.0	344	8.823529

Table 6.9: Measurement data of Sensor_3 for mussel samples

Samples	Air		Sensor_3		
	Vout	ADC	Vout	ADC	Sensitivity
Mussel_1	481.3	393	518.8	422	7.228219
Mussel_2	481.3	393	537.5	440	10.45581
Mussel_3	481.3	393	525.0	430	8.32381
Mussel_4	481.3	393	537.5	441	10.45581
Mussel_5	481.3	393	518.8	423	7.228219
Mussel_6	481.3	393	525.0	430	8.32381
Mussel_7	481.3	393	518.8	422	7.228219
Mussel_8	481.3	393	543.8	444	11.4932
Mussel_9	481.3	393	531.3	435	9.410879
Mussel_10	481.3	393	518.8	426	7.228219

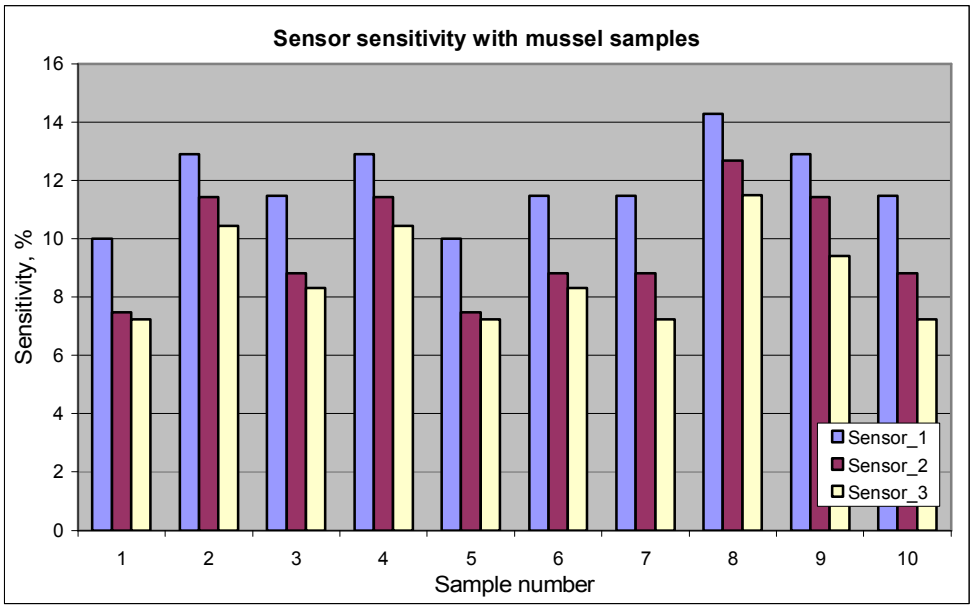

Figure 6.13: Comparison of sensors' sensitivity with mussel samples

The last experiment with seafood products has been conducted. Squid samples as in figure 6.14 were prepared and the measurement data were recorded. Table 6.10 shows the measurement data of Sensor_1 for squid samples. Table 6.11 shows the measurement data of Sensor_2 and Table 6.12 for Sensor_3 respectively. Figure 6.15 shows the comparison of sensors' sensitivity with squid samples. From the graph in figure 6.15, it can be said that Sensor_1 has better sensor's sensitivity compared to Sensor_2 and Sensor_3.

Figure 6.14: 10 samples of squid prepared for the experiment

Table 6.10: Measurement data of Sensor_1 for squid samples

Samples	Air		Sensor_1		
	Vout	ADC	Vout	ADC	Sensitivity
Squid_1	312.5	248	375.0	302	16.66667
Squid_2	312.5	248	356.3	282	12.29301
Squid_3	312.5	248	381.3	311	18.04354
Squid_4	312.5	248	362.5	291	13.7931
Squid_5	312.5	248	375.0	300	16.66667
Squid_6	312.5	248	381.3	309	18.04354
Squid_7	312.5	248	362.5	290	13.7931
Squid_8	312.5	248	381.3	307	18.04354
Squid_9	312.5	248	381.3	311	18.04354
Squid_10	312.5	248	368.8	297	15.26573

Table 6.11: Measurement data of Sensor_2 for squid samples

Samples	Air		Sensor_2		
	Vout	ADC	Vout	ADC	Sensitivity
Squid_1	393.8	318	456.3	373	13.69713
Squid_2	393.8	318	437.5	356	9.988571
Squid_3	393.8	318	462.5	377	14.85405
Squid_4	393.8	318	443.8	362	11.26634
Squid_5	393.8	318	462.5	378	14.85405
Squid_6	393.8	318	468.8	385	15.99829
Squid_7	393.8	318	443.8	361	11.26634
Squid_8	393.8	318	462.5	379	14.85405
Squid_9	393.8	318	462.5	378	14.85405
Squid_10	393.8	318	456.3	373	13.69713

Table 6.12: Measurement data of Sensor_3 for squid samples

Samples	Air		Sensor_3		
	Vout	ADC	Vout	ADC	Sensitivity
Squid_1	475.0	389	531.3	436	10.59665
Squid_2	475.0	389	518.8	423	8.44256
Squid_3	475.0	389	537.5	440	11.62791
Squid_4	475.0	389	531.3	436	10.59665
Squid_5	475.0	389	543.8	448	12.65171
Squid_6	475.0	389	556.3	459	14.61442
Squid_7	475.0	389	531.3	436	10.59665
Squid_8	475.0	389	550.0	451	13.63636
Squid_9	475.0	389	550.0	450	13.63636
Squid_10	475.0	389	543.8	448	12.65171

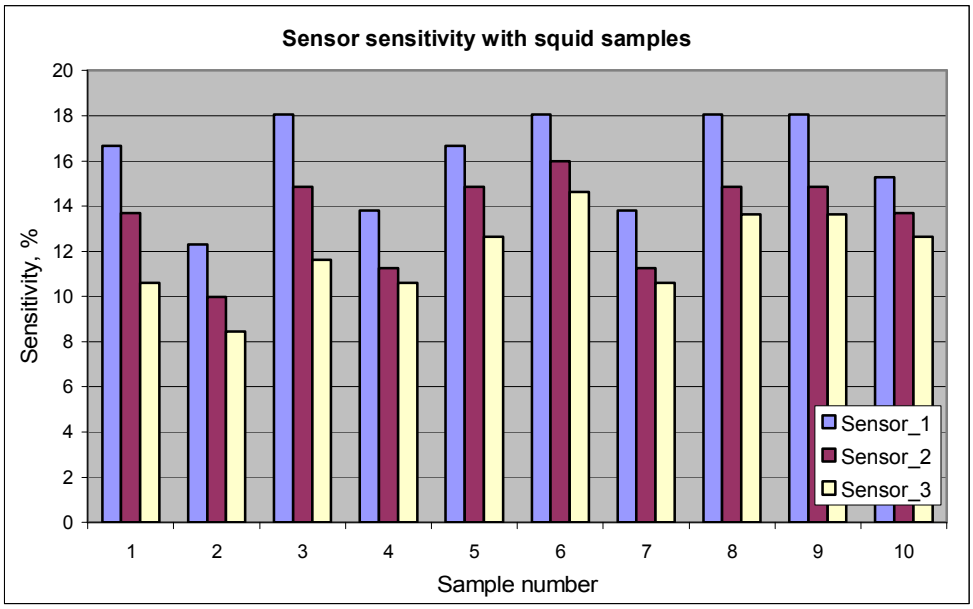

Figure 6.15: Comparison of sensors' sensitivity with squid samples

Experiments with seafood products were successfully conducted. Results from the experiments have shown that all novel interdigital sensors respond very well with seafood products. Results also shown that Sensor_1 shows better response and give better sensitivity compare to other novel interdigital sensors. Therefore Sensor_1 has been chosen for further analysis with proline and domoic acid (DA).

6.5 Experiments with Mussels and Proline

Blue mussles or Mytilus edulis has been used as samples for the experiments. This is because, it was reported that the amnesic shellfish poisoning (ASP) was caused after eating the contaminated blue mussels [68]. Assuming all mussels in the market are good (at regulatory level of DA is 20 µg/g), a set of 8 mussels were randomly selected and were cut from 5 different locations. Figure 6.16 shows that how the samples were cut from each mussel. Location 1 to location 4 is known as the ctenidia and location 5 is the digestive gland of the mussel. Normally the digestive gland is thicker compare to other parts of the mussel.

All samples were placed onto the non-stick paper. Samples were wiped with tissue paper to remove the water and then left them to be dried for 1-2 hours at a controlled laboratory temperature of 23 ºC with humidity of 40%. In practical situation, it may not be a mandatory requirement to dry the samples. But it is important to wipe out water present in

and out of the samples. Each sample thickness and surface temperature was measured using digital calliper and temperature tester respectively. The samples thickness measured were between 1.4 mm to 3.2 mm having the temperature of range between 22.0 ºC to 22.5 ºC which was closed to laboratory temperature.

The experimental setup shown in figure 6.1 was constructed to test the samples. Each sample was placed on the sensor as shown in figure 6.17. The output voltage from the signal rectification circuit and the digital values from microcontroller were taken. Data of each sample was taken for analysis before and after a very small amount of proline (0.7 mg) was put on the surface of the samples.

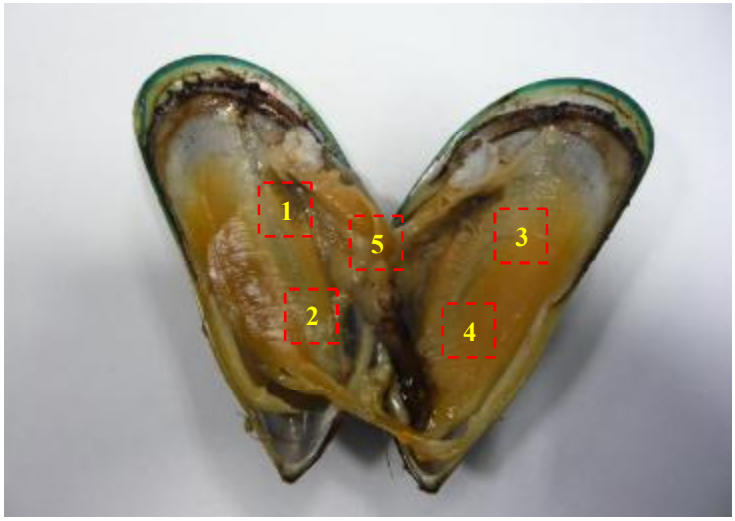

Figure 6.16: The samples were cut from each mussel

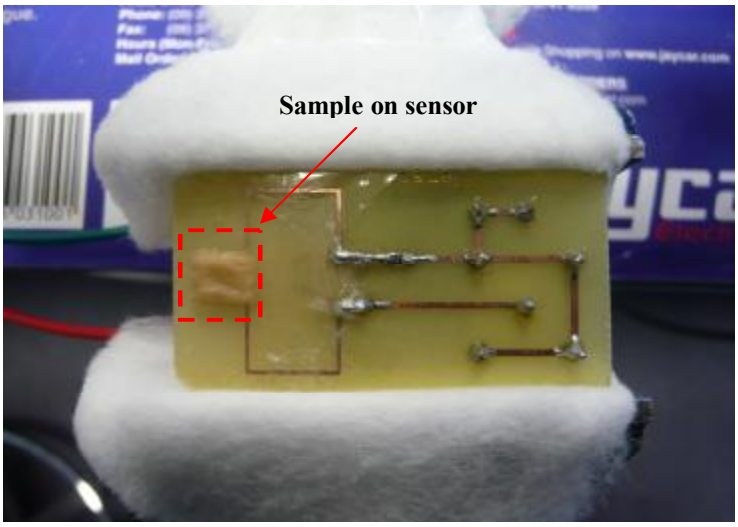

Figure 6.17: The sample (mussel) on the sensor of measurement

6.5.1 Experimental Results with Mussels and Proline

The objective of the experiments is to observe the response of Sensor_1 to chemical samples such as proline. Proline was chosen in the experiment because it has a close chemical structure to domoic acid and is affordable to start with. The experiment was conducted at a laboratory temperature of 22.9 ºC with humidity of 40%. Table 6.13 shows the measurement data before and after adding proline on the surface of the samples. Result in figure 6.18 shows that there was a significant difference of Sensor_1 sensitivity before and after adding the proline. It is shown that Sensor_1 was able to detect the presence of proline on the mussel's surface. Graph on figure 6.19 shows the average sensor sensitivity is higher at location 5 and lower at location 1. This is because the average thickness at location 5 is 2.7 mm, which is thicker compared to other locations. The sensitivity is lowest at location 1 of having average thickness of 2.3 mm. The graph in figure 6.20 shows a good correlation with $R^2 = 0.717$, between sensor's sensitivity with sample thickness. This is true for certain level of thickness because as the thickness increase the electric field distribution becomes weak and the sensitivity is expected to be indifferent.

Table 6.13: Measurement data of sample before and after adding proline on the sample surface

Sample No	Sample		Voltage			ADC Value		Sensitivity	
	Thickness mm	Temp (ºC)	Vair	Vout Sample	Vout +Proline	Sample	+Proline	Before	+Proline
1	2.5	22.1	300.0	331.3	337.5	274	278	10.43	12.50
2	2.6	22.1	300.0	337.5	343.8	279	280	12.50	14.60
3	2.1	22.0	300.0	331.3	337.5	273	276	10.43	12.50
4	1.9	22.0	300.0	331.3	343.8	272	282	10.43	14.60
5	3.0	22.2	300.0	343.8	356.3	280	292	14.60	18.77
6	1.6	22.7	300.0	325.0	337.5	265	276	8.33	12.50
7	2.1	22.2	300.0	331.3	343.8	272	281	10.43	14.60
8	1.5	22.4	300.0	331.3	343.8	272	280	10.43	14.60
9	2.7	22.0	300.0	350.0	362.5	287	297	16.67	20.83
10	1.9	22.2	300.0	331.3	343.8	272	282	10.43	14.60
11	2.4	22.4	300.0	337.5	350.0	279	286	12.50	16.67
12	2.5	22.1	300.0	350.0	350.0	286	286	16.67	16.67
13	2.2	22.1	300.0	343.8	356.3	284	290	14.60	18.77
14	2.0	22.1	300.0	337.5	350.0	279	286	12.50	16.67
15	2.5	22.3	300.0	356.3	368.8	290	302	18.77	22.93
16	1.7	21.9	306.3	331.3	343.8	273	279	8.16	12.24
17	1.9	22.0	306.3	331.3	337.5	272	276	8.16	10.19
18	1.7	21.9	306.3	337.5	350.0	276	286	10.19	14.27

19	1.7	22.0	306.3	331.3	343.8	271	281	8.16	12.24
20	2.9	22.0	306.3	362.5	375.0	298	306	18.35	22.43
21	2.4	22.4	306.3	343.8	350.0	282	286	12.24	14.27
22	2.1	22.1	306.3	343.8	356.3	280	292	12.24	16.32
23	2.3	22.2	306.3	350.0	356.3	287	292	14.27	16.32
24	2.4	22.3	306.3	350.0	362.5	287	296	14.27	18.35
25	2.5	22.4	306.3	350.0	362.5	286	295	14.27	18.35
26	1.2	22.4	306.3	331.3	337.5	270	276	8.16	10.19
27	1.6	22.0	306.3	331.3	343.8	270	280	8.16	12.24
28	1.5	22.0	306.3	331.3	337.5	270	278	8.16	10.19
29	2.1	22.0	306.3	343.8	356.3	291	291	12.24	16.32
30	2.9	22.1	306.3	362.5	368.8	297	299	18.35	20.40
31	1.8	22.0	306.3	343.8	356.3	282	290	12.24	16.32
32	2.2	22.2	306.3	343.8	356.3	282	291	12.24	16.32
33	2.5	22.0	306.3	356.3	362.5	290	296	16.32	18.35
34	1.7	22.0	306.3	343.8	350.0	282	287	12.24	14.27
35	2.7	22.2	306.3	356.3	368.8	290	299	16.32	20.40
36	2.0	22.2	306.3	337.5	343.8	276	283	10.19	12.24
37	3.0	22.0	300	356.3	362.5	289	296	18.77	20.83
38	2.6	22.3	300	350.0	362.5	286	296	16.67	20.83
39	3.0	22.4	300	343.8	356.3	283	290	14.60	18.77
40	2.9	22.3	300	356.3	362.5	290	297	18.77	20.83

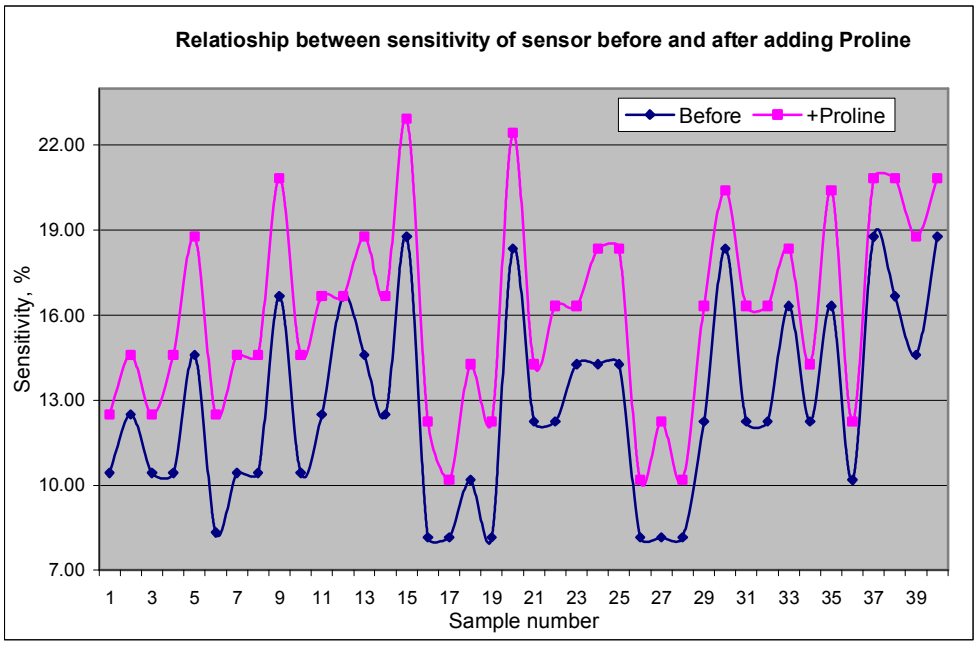

Figure 6.18: Sensor sensitivity with sample before and after adding proline

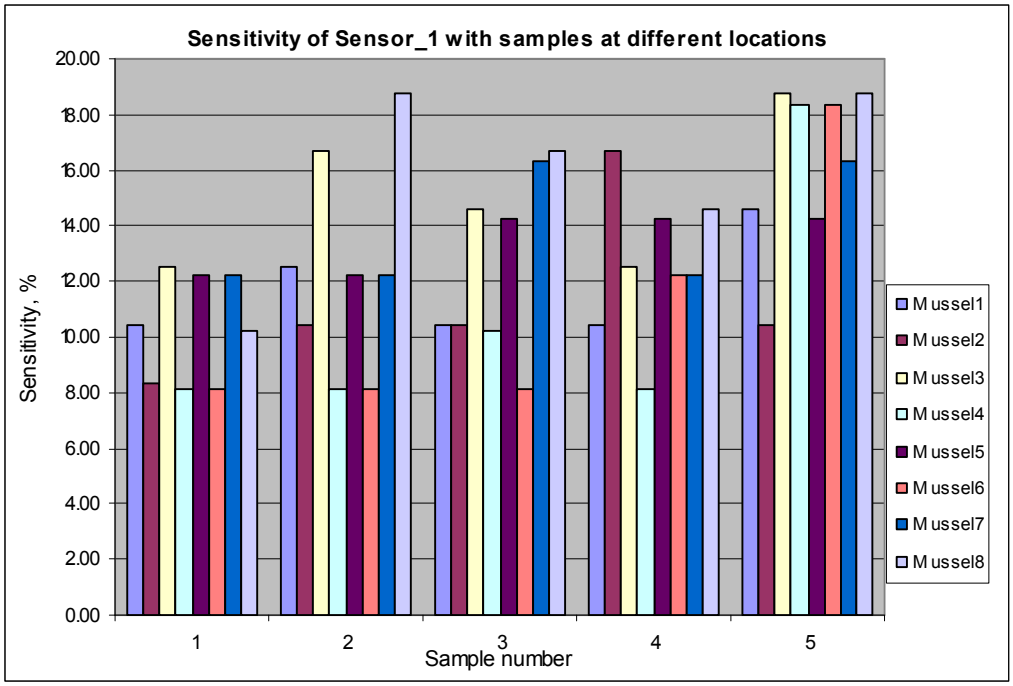

Figure 6.19: Results of mussel samples from different locations (before + proline)

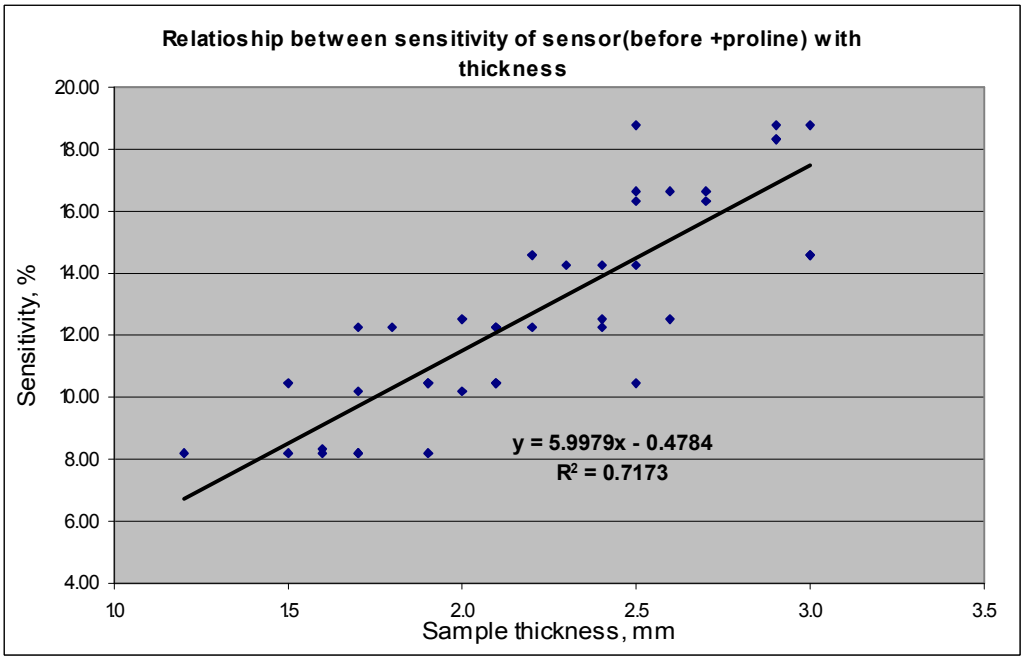

Figure 6.20: The relationship between sensor sensitivity with sample thickness (before +proline).

Experiment was repeated with another 20 samples of mussels at the same location 5. Location 5 was chosen because it is thicker compared to other locations and the sensor sensitivity is higher at location 5 compared to other locations which is shown in figure 6.19. Although samples were taken from the same location, but the thickness of each sample is not homogeneous. This is because of the different size of mussels. In the experiment, a small amount of proline was injected to the sample, instead of putting it on the sample surface. The experiment was conducted at the laboratory temperature of 21.4 ºC with humidity of 41%. Each sample was injected with 0.7 mg of proline. Data was collected before and after the proline was injected. Table 6.14 shows the measurement data for samples before and after injected with proline. Figure 6.21, shows that the sensor is able to detect the present of proline injected to the samples. This result also shows that, it is possible to evaluate different amount of chemicals injected to mussel samples.

Table 6.14: Measurement data of samples before and after injected with 0.7 mg proline

Sample No	Sample		Voltage			ADC Value		Sensitivity	
	Thickness mm	Temp (ºC)	Vair	Vout Sample	Vout +Proline	Sample	Injected Proline	Before	Injected Proline
1	2.7	20.8	331.3	400.0	418.8	324	340	17.18	20.89
2	2.9	20.9	331.3	406.3	425.0	331	344	18.46	22.05
3	3.3	20.7	331.3	412.5	431.3	334	352	19.68	23.19
4	3.2	20.8	331.3	412.5	425.0	334	344	19.68	22.05
5	3.6	20.8	331.3	425.0	437.5	344	355	22.05	24.27
6	2.8	20.9	331.3	400.0	412.5	324	335	17.18	19.68
7	2.5	20.9	331.3	393.8	400.0	321	326	15.87	17.18
8	2.9	21.0	331.3	412.5	418.8	336	340	19.68	20.89
9	2.5	20.8	331.3	387.5	393.8	316	322	14.50	15.87
10	3.4	20.6	331.3	425.0	437.5	344	355	22.05	24.27
11	2.8	21.4	325.0	393.8	400.0	319	322	15.87	18.75
12	3.1	21.6	325.0	406.3	406.3	331	330	18.46	20.01
13	2.6	21.8	325.0	406.3	406.3	331	332	18.46	20.01
14	2.7	21.6	325.0	400.0	400.0	324	325	17.18	18.75
15	2.6	21.7	325.0	393.8	393.8	320	322	15.87	17.47
16	3.3	21.5	325.0	412.5	412.5	334	337	19.68	21.21
17	2.1	21.6	325.0	393.8	393.8	321	320	15.87	17.47
18	3.2	21.5	325.0	412.5	412.5	336	335	19.68	21.21
19	2.3	21.7	325.0	387.5	387.5	316	317	14.50	16.13
20	2.1	21.5	325.0	381.3	381.3	310	312	13.11	14.77

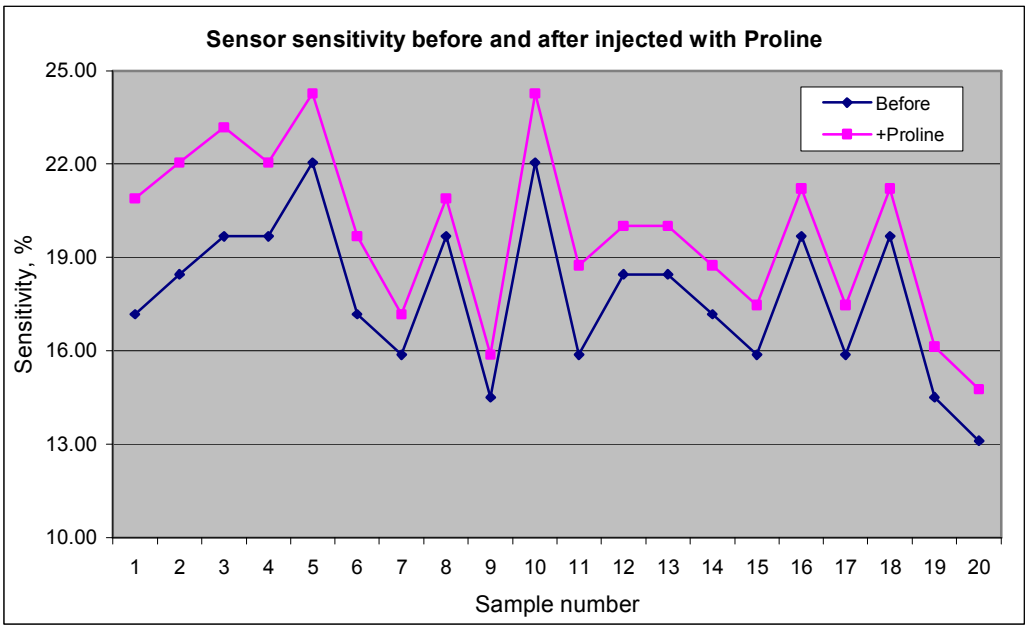

Figure 6.21: Sensor sensitivity with sample before and after injected by proline

In order to get more convincing results, 10 samples (Sample 11-20) have been used for further analysis with different amount of proline. The amount of proline injected to the samples was 1.4 mg and 2.1 mg and data of each sample was measured and analysed. Data was collected as shown in Table 6.15. Figure 6.22 shows that there was an increase in sensor sensitivity for different amount of proline injected. The result has shown a good linearity between injected proline with sensor sensitivity as shown in figure 6.23. Taking sample M_10, the thinnest (2.3 mm) among the samples, the equivalent linear equation is

$$y = 2.3396\ x + 10.491 \tag{11}$$

It was observed from the experimental results that we can estimate small amount of proline present in the mussel samples. Sensor_1 has shown a good response with proline and from the experimental results with proline, it can be said that Sensor_1 will be able to detect the presence of DA in mussel samples. Therefore, Sensor_1 has been used for further analysis with domoic acid (DA).

Table 6.15: Measurement data of samples before and after injected with 0.7 mg, 1.4 mg and 2.1 mg of proline

Sample Number	Sample		Sensor Sensitivity			
	Thickness, mm	Temp ºC	Before	+Proline 0.7 mg	+Proline 1.4 mg	+Proline 2.1 mg
1	2.8	21.4	15.87	18.75	20.01	21.21
2	3.1	21.6	18.46	20.01	21.21	22.40
3	2.6	21.8	18.46	20.01	22.40	23.53
4	2.7	21.6	17.18	18.75	21.21	23.53
5	2.6	21.7	15.87	17.47	22.40	24.65
6	3.3	21.5	19.68	21.21	24.65	27.78
7	2.1	21.6	15.87	17.47	20.01	21.21
8	3.2	21.5	19.68	21.21	23.53	25.71
9	2.3	21.7	14.50	16.13	18.75	21.21
10	2.1	21.5	13.11	14.77	17.47	20.01

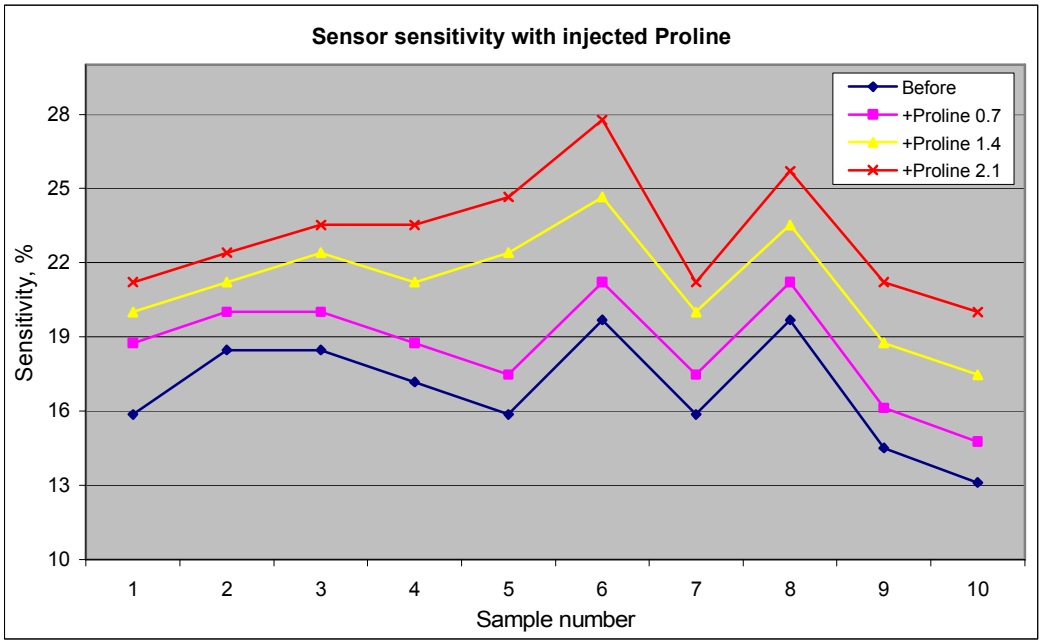

Figure 6.22: Sensor sensitivity with different amount of injected proline

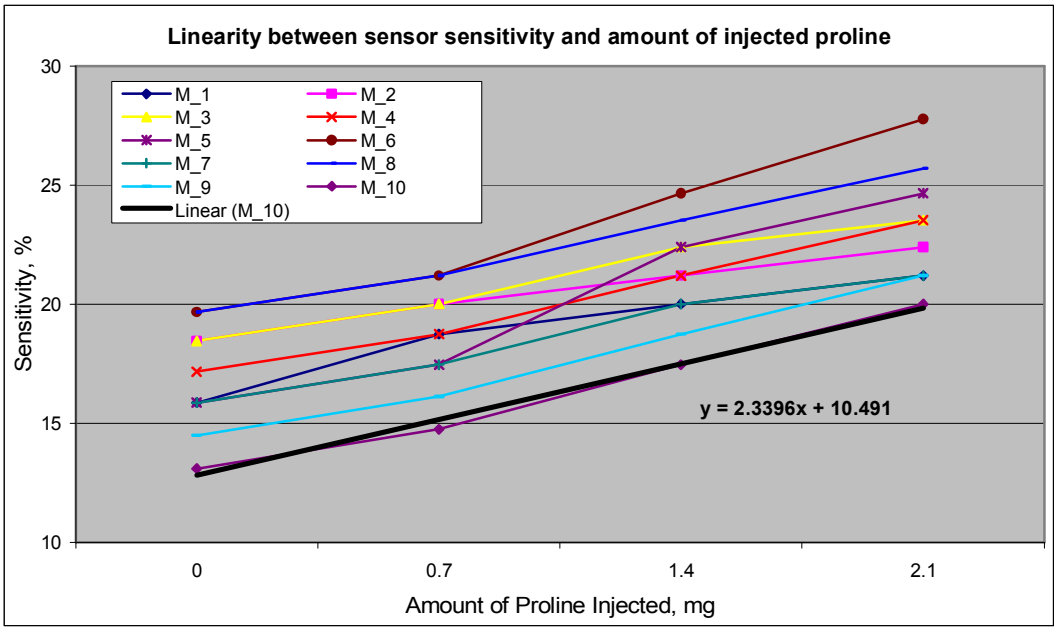

Figure 6.23: Linearity of sensor sensitivity with injected proline

6.6 Experiments with Mussels and Domoic Acid

The main objective of this research work is to detect the presence of domoic acid (DA) in seafood. DA, the neurotoxin which causes amnesic shellfish poisoning (ASP) is an amino acid produced by the diatom Pseudo-nitzschia. Figure 6.24 shows the chemical structure of DA. DA was purchased from CALBIOCHEM, EMD Biosciences, Inc. with the cost of USD 500 for 2 mg of DA. Figure 6.25 shows the sample of DA used for the experiments.

Three experiments with DA were conducted using mussel samples. The first experiment was conducted to analyse how much Sensor_1 can response to DA. Measurement data of air, voltage output and digital value were collected. Sensitivity measurement (equation 11) was used to analyse the sensor. Second experiment was conducted with different amount of DA concentrations and also with water. The experiment was conducted to analyse the effect of water and different concentrations of DA in mussel samples. Third experiment was conducted by injecting 1.0 µg of DA into several mussel samples of different thickness. The experiment was conducted to find the threshold level of sensor sensitivity with respect to sample thickness.

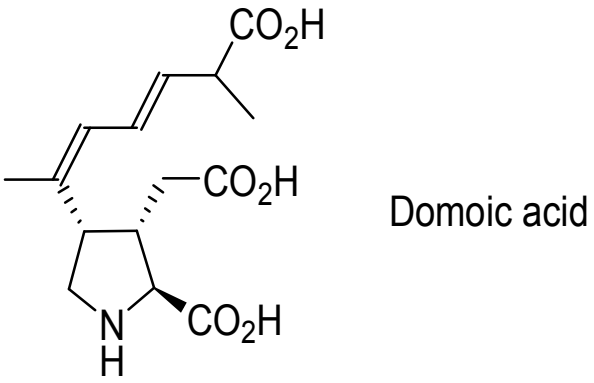

Figure 6.24: The chemical structure of DA

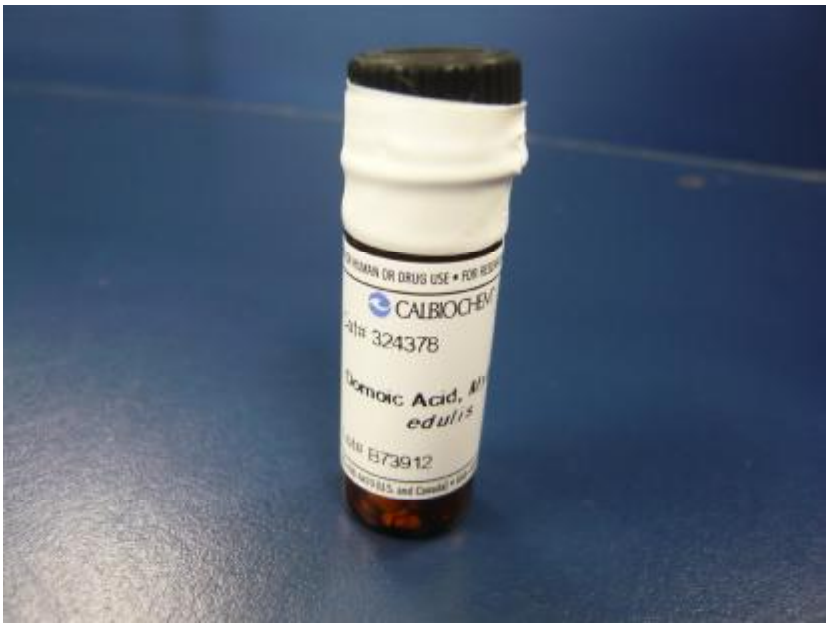

Figure 6.25: Domoic acid used for the experiments

6.6.1 Experimental Results with Mussel and Domoic Acid

Experiments with domoic acid (DA) were successfully conducted in the laboratory. The experiments were conducted at the laboratory temperature of 22 ℃ with humidity of 48%. Small amount of DA of 0.1 mg was diluted in 2.0 ml (2.0 g) of water to give 50 ppm of DA (50 µgm of DA in 1 gm of produced mixture sample). Mussel sample was injected with domoic acid from 0.5 µg until 5.0 µg. Table 6.16 shows the particulars of the prepared mussel samples. Table 6.17 shows the measurement data collected from the experiment. Result in figure 6.26 shows that Sensor_1 respond to the presence of DA after 1.0 µg of DA injected into the mussel with minimum weight of 0.0795 g. The result shows that Sensor_1 was able to detect approximately 12.6 µg/g of DA in mussel meat. The regulatory guideline for DA is 20

µg/g. The sensor has the potential to detect an amount even lower than 10 µg/g of DA in mussel meat.

Table 6.16: Sample prepared for the experiment with domoic acid

Sample	Weight (g)	Thickness (mm)	Surface Temperature (°C)
Mussel	0.0795	2.2	22

Table 6.17: Measurement data of samples injected with domoic acid

Domoic Acid, µg	Air	Sensor_1	
	Vair	Vout	Sensitivity
0.0	334.4	384.4	14.95
0.5	334.4	384.4	14.95
1.0	334.4	390.6	16.81
1.5	334.4	393.8	17.76
2.0	334.4	396.9	18.69
2.5	334.4	400.0	19.62
3.0	334.4	400.0	19.62
3.5	334.4	403.1	20.54
4.0	334.4	406.3	21.50
4.5	334.4	406.3	21.50
5.0	334.4	409.4	22.43

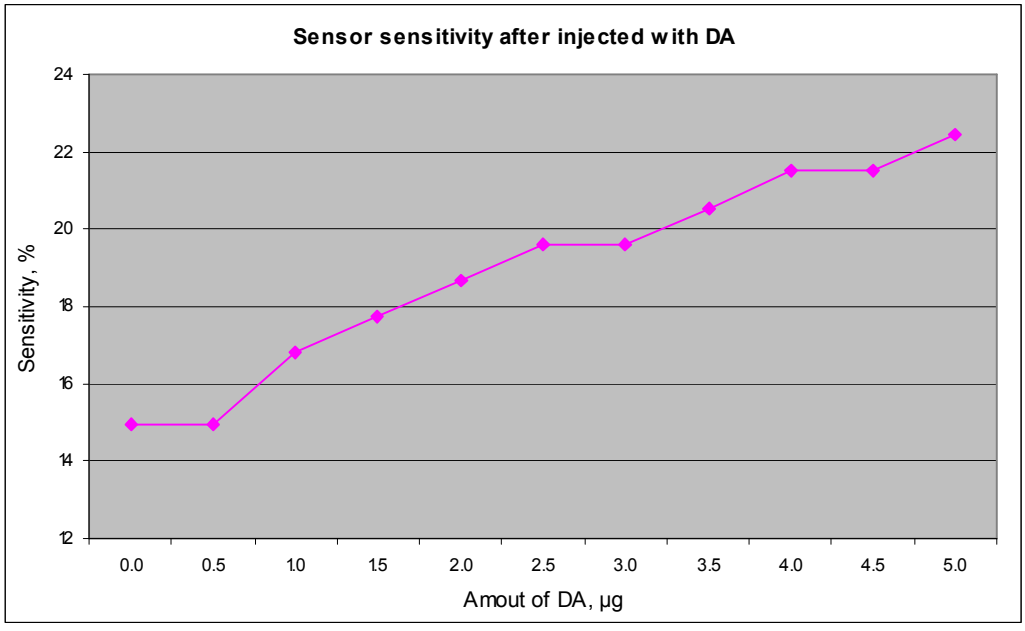

Figure 6.26: Sensor sensitivity with injected DA to a sample

The experiment was repeated by injecting very small amount of water and DA of different concentrations to the samples having the same thickness of 2.4 mm. Different concentrations of DA (10.1 µg, 21.2 µg, 42.5 µg, 85.0 µg and 170 µg) were prepared for the experiments. Each sample was injected with the initial amount of water and DA of 0.01 ml and this amount was increased by 0.01 ml until the total amount injected to the samples was 0.05 ml. The purpose of this experiment is to observe the effect of sensor sensitivity with water and also DA of different concentrations. Table 6.18 shows the measurement data collected from the experiment. Result from the experiment is shown in figure 6.27, where the sensor able to clearly discriminate the water and also the DA at different concentrations. Results from both experiments indicate that novel interdigital sensing system has a good potential to detect the contaminated domoic acid in mussels.

Table 6.18: Measurement data of samples injected with water and domoic acid of different concentrations

Sample Number	SurfaceTemp	Amount of chemical, ml	Sensor Sensitivity for water and DA of different concentrations					
			Water	10.1 µg DA	21.2 µg DA	42.5 µg DA	85.0 µg DA	170 µg DA
1	21.3	0.00	15.11	15.88	15.88	15.07	15.07	15.53
2	21.6	0.01	16.81	18.69	18.69	19.48	19.48	18.98
3	21.4	0.02	18.47	20.54	20.54	21.24	21.24	20.69
4	21.4	0.03	19.33	21.50	22.43	23.02	23.02	23.28
5	21.3	0.04	21.00	23.36	24.28	24.78	25.69	25.88
6	21.4	0.05	22.69	24.28	26.17	26.56	27.44	28.44

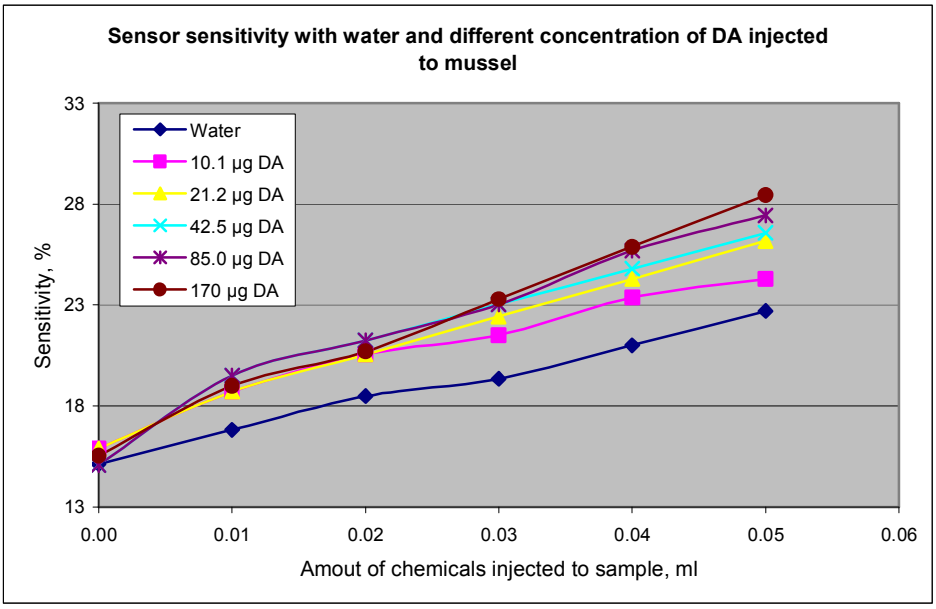

Figure 6.27: Sensor sensitivity with water and different concentrations of DA injected to the mussels

Further experiment with DA was conducted by injecting 1.0 µg of DA into several mussel samples of different thickness. The experiment was conducted to find the threshold level of sensor sensitivity with respect to sample thickness. The sensitivity will change depends on the corresponding samples thickness, therefore it is very important to determine the sensitivity threshold level of samples at different thickness. Data was collected for normal samples and also samples injected with DA of respective samples thickness. The experiment was conducted at a room temperature of 22 ℃ with humidity of 42%. Figure 6.28 shows that the threshold sensitivity level can be determined with respect to different thickness of mussel samples. There are three level of sensitivity threshold that were observed from the experiment. The result is simplified into a table shown in Table 6.19.

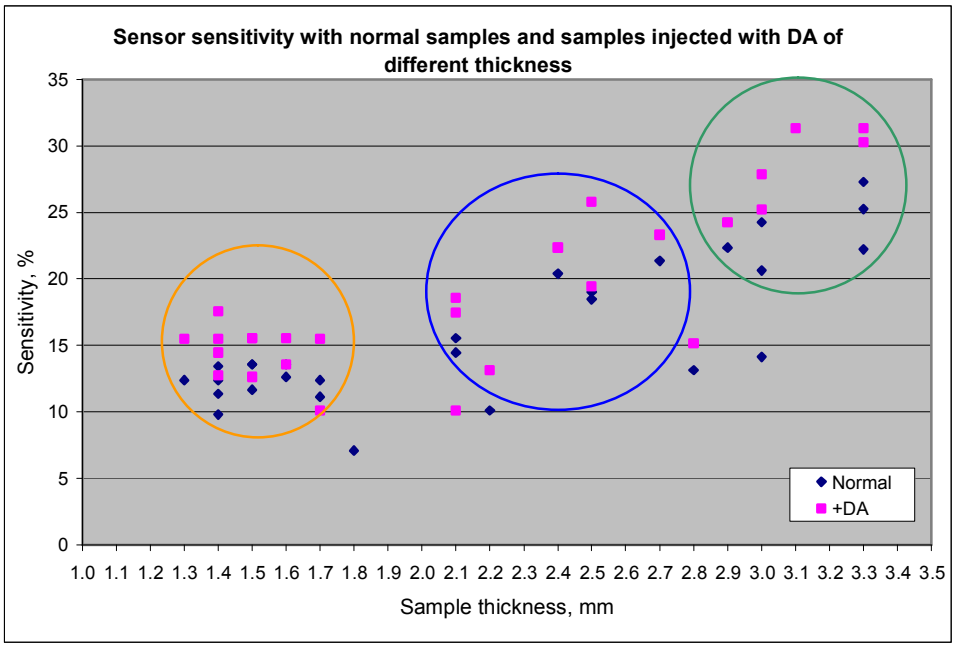

Figure 6.28: Sensitivity threshold levels for normal samples and samples injected with DA of different thickness

Table 6.18: Sensitivity threshold level with respect to sample thickness

Sample Thickness, mm	No. of Samples	Threshold Sensitivity, %	Sensor Detection
1.3 – 1.9	23	13.0	Yes
2.0 – 2.8	17	19.0	Yes
2.9 – 3.4	13	25.0	Yes

6.7 Conclusion

Initial studies were conducted with three chemicals (sarcosine, proline and hydroxylproline) to evaluate which of the fabricated sensors (conventional and novel interdigital sensors) give a good response and could clearly discriminate between these three chemicals. Results from the initial studies have shown that novel interdigital sensors have better sensing performance compared to the conventional sensors. It is also shown that novel interdigital Sensor_1 was the best among all sensors. Experiments of novel interdigital sensors with seafood products have shown that all sensors respond very well with seafood products. Results also shown that Sensor_1 shows better sensitivity compared to other novel interdigital sensors. Sensor_1 has been chosen for further analysis with proline and domoic acid (DA). Sensor_1 has shown a good response with proline. Results from experiments, have shown that Sensor_1 was able to detect the small amount of proline presence in mussel samples. It can be said that Sensor_1 can be used to detect small percentage of domoic acid (DA) in mussel samples. Experimental results with DA have shown that Sensor_1 was able to detect approximately 12.6 µg/g of DA in mussel meat (regulatory guideline for DA is 20 µg/g). The sensor has the potential to detect an amount even lower than 10 µg/g of DA in mussel meat. Results of experiments with water and different concentration of DA have shown that Sensor_1 able to clearly discriminate the water and also the DA at different concentrations. The threshold sensitivity level can be determined with respect to different thickness of mussel samples. There are three levels of sensitivity threshold that were observed from the experiment. This result can be used as a guideline to a user (for e.g. fisherman having a little technical knowledge) who will conduct the pre-screening or sampling process at their site. Results from experiments with DA indicate that novel interdigital sensing system has a good potential to detect the contaminated DA in seafood.

Chapter 7

Development of A Low Cost Sensing System

7.1 Introduction

A low cost sensing system for inspection of raw seafood was developed. The developed low cost sensing system may be used by fisherman for first-hand pre-screening process. The sensing system analyse the samples from the ranch site and then provide pass or fail analysis. If the results showing certain number of fail analysis (suspicious results), the samples at that ranch site have to be sent to the laboratory for further analysis of contaminated chemicals (DA) in the seafood using expensive techniques. The developed sensing system is easy to be used for the purpose of sampling inspection and can provide fast analysis of DA within shellfish meat for in-situ monitoring. The developed sensing system should be reliable and cost effective.

The developed low cost sensing system consist of microcontroller, novel interdigital sensor, power supply circuit from 9V battery and signal processing circuit. This chapter will highlight details on the embedded system developed for a low cost sensing system called Seafood Inspection Tool or SIT.

7.2 Interfacing to Microcontroller

A SiLab C8051F020 microcontroller was used both for generating the necessary excitation signal as well as for data acquisition. The main purpose of using microcontroller based sensing system is to develop a low-cost system. A SiLab C8051F020 microcontroller board is shown in figure 7.1. The micro-controller was programmed to generate a sinusoidal voltage for excitation of the sensor. A sinusoidal waveform of 7.5 V peak-to-peaks at an operating frequency of 10 kHz was generated. The stepped sine wave was first generated by the micro-controller and the smoothed sine wave was obtained from a smoothing circuit output, which was fabricated on a single fabricated board of signal processing circuit.

The signal coming from the sensor is alternating in nature. The interfacing circuit used for this setup is shown in figure 7.2. The sensor input needs to have an offset since the 12-Bit Analog to Digital Converter (ADC) cannot process values less than zero.

Figure 7.1: A SiLab C8051F020 microcontroller board

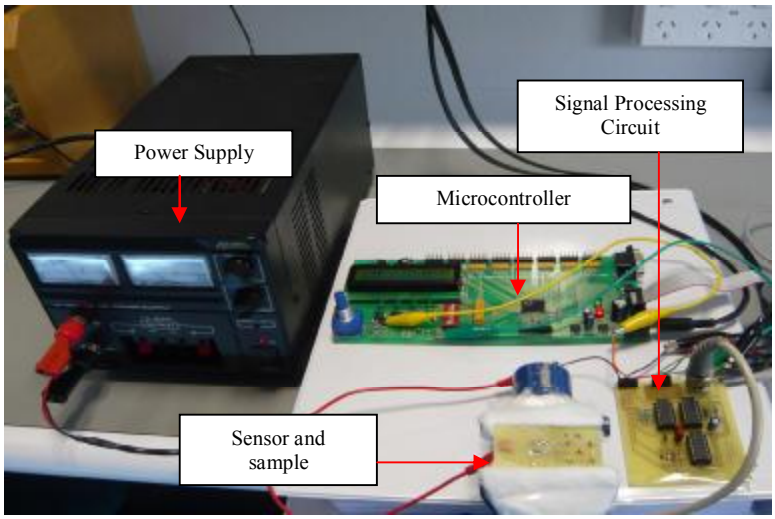

Figure 7.2: Experimental setup of a low cost sensing system

Two LM324 Low Power Quad Operational Amplifier were used in the circuit. The sensor signal is amplified by a gain of around 8.2. VCC is set to 9V, and a Zener diode can be used as a protection to make sure the signal into the ADC input in the microcontroller doesn't exceed 3.3 V as the microcontroller C8051F020 operates at 3.3 V. The output signal from the sensor was fed to the ADC pin of the microcontroller. The program is developed to set the calibration with air and then read the measurement value with samples. The sensor sensitivity was calculated from the measurement data. So as the response of the sensor changes with the

samples, the output digital value will change accordingly. The pass and fail analysis will be display on the LCD and LED will be on.

7.2.1 Initialisation of Important Parts of Microcontroller

The ADC and DAC use a 2.4 V reference by default. The stepped sine wave was first generated by the microcontroller for the excitation voltage. It was generated from DAC 0 and is connected to a sine-wave smoothing circuit, to obtain a desired excitation signals. AIN0.2 was selected to be the sensor input in order to get digital values. The initialisation of ADC and DAC are as follows:

```
//-----------------------------------------------------------------------------
// converter_init
//-----------------------------------------------------------------------------
//
//              Initialise the required ADCs and DACs
//
void converter_init(void) {

        //--- Set up ADCs & DACs ---
        // Enable the internal bias generator & internal refernece buffer.
        // ==> ADCs & DACs use a 2.4V reference by default
        // Configure the reference for ADC0 to be the VREF0 pin. Turn the temperature sensor off.
        REF0CN = 0x03;

        //*** ADCs ***
        ADC0CF = 0x38;                          // SAR0 conversion clock ~2.2 MHz, gain = 1

        AMX0CF = 0x00;                          // Configure for 8 single-ended inputs
        AMX0SL = 0x02;                          // Select AIN0.2 (sensor input)
        ADC0CN = 0x80;                          // Enable ADC0 in continuous Tracking Mode
                                                // Conversion initiated on write to AD0BUSY
                                                // ADC0 data is right justified

        EIE2 |= 0x02;                           // Enable ADC0 interrupt


        //*** DACs ***
        DAC0CN = 0x80;                          // Enable DAC0 in on demand mode;
                                                // Data is left justified
        DAC1CN = 0x87;                          // Enable DAC1 in on demand mode;
                                                // Data is left justified


        DAC1H = 0x63;                           // Set a reasonable contrast (in case DAC1 is
                                                // controlling contrast)
}
```

The sine wave is generated by a sequence of 20 digital samples. The sine wave was program using Timer 3. Timer 3 is initialised as follows:

```
//-----------------------------------------------------------------------------
// sine_timer_init
//-----------------------------------------------------------------------------
//              Initialise timer 3 in preparation for using it to generate a sine wave
//
void sine_timer_init(void) {

              TMR3CN = 0x06;                                  // Timer 3 uses the system clock; clear its interrupt flag
              TMR3 = 0xFFFF;                                  // The timer will overflow straight away
              TMR3RL = 0xFF5F;                                // The timer counts from 0x0000 to 0xFFFF
              EIE2 |= 0x01;                                   // Enable timer 3's interrupt
              EIP2 |= 0x01;                                   // This interrupt is high priority
              TMR3CN |= 0x04;                                 // Start the timer
}
```

The sensor related variables used in the program as indicated by AIR is the digital value of the sensor output with air (NO sample), SENSE is the initial digital value of sensor output with sample, TRESH is the threshold value which in this initial design is set to 2048, NEW_SENSE is the new digital value of the sensor output and VIRT_TICKS is used for virtual timer. Software initialisation is as follows:

```
//-----------------------------------------------------------------------------
// software_init
//-----------------------------------------------------------------------------
// This function initialises all the global variables
//
void software_init(void) {

              //--- Sensor Related Variables
              AIR = 0;
              SENSE = 0x0019;
              THRESH = 2048;                  // Change the treshold value for DEMO
              NEW_SENSE = 0;
              VIRT_TICKS = 0;
              //--- Sine Wave Generator Related Variables ---
              SINE_SAMPLES = 20;
              SINE_INDEX = 0;
}
```

Hardware initialisation function is used to disable the watch dog timer, to set up the clock, to set up the crossbar and to configure the required LED for the indicator of power, pass and fail results. The hardware initialisation is follows:

```
//-------------------------------------------------------------------------
// hardware_init
//-------------------------------------------------------------------------
// Hardware related initialisation
//
void hardware_init(void) {

        //--- Disable watch dog timer ---
        WDTCN = 0x07;
        WDTCN = 0xDE;
        WDTCN = 0xAD;

        //--- Set up the clock ---
        OSCXCN = 0x00;                                  // Don't use any external oscillators
        OSCICN = 0x07;                                  // Instead use the internal 16MHz clock
        while ((OSCICN & 0x10) == 0);                   // Wait for the oscillator to stabilize
        //--- Set up the crossbar ---
        XBR2 = 0x40;                                    // Crossbar is enabled
        //--- Configure ports 0..3 ---
        //*** OUTPUTS ***
        // Push-pull:          P1.6 (LED)
        //                                  P2.0-2 (Indicator LEDs)
        //*** INPUTS ***
        // Open drain:         P3.7 (Start button)

        P0MDOUT = 0x00;
        P1MDOUT = 0x40;                                 // P1.6 is in push-pull mode
        P2MDOUT = 0xFF;                                 // P2.0-2 are in push-pull mode
        P3MDOUT = 0x00;                                 // P3.7 is open drain

        // Write logic 1 to inputs
        P3 = 0x80;
        //--- Configure ports 4..7 ---
        //*** OUTPUTS ***
        // Push-pull:          P7.0 - P7.3 (LCD control)
        // Open drain:         P6 (LCD data)

        P74OUT = 0x40;
        P2 = 0x01;                                      // Turn on the power LED
}
```

7.3 Electronics and Signal Processing Circuit for the Low Cost Sensing System

Efficient data acquisition system is very important in the development of a low cost sensing system. Since the output measurement from the sensor is small (in mV) therefore a good circuit design has to be designed and developed to minimise the effect of noise. A signal processing circuit consist of sine-wave smoothing circuit and signal conditioning circuit were developed to be connected to the microcontroller. Both circuits were fabricated on a single board as shown in figure 7.3.

The main function of the software is to initialise all components ready for testing, then calls introScreen to let the user run through a complete test or run individual tests via serial control. The main function of the program code is follows:

```
//-------------------------------------------------------------------------
// main routine
//-------------------------------------------------------------------------
//
// The main function initialises all components ready for testing, then calls
// introScreen to let the user run through a complete test or run individual tests
// via serial control.
//
main() {

        uint reading = 0;
        bit first = 1;

        EA = 0;                                         // Disable all interrupts temporarily
        software_init();
        hardware_init();
        lcd_init();
        reading_timer_init();
        sine_timer_init();
        converter_init();
        EA = 1;                                         // Re-enable all interrupts

        AD0BUSY = 1;                                    // Start monitoring the sensor

//      while (1) {                                     // Forever...

                lcd_reset();
                printf("Press <START>");
                lcd_goto(0x40);
                printf("to calibrate");

                while (P3 | 0x7F != 0x7F) {     // Wait for the user
                        // wait...
                }

                calibrate();

                lcd_reset();
                printf("Press <START>");
                lcd_goto(0x40);
                printf("to Measure");

                while (P3 | 0x7F != 0x7F) {     // Wait for the user
                        // wait...
                }
```

```
                VIRT_TICKS = 0;
                reading = SENSE;

                while (VIRT_TICKS < 40) {                    // For ~2 seconds
                        if (NEW_SENSE) {                              // New reading to incorporate in the average
                                NEW_SENSE = 0;
                                reading = (reading + SENSE) >> 1;
                                meter();
                        }
                }
                reading = SENSE - AIR;
                lcd_reset();
                lcd_goto(0x40);
                printf("Press <RESET> ", reading);
                lcd_goto(0x0C);
                if (reading > THRESH) {
                // failed
                        printf("FAIL");
                        P2 |= 0x14;                                                   // Turn on the fail LED
                }
                else {
                // passed
                        printf("PASS");
                        P2 |= 0x40;                                                   // Turn on the pass LED
                }
                while (1) {
                                                                                      // stop the program here
                }

}
```

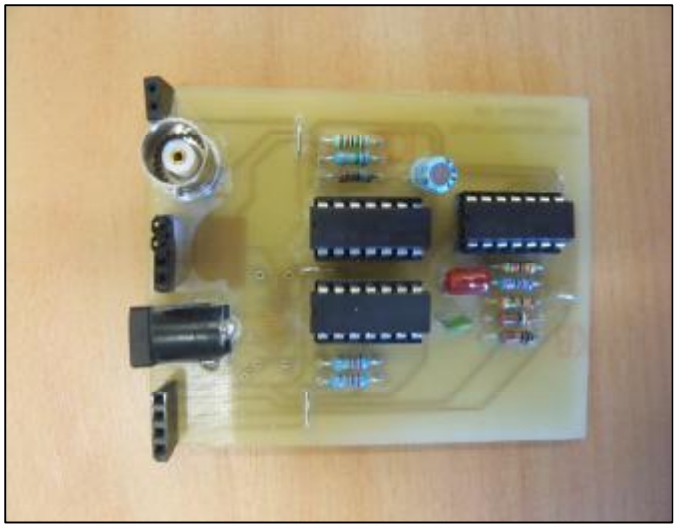

Figure 7.3: Fabricated electronic circuit for signal processing

7.3.1 Smooth Sine Wave Generation

The smoothed sine wave was obtained using a smoothing circuit. The circuit diagram of sine-wave smoothing circuit is shown in figure 7.4. The step sine wave generated by the microcontroller has high frequency, therefore a low pass filter is needed to make the sine wave has smooth steps. The decoupling capacitor was used to dampen the noise. A pull down resistor of 1 MΩ was used to bring the sine wave at zero axis. The 100 kΩ resistor is used to minimise the current input to the non-inverting op-amp to get a better gain. The sine-wave generated by the micro-controller before and after the smoothing circuit is shown in figure 7.5. The developed sine wave was used as excitation signal and is fed to the developed novel interdigital sensor.

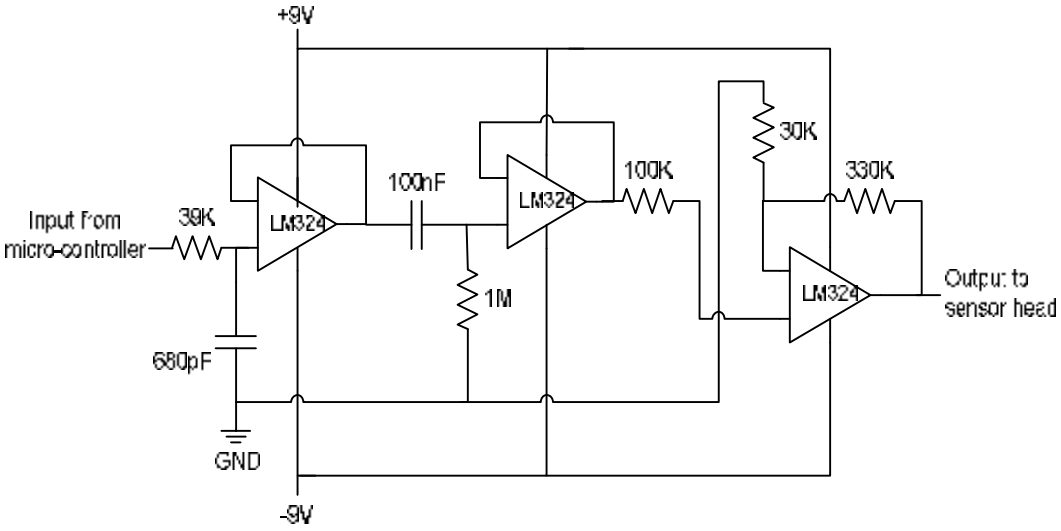

Figure 7.4: Sine-wave smoothing circuit

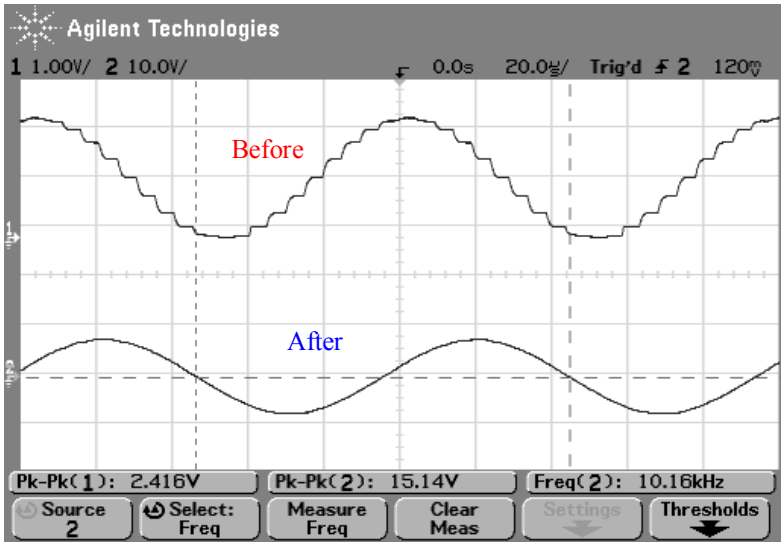

Figure 7.5: Sine-wave generated by the micro-controller before and after the smoothing circuit

7.3.2 Signal Rectification and Amplification

The second part of the signal processing circuit is the signal conditioning circuit. This signal conditioning circuit were built by several operational amplifiers in order to develop a good signal conditioning of sensor signals. A signal conditioning circuit has been fabricated for interfacing the sensor signal to the microcontroller as shown in figure 7.6. It consists of a full wave rectification circuit and an amplification circuit. An ideal output signal of full wave rectifier is shown in figure 7.7, where circuit's input signal at V_{IN}; its intermediate voltage, V_{HALF}; and its output voltage, V_{OUT}.

The operation of the circuit is as follows: The output voltage from sensor is fed to the op-amp #1 to generate a full sine wave input (positive and negative) as shown in figure 7.8. If the input voltage form the sensor, V_{SEN}>0V, then the output from Op-amp #2, V_{HALF}, equals $V_{SEN}/2$. The half wave generated is shown in figure 7.9. Op-amp #3 operates as a substracter, delivering an output voltage, V_{OUT}, equals V_{SEN} (other half of the signals). In effect, the circuit operates as a unity-gain follower. If V_{SEN}, is 0V, then V_{HALF} = 0V, and the circuit behaves as a unity-gain inverter and delivers an output of $V_{OUT} = -V_{SEN}$. The rectified voltage will pass through the op-amp #4 with gain of 8.2. The amplified signal is shown in figure 7.10. The amplified signal will pass through a low pass filter with a cut off frequency of 13 Hz. The dc signal from op-amp #5 is connected to a digital input of the microcontroller for the necessary conversion into digital value.

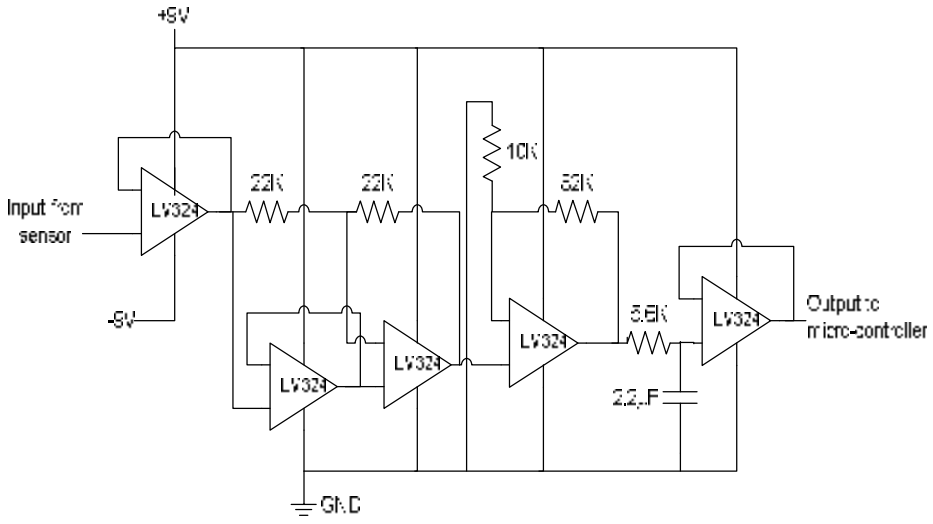

Figure 7.6: Signal conditioning circuit diagram

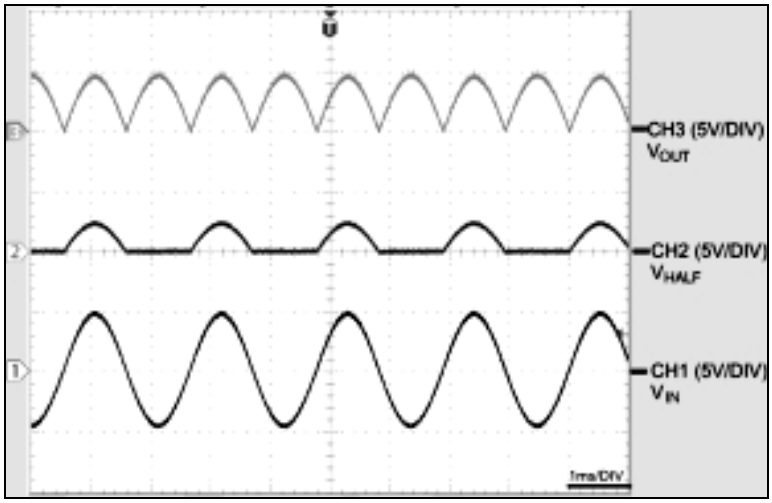

Figure 7.7: Ideal output signal of full wave rectifier. From bottom to top, the waveforms show VIN (CH1), VHALF (CH2), and VOUT (CH3).

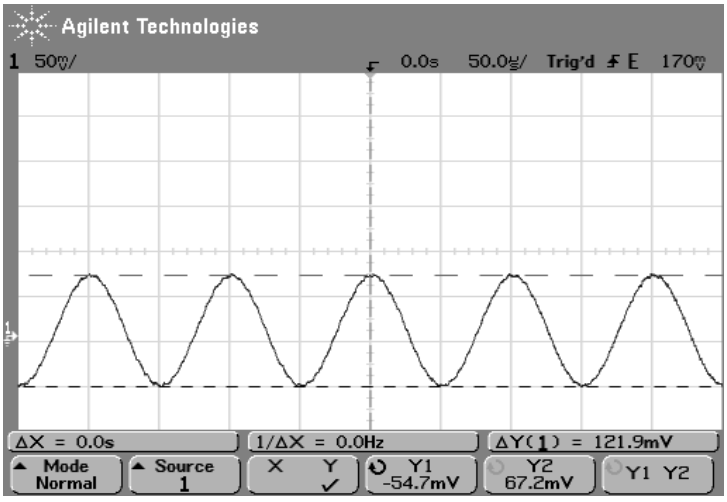

Figure 7.8: Signal from the sensor output feed to full wave signal rectification circuit

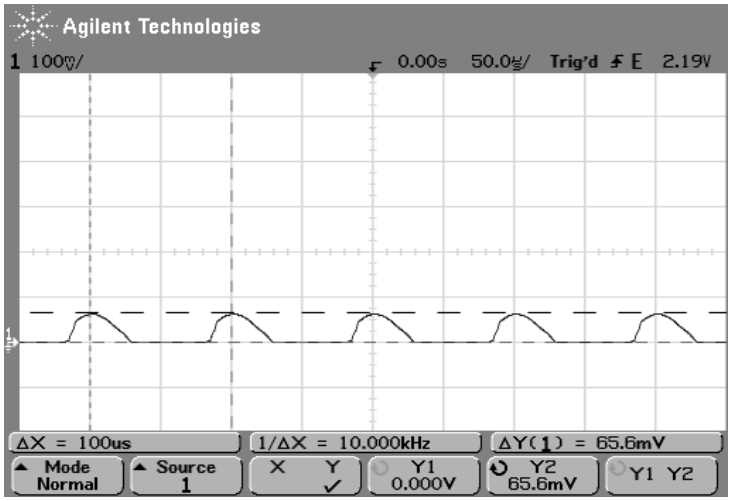

Figure 7.9: Half wave signal

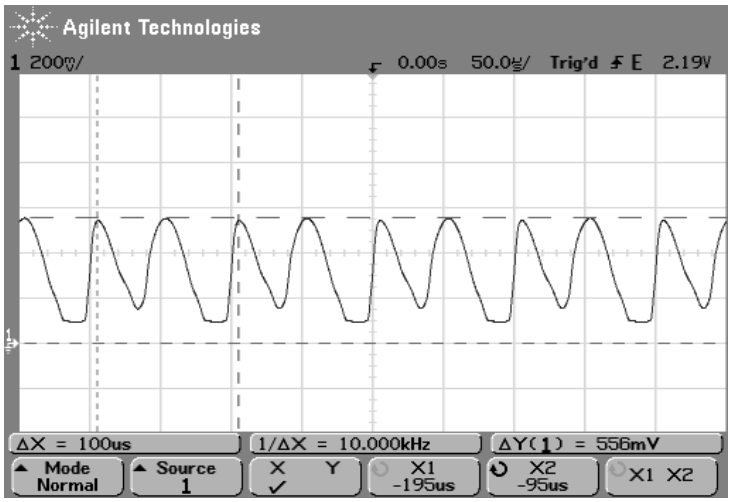

Figure 7.10: Full-wave rectification after introduce gain of 8.2

7.4 Calibration, Sensitivity Threshold and Signal Definitions

The sensing system need to be calibrated before it can start measurement and provide analysis of the samples under test. The calibration is based on the digital value of the sensor output at air, ADC_{AIR} (sensor without sample). The microcontroller will read this data first and use this data for calibration. The sample with known thickness will be placed on the sensor for measurement. The microcontroller then recorded the sensor reading in terms of digital value of that sample, ADC_{OUT}. The sensitivity measurement of the sensor is then given by;

$$Sensitivity = \frac{(ADC_{OUT} - ADC_{AIR})}{ADC_{AIR}} * 100 \quad (12)$$

where

ADC_{AIR} = Digital value of the sensor output at air

ADC_{OUT} = Digital value of the sensor output with sample

The current sensitivity value is compared to the sensitivity threshold (obtained from the calibrated experiments) to get a pass or fail analysis of the particular samples. The initial code was designed as a demo version which only calibrates and compares the measurement data from the sensor with a single threshold value (2048). The above formula and the threshold values obtained from the experiment are not in the code as follows:

```
//---------------------------------------------------------------------------
// calibrate
//---------------------------------------------------------------------------
//
// Calibrate the sensor by sensing the air for ~2 seconds (to get a good average
// reading)
//
void calibrate(void) {

        uchar count = 0;
        bit flash = 0;

        lcd_reset();
        printf("Prepare to");
        lcd_goto(0x40);
        printf("calibrate sensor");
        huge_delay(50);

        while (P3 | 0x7F != 0x7F) {                     // While the user hasn't responded...// Flash text
                if  (!flash) {                          // If flash is off...
                        lcd_goto(0x00);
                        printf("Press the button");
                        lcd_goto(0x40);
                        printf("   when ready   ");
                }
                else {

                        lcd_reset();
                }

                large_delay(122);                       // Check the button every 10ms or so

                if (count == 25) {                      // Flash on for 35ms
                        count = 0;
                        flash = ~flash;
                }
                count++;
        }

        lcd_reset();
        printf("Calibrating...");
        AIR = SENSE;
        T4 = 0;
        VIRT_TICKS = 0;

        while (VIRT_TICKS < 40) {                       // For ~2 seconds
                if (NEW_SENSE) {                        // New reading to incorporate in the average
                        NEW_SENSE = 0;
                        AIR = (AIR + SENSE) >> 1;
                        meter();
                }
        }

}
```

7.5 Power Supply for A Low Cost Sensing System

A dc voltage of ± 9 V is needed to power the developed sensing system. A battery of 9V supply was introduced to the sensing system. A negative 9V power supply was generated using the NE 555. The circuit diagram in figure 7.11 show how negative 9V is generated from a 9V battery. The fabricated power supply board is shown in figure 7.12. The generated negative voltage together with the positive supply was used to power the op-amps and other circuits requiring a dual supply.

The NE 555 operates as an astable multivibrator. A square wave is obtained at the Output pin 3 of the IC. The 22uF capacitor charges through the diode D1(1N4001) when the output is positive. When the output at pin 3 is ground, the 22uF discharges through the diode D2 (1N4001) and charges the 100uF capacitor is charged. The output is taken across the 100uF capacitor.

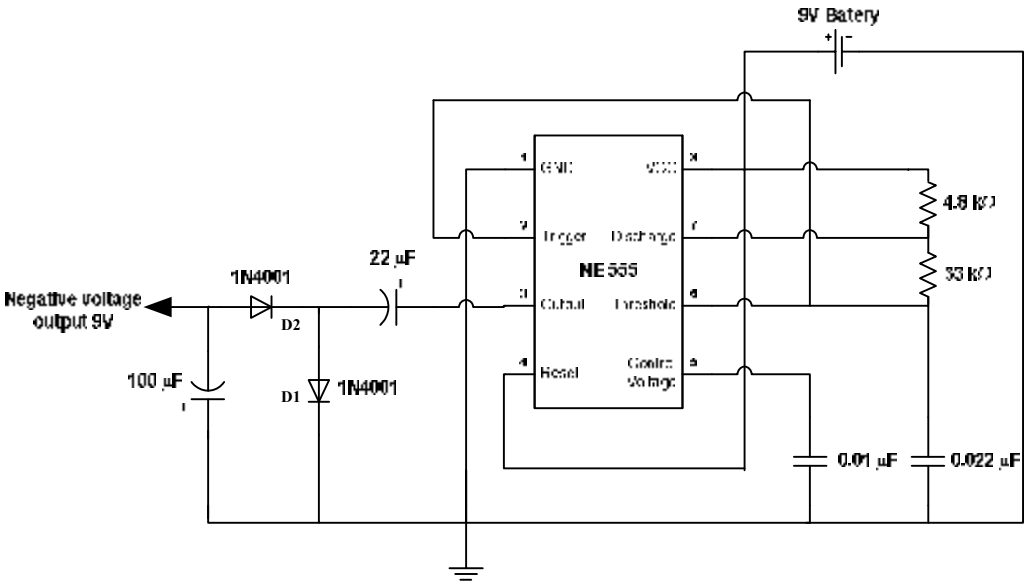

Figure 7.11: A negative voltage from a single positive supply

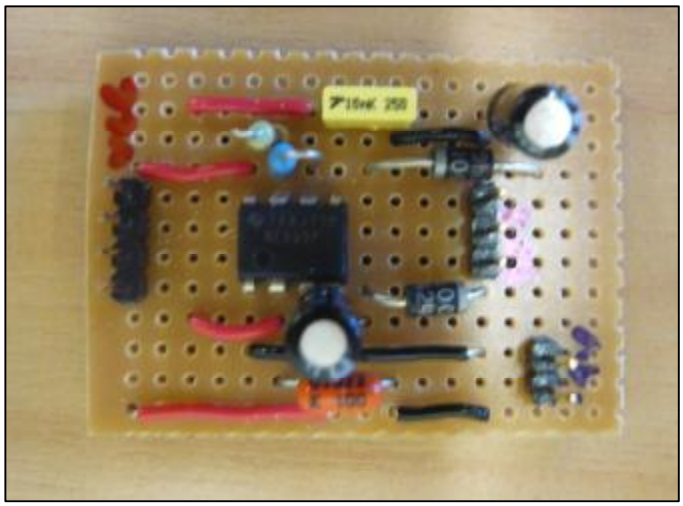

Figure 7.12: Fabricated electronic circuit to power the sensing system

7.6 Prototype of Seafood Inspection Tool (SIT)

The first prototype of seafood inspection tool (SIT) was developed to detect the domoic acid (DA) in mussels. SIT consist of ± 9 V power supply, novel planar interdigital sensor, a SiLab C8051F020 microcontroller, a signal processing circuit and an expansion board (for display). A user friendly software was developed to make it ease of use. It can be used by anyone especially by fisherman for pre-screening process at the ranch site. The first prototype of SIT is shown in figure 7.13.

Figure 7.13: Seafood Inspection Tool (1st prototype)

7.7 Conclusion

Smart sensing system for health and environmental was developed to be used to access the contaminated seafood with marine bio-toxins. A low cost sensing system using microcontroller and local fabricated board has been developed. This chapter has discussed the development of each component of the low cost sensing system. The first prototype of SIT was introduced to help the fisherman to conduct pre-screening process for domoic acid detection. If the results of from the sampling are suspicious, the whole products should be isolated and detail analysis using expensive equipments (laboratory analysis) should be conducted.

Chapter 8

Conclusion

The works in this thesis was mainly to get a first-hand information about the seafood poisoning issues i.e., to detect dangerous contaminated chemical produced by marine bio-toxins. Amnesic Shellfish Poisoning that was caused by eating contaminated mussels with domoic acid was the main concern of the research work that has been conducted for this thesis. Therefore, it is important to design and develop a tool which can provide a fast analysis of seafood poisoning before the products can be released to the market. The tool can be used easily by the fisherman at the ranch site for pre-screening process. If the result from analysis is suspicious the seafood products should be isolated and samples need to be sent to laboratory for detailed analysis using expensive equipment.

This thesis includes the design, fabrication and analysis of conventional planar interdigital sensors and novel planar interdigital sensors. The principles behind planar interdigital sensors have been used in many new technologies of various research areas. Planar interdigital sensors were used as the non-destructive techniques because they can provide reliable, fast and rapid analysis. The interdigital sensors are capacitive type and are based on the measurement of capacitance and capacitive reactance. The interdigital sensors have a strong response to materials with high dielectric properties especially liquid. That is why the interdigital type of sensors was chosen to detect the presence of small amount of domoic acid in mussels. Detailed designs of the fabricated sensors were discussed and analysis of the sensor designed has been reported using circuit analysis and simulation with COMSOL Multiphysics. Both analyses have indicated that novel planar interdigital sensors can be one of the options to access the chemical structure in material under test (MUT). The experimental results supported both analyses.

Three peptide derivatives namely sarcosine, proline and hydroxylproline were used for the initial studies, which are structurally close to the target molecule (domoic acid). The initial goal is to evaluate which of these fabricated sensors give a good response and could discriminate well between these three different chemical samples. Among these three

chemical samples, proline molecule is arguably the most important amino acid in peptide conformation, containing the basic structural similarity to the domoic acid.

Three conventional sensors were first designed and fabricated. The response of the sensors with chemical samples were analysed and it was shown that these sensors can detect the presence of different chemicals on the each sensor. The conventional sensor with configuration #3 has shown better sensitivity measurement compared to other conventional sensors. This is because conventional sensor with configuration #3 has better penetration depth, higher capacitive reactance value and has uniform distribution of electric field strength. It was found that these characteristics related to the number of negative electrodes designed for the particular sensor. This initial result has given us idea to design and to fabricate better sensors with more number of negative electrodes in between the positive electrodes.

Three novel interdigital sensors have been designed, fabricated and tested. The optimum number of negative electrodes is important in the design consideration of interdigital sensors. Sensor with greater penetration depth has uniformity of electric field distribution and uniformity of capacitance distribution within sensor geometry contributes to better sensitivity measurement. Results from circuit analysis and COMSOL simulations have shown that these three factors are very important for planar interdigital sensor design. All novel interdigital sensors were designed to have 13 numbers of electrodes, having the same effective area and electrodes spacing. Results from circuit analysis and simulation also have shown that sensor with configuration #1 (Sensor_1) has a better sensor sensitivity compared to other novel interdigital sensors.

Initial studies with three chemicals samples have shown that the fabricated novel interdigital sensors can respond very well to each sample and can clearly discriminate between them. Experimental results also shown that novel interdigital sensors have better sensitivity measurement compared to the conventional sensors. Experiments with seafood products were conducted to choose the best novel interdigital sensor. Samples of fish, mussel and squid were prepared for the experiments. Results from the experiments have shown that all novel interdigital sensors respond very well with seafood products. Results also shown that Sensor_1 shows better response and give better sensitivity measurement compared to other novel interdigital sensors. Results from the initial studies and experiments with seafood

products have shown that Sensor_1 was the best sensor. Therefore, Sensor_1 has been chosen for further analysis with proline and domoic acid (DA).

Experimental results with mussels and proline have shown that Sensor_1 can detect the presence of proline on the surface as well as injected proline to each sample. Sensor_1 was also able to detect the presence of different amount of proline, which is structurally close to domoic acid chemical structure. Results from the experiments also indicated that the presence of small amount of proline can be estimated by using the linear equation obtained from the experiment. Therefore, Sensor_1 can be used for the experiment with domoic acid which is actually more expensive compared to those three chemicals used for the initial studies.

Experiments with domoic acid have shown that novel interdigital sensor can be used to detect the small amount of domoic acid in mussels. The experimental results have shown that Sensor_1 was able to detect approximately 12.6 µg/g of DA in mussel meat. The sensor detection is very good as the regulatory guideline for DA is 20 µg/g. The sensor has the potential to detect an amount even lower than 10 µg/g of DA in mussel meat with some precautions. Results on the effect of water and different concentration of DA were also presented, where the sensor is able to clearly discriminate the water and also the DA at different concentrations. Threshold levels of sensor's sensitivity with different mussel thickness were also established. Mussels sample thickness of 1.3 mm – 1.9 mm, the threshold sensitivity level was 13%. Samples with thickness of 2.0 mm – 2.8 mm will have the threshold level of 19%. And for samples of 2.9 mm – 3.4 mm, the threshold level was 25%. This result will be used as a guideline to a user (for e.g. fisherman having a little technical knowledge) who will conduct the pre-screening or sampling process at their ranch site. Results from the experiments have shown that the novel interdigital sensing system has the potential to be one of the options to assess the quality of seafood products for in-situ monitoring. The outcomes from the experiments provide chances of opportunity for further research in developing a low cost miniature type of sensors with reliable sensing system for commercial use.

A smart sensing system for health and environmental was developed to be used to access the contaminated seafood with marine bio-toxins. We have developed a low cost smart sensing system using a microcontroller and local fabricated circuits with dual supply and

signal processing for data acquisition. The first prototype is called seafood inspection tool or SIT consist of a SiLab C8051F020 microcontroller, a signal processing circuit, novel planar interdigital sensor, an expansion board (for display) and dual power supply circuit. A user friendly software was also developed to make SIT easy to be used by users who has a little technical knowledge. SIT was developed to be tested by the fisherman who can do a pre-screening process of the mussels at their ranch site. With SIT they can do a fast sampling check and if the result from the sampling is bad, the whole mussels should be isolated for details analysis using high sophisticated equipments.

Chapter 9

Future Work

Further research work need to be conducted for detection of different acids presents in seafood. The works done for this thesis only evaluate water, domoic acids and chemicals which are closely related to domoic acids. We believe that there are other acids that can affect the result of the sensor sensitivity. Therefore continuous studies should be conducted to access these chemicals. Identification of these chemicals will help to develop a reliable sensing system in the future.

The effect of temperature, water content, and humidity will also affect the results. A proper experiment need to be conducted in an environmental chamber where the effect of temperature and humidity can be controlled. It is important to evaluate these parameters as both can give significant effect of the sensor sensitivity. Water content in the material should also be analysed and evaluate. This is because the water content has strong effect for planar interdigital sensor. The effect of temperature and humidity can be included in the software.

There is a need of developing a comprehensive model for accurate prediction. The model could be used as a reference for certain contaminated chemicals in seafood products. This comprehensive model is also important in developing a reliable tool to access the contaminated seafood with marine bio-toxins. Detail experiments need to be conducted in order to develop the comprehensive model.

A new approach should be considered of developing novel planar interdigital sensor with different substrate layers. There are three possible layers, which are conducting layer, shielding layer and ground layer. This design will improve the sensor sensitivity as well as to make a reliable sensor. A collaborative work with other agencies or universities should be emphasised in order to get the facilities of developing this kind of sensors. One professor from University of North Illinois has already agreed to do collaborative research in developing novel interdigital sensors of different substrate layer. The designed of the novel planar interdigital sensor will be redesigned to make it suitable to be fabricated for different layers.

It is important to develop a small and compact tool for the second prototype of SIT. There is a need to develop a new microcontroller circuit board which is even smaller than the current microcontroller used for SIT. This is because only a few ports of the current microcontroller were used. The display can be reduced to a smaller size, better resolution and with small power usage. The size for dual supply and the signal processing circuit can be reduced and make them more compact. The second prototype should be smaller and more compact compared to the first prototype. The developed system should be able to operate from a small 3V battery.

There is a strong possibility of using novel planar interdigital sensor to detect dangerous pathogens or biological agents (bacteria, viruses or toxins) on food, which is used for bioterrorism. Human exposure to pathogens may occur through inhalation, skin exposure, or ingestion of contaminated food or water. The planar interdigital sensor could be used to access the contaminated food with the pathogens by sensing the difference of dielectric properties of food that is affected with the pathogens.

Chapter 10

References:

[1] M. J. Usher, *Sensors and transducers* London: Macmillan, 1985.

[2] P. D. Andersen, B. H. Jorgensen, L. Lading, and B. Rasmussen, "Sensor foresight - technology and market," *Technovation,* vol. 24, pp. 311-320, Apr 2004.

[3] N. Schroder, "Sensor Markets 2008: Worldwide Analyses and Forecasts for Sensor Markets until 2008," Intechno Consulting, Basle, Switzerland, pp. 1-11, May 12 1999.

[4] L. M. Davies, "Role of NDT in condition based maintenance of nuclear power plant components," in *15th World Conference on Nondestructive Testing*, Roma, Italy, pp. 239-245, 15-21 Oct 2000.

[5] N. J. Goldfine, " Magnetometers for improved material characterization in aerospace application," *Material Evaluation,* pp. 396-405, 1993.

[6] N. J. Goldfine, D. Clark, and T. Lovett, "Material characterization using model based meandering winding eddy current testing (MW-ET)." in *EPRI Topical workshop: Electromagnetic NDE applications in the Electric Power Industry* Charlotte, N Carolina (USA), pp. 285-292, 1995.

[7] Y. Bi, M. R. Gobindaraju, and D. C. Jiles, "The dependence of magnetic properties on fatigue in A533B nuclear pressure vessel steels.," *IEEE Transactions on Magnetics* pp. 3928-3930, 1997.

[8] Y. Shi and D. C. Jiles, "Finite element analysis of the influence of a fatigue crack on magnetic properties of steel. ," *Journal of Applied Physics* pp. 6353-6355., 1998.

[9] Y. Bi and D. C. Jiles, "Dependence of magnetic properties on crack size in steels.," *IEEE Transactions on Magnetics* pp. 2021-2023, 1998.

[10] H. Thiele, "NDT Methods for Surveillance of Plants in Chemical and Petrochemical Industry," in *7th European Conference on Non-Destructive Testing (ECNDT)*, Copenhagen, pp. 92-95, 1998.

[11] D. F. Cannon, K. O. Edel, S. L. Grassie, and K. Sawley, "Rail defects: An overview," *Fatigue & Fracture of Engineering Materials & Structures,* vol. 26, pp. 865-886, 2003.

[12] S. C. Mukhopadhyay, "Novel high performance planar electromagnetic sensors," *The e-Journal on Nondestructive Testing,* vol. 10, Aug 2005.

[13] C. P. Gooneratne, "Planar Electromagnetic Sensors: Characteristic and Experimental Results," *Institute of Information Sciences and Technology*. Master of Engineering Thesis, Palmerston North: Massey University, pp. 1-108, 2005.

[14] S. C. Mukhopadhyay, "A Novel Planar Mesh-Type Microelectromagnetic Sensor—Part II: Estimation of System Properties," *IEEE Sensors Journal,* vol. 4, pp. 308-312, 2004.

[15] S. C. Mukhopadhyay, "A novel planar mesh type micro-electromagnetic sensor: Part I - Model Formulation," *IEEE Sensors Journal,* vol. 4, pp. 301-307, 2004.

[16] S. Yamada, H. Fujiki, M. Iwahara, S. C. Mukhopadhyay, and F. P. Dawson, " Investigation of printed wiring board testing by using planar coil type ECT probe," *IEEE Transactions on Magnetics,* vol. 33, pp. 3376–3378, 1997.

[17] S. C. Mukhopadhyay, S. Yamada, and M. Iwahara, "Investigation of near-surface material properties using planar type meander coil," *JSAEM Studies on Applied Electromagnetics and Mechanics,* vol. 11, pp. 61–69, 2001.

[18] S. C. Mukhopadhyay, S. Yamada, and M. Iwahara, "Evaluation of near- surface material properties using planar mesh type coils with post-processing from neural network model. ," *International Journal on Electromagnetic Nondestuctive Evaluation,* vol. 23, pp. 181-188, 2002.

[19] S. C. Mukhopadhyay, S. Yamada, and M. Iwahara, "Experimental determination of optimum coil pitch for a planar mesh type micro-magnetic sensor," *IEEE Transactions on Magnetics,* vol. 38, pp. 3380-3382, 2002.
[20] S. C. Mukhopadhyay, S. Yamada, and M. Iwahara, "Optimum coil pitch selection for planar mesh type micro-magnetic sensor for the estimation of near-surface material properties " *JSAEM series on Applied Electromagnetics and Mechanics,* vol. 14, pp. 1-9, 2003.
[21] S. Yoshida, T. Gyoji, and K. Toda, "Position-Sensitive Photodetector Using Interdigital Electrodes on Pb2cro5 Thin-Films," *International Journal of Electronics,* vol. 68, pp. 525-531, Apr 1990.
[22] S. Averin, R. Sachot, J. Hugi, M. deFays, and M. Ilegems, "Two-dimensional device modeling and analysis of GaInAs metal-semiconductor-metal photodiode structures," *Journal of Applied Physics,* vol. 80, pp. 1553-1558, Aug 1 1996.
[23] S. H. Lee, S. L. Lee, H. Y. Kim, and T. Y. Eom, "Analysis of light efficiency in homogeneously aligned nematic liquid crystal display with interdigital electrodes," *Journal of the Korean Physical Society,* vol. 35, pp. S1111-S1114, Dec 1999.
[24] Y. J. Chen, C. L. Zhu, M. S. Cao, and T. H. Wang, "Photoresponse of SnO2 nanobelts grown in situ on interdigital electrodes," *Nanotechnology,* vol. 18, pp. -, Jul 18 2007.
[25] T. M. A. Gronewold, "Surface acoustic wave sensors in the bioanalytical field: Recent trends and challenges," *Analytica Chimica Acta,* vol. 603, pp. 119-128, Nov 12 2007.
[26] R. Weigel and R. Hauser, "Introduction to the special issue on acoustic wave sensors and applications," *Ieee Transactions on Ultrasonics Ferroelectrics and Frequency Control,* vol. 51, pp. 1365-1366, Nov 2004.
[27] S. Shiokawa and J. Kondoh, "Surface acoustic wave sensors," *Japanese Journal of Applied Physics Part 1-Regular Papers Brief Communications & Review Papers,* vol. 43, pp. 2799-2802, May 2004.
[28] B. Drafts, "Acoustic wave technology sensors," *Ieee Transactions on Microwave Theory and Techniques,* vol. 49, pp. 795-802, Apr 2001.
[29] M. Hoummady, A. Campitelli, and W. Wlodarski, "Acoustic wave sensors: design, sensing mechanisms and applications," *Smart Materials & Structures,* vol. 6, pp. 647-657, Dec 1997.
[30] J. J. Steele, M. T. Taschuk, and M. J. Brett, "Nanostructured metal oxide thin films for humidity sensors," *Ieee Sensors Journal,* vol. 8, pp. 1422-1429, Jul-Aug 2008.
[31] J. J. Steele, G. A. Fitzpatrick, and M. J. Brett, "Capacitive humidity sensors with high sensitivity and subsecond response times," *Ieee Sensors Journal,* vol. 7, pp. 955-956, May-Jun 2007.
[32] C. Y. Lee and G. B. Lee, "Humidity sensors: A review," *Sensor Letters,* vol. 3, pp. 1-15, Mar 2005.
[33] P. Furjes, A. Kovacs, C. Ducso, M. Adam, B. Muller, and U. Mescheder, "Porous silicon-based humidity sensor with interdigital electrodes and internal heaters," *Sensors and Actuators B-Chemical,* vol. 95, pp. 140-144, Oct 15 2003.
[34] M. Kitsara, D. Goustouridis, S. Chatzandroulis, M. Chatzichristidi, I. Raptis, T. Ganetsos, R. Igreja, and C. J. Dias, "Single chip interdigitated electrode capacitive chemical sensor arrays," *Sensors and Actuators B-Chemical,* vol. 127, pp. 186-192, Oct 20 2007.
[35] R. Igreja and C. J. Dias, "Dielectric response of interdigital chemocapacitors: The role of the sensitive layer thickness," *Sensors and Actuators B-Chemical,* vol. 115, pp. 69-78, May 23 2006.
[36] R. Igreja and C. J. Dias, "Organic vapour discrimination using sorption sensitive chemocapacitor arrays," *Advanced Materials Forum Iii, Pts 1 and 2,* vol. 514-516, pp. 1064-1067, 2006.
[37] R. Igreja and C. J. Dias, "Capacitance response of polysiloxane films with interdigital electrodes to volatile organic compounds," *Advanced Materials Forum Ii,* vol. 455-456, pp. 420-424, 2004.
[38] C. Ziegler, J. Maier, and H. D. Wiemhofer, "Chemical sensors and sensor technology," *Physical Chemistry Chemical Physics,* vol. 5, pp. 1-7, Dec 1 2003.
[39] C. Hagleitner, A. Hierlemann, D. Lange, A. Kummer, N. Kerness, O. Brand, and H. Baltes, "Smart single-chip gas sensor microsystem," *Nature,* vol. 414, pp. 293-296, Nov 15 2001.

[40] W. Olthuis, A. J. Sprenkels, J. G. Bomer, and P. Bergveld, "Planar interdigitated electrolyte-conductivity sensors on an insulating substrate covered with Ta2O5," *Sensors and Actuators B- Chemical,* vol. 43, pp. 211-216, 1997.
[41] K. Toda, Y. Komatsu, S. Oguni, S. Hashiguchi, and I. Sanemasa, "A planar gas sensor combined with interdigitated array electrodes," *Analytical Sciences,* vol. 15, pp. 87-89, Jan 1999.
[42] K. Sundara-Rajan, L. Byrd, and A. V. Mamishev, "Moisture content estimation in paper pulp using fringing field impedance Spectroscopy," *Ieee Sensors Journal,* vol. 4, pp. 378-383, Jun 2004.
[43] K. Sundara-Rajan, L. Byrd, and A. V. Mamishev, "Measuring moisture, fiber, and titanium dioxide in pulp with impedance spectroscopy," *Tappi Journal,* vol. 4, pp. 23-27, Feb 2005.
[44] E. Fratticcioli, M. Dionigi, and R. Sorrentino, "A simple and low-cost measurement system for the complex permittivity characterization of materials," *Ieee Transactions on Instrumentation and Measurement,* vol. 53, pp. 1071-1077, Aug 2004.
[45] X. Li, "Impedance Spectroscopy for Manufacturing Control of Material Physical Properties," *Department of Electrical Engineering*. Master of Science Thesis in Electrical Engineering Washington: University of Washington, pp. 1-110, 2003.
[46] S. Baglio, S. Castorina, and N. Savalli, "Integrated inductive sensors for the detection of magnetic microparticles," *Ieee Sensors Journal,* vol. 5, pp. 372-384, Jun 2005.
[47] V. Kasturi and S. C. Mukhopadhyay, "Estimation of Property of Sheep Skin to Modify the Tanning Process Using Interdigital Sensors " in *Sensors: Advancements in Modeling, Design Issues, Fabrication and Practical Applications* vol. 21, S. C. Mukhopadhyay, R. Y. M. Huang, Ed.: Springer Berlin Heidelberg, pp. 91-110, 2008.
[48] S. C. Mukhopadhyay, S. D. Choudhury, T. Allsop, V. Kasturi, and G. E. Norris, "Assessment of pelt quality in leather making using a novel non-invasive sensing approach," *Journal of Biochemical and Biophysical Methods,* vol. 70, pp. 809-815, Apr 24 2008.
[49] S. C. Mukhopadhyay, G. Sen Gupta, and S. N. Demidenko, "Special issue on intelligent sensors - Guest Editorial," *Ieee Sensors Journal,* vol. 7, pp. 608-610, May-Jun 2007.
[50] S. C. Mukhopadhyay, "Planar electromagnetic sensors: Characterization, applications and experimental results," *Tm-Technisches Messen,* vol. 74, pp. 290-297, 2007.
[51] S. C. Mukhopadhyay, "Novel planar electromagnetic sensors: Modeling and performance evaluation," *Sensors,* vol. 5, pp. 546-579, Dec 2005.
[52] S. C. Mukhopadhyay, J. D. M. Woolley, G. S. Gupta, and S. Deidenko, "Saxophone Reed Inspection Employing Planar Electromagnetic Sensors," *IEEE Transactions on Instrumentation and Measurements,* vol. 56, pp. 2492-2503, Dec 2007.
[53] S. C. Mukhopadhyay, C. Goonerate, G. S. Gupta, and S. Demidenko, "A Low Cost Sensing System for Quality of Dairy Products," *IEEE Transactions on Instrumentation and Measurements,* vol. 55, pp. 1331-1338, Aug 2006.
[54] S. C. Mukhopadhyay and C. P. Gooneratne, "A Novel Planar-Type Biosensor for Noninvasive Meat Inspection," *IEEE Sensors Journal,* vol. 7, pp. 1340-1346, Sep 2007.
[55] A. V. Mamishev, Y. Du, J. H. Bau, B. C. Lesieutre, and M. Zahn, "Evaluation of diffusion-driven material property profiles using three-wavelength interdigital sensor," *Ieee Transactions on Dielectrics and Electrical Insulation,* vol. 8, pp. 785-798, Oct 2001.
[56] S. Radke and E. Alocilja., "A Microfabricated Biosensor for Detecting Foodborne Bioterrorism Agents," *IEEE Sensors Journal,* vol. 5, pp. 744-750, Aug 2005.
[57] S. Radke and E. Alocilja., "Design and Fabrication of a Microimpedance Biosensor for Bacterial Detection," *IEEE Sensors Journal,* vol. 4, pp. 434-440, Aug 2004.
[58] F. L. Dickert, G. K. Zwissler, and E. Obermeier, "Liquid-Crystals on Interdigital Structures - Applications as Capacitive Chemical Sensors," *Berichte Der Bunsen-Gesellschaft-Physical Chemistry Chemical Physics,* vol. 97, pp. 184-188, Feb 1993.
[59] A. V. Mamishev, K. Sundara-Rajan, F. Yang, Y. Q. Du, and M. Zahn, "Interdigital sensors and transducers," *Proceedings of the Ieee,* vol. 92, pp. 808-845, May 2004.
[60] V. Kasturi, "Quality Inspection of Leather Using Novel Planar Sensor," *School of Engineering and Advanced Technology*. Master of Engineering Thesis, Palmerston North: Massey University, pp. 1-130, 2008.

[61] S. D. Karunanayaka, C. P. Gooneratne, S. C. Mukhopadhyay, and G. Sen Gupta, "A Planar Electromagnetic Sensors Aided Non-destructive Testing of Currency Coins," *The e-Journal on Nondestructive Testing,* vol. 11, pp. 1-10, 2006.
[62] J. M. Bourre and P. Paquotte, "Seafood (wild and farmed) for the elderly: Contribution to the dietary intakes of iodine, selenium, DHA and vitamins B12 and D," *Journal of Nutrition Health & Aging,* vol. 12, pp. 186-192, Mar 2008.
[63] M. C. H. Soccol and M. Oetterer, "Seafood as functional food," *Brazilian Archives of Biology and Technology,* vol. 46, pp. 443-454, Jun 2003.
[64] F. Valfre, F. Caprino, and G. M. Turchini, "The health benefit of seafood," *Veterinary Research Communications,* vol. 27, pp. 507-512, Sep 2003.
[65] FAO, "Marine Biotoxins : Food and Nutrition Paper 80," Food and Agriculture Organization (FAO) Rome, pp. 1-294, Dec 2004.
[66] J. Osek, K. Wieczorek, and M. Tatarczak, "Seafood as potential source of poisoning by marine biotoxins," *Medycyna Weterynaryjna,* vol. 62, pp. 370-373, Apr 2006.
[67] M. Campas, B. Prieto-Simon, and J. L. Marty, "Biosensors to detect marine toxins: Assessing seafood safety," *Talanta,* vol. 72, pp. 884-895, May 15 2007.
[68] F. M. V. Dolah, "Marine Algal Toxins: Origins, Health Effect, and Their Increased Ocurrence," *Environmental Health Perspectives,* vol. 108, pp. 133-141, Mar 2000.
[69] I. Garthwaite, "Keeping shellfish safe to eat: a brief review of shellfish toxins, and methods for their detection," *Trends in Food Science & Technology,* vol. 11, pp. 235-244, Jul 2000.
[70] R. F. Clark, S. R. Williams, S. P. Nordt, and A. S. Manoguerra, "A review of selected seafood poisonings," *Undersea & Hyperbaric Medicine,* vol. 26, pp. 175-184, Apr 1999.
[71] B. Hamilton, M. Hurbungs, J. P. Vernoux, A. Jones, and R. J. Lewis, "Isolation and characterisation of Indian Ocean ciguatoxin," *Toxicon,* vol. 40, pp. 685-693, Jun 2002.
[72] I. Pottier, J. P. Vernoux, and R. J. Lewis, "Ciguatera fish poisoning in the Caribbean islands and western Atlantic," *Reviews of Environmental Contamination and Toxicolgy,* vol. 168, pp. 99-141, 2001.
[73] P. R. Costa, R. Rosa, J. Pereira, and M. A. M. Sampayo, "Detection of domoic acid, the amnesic shellfish toxin, in the digestive gland of Eledone cirrhosa and E-moschata (Cephalopoda, Octopoda) from the Portuguese coast," *Aquatic Living Resources,* vol. 18, pp. 395-400, Oct-Dec 2005.
[74] C. K. Cusack, S. S. Bates, M. A. Quilliam, J. W. Patching, and R. Raine, "Confirmation of domoic acid production by Pseudo-nitzschia australis (Bacillariophyceae) isolated from Irish waters," *Journal of Phycology,* vol. 38, pp. 1106-1112, Dec 2002.
[75] J. A. Maucher and J. S. Ramsdell, "Ultrasensitive detection of domoic acid in mouse blood by competitive ELISA using blood collection cards," *Toxicon,* vol. 45, pp. 607-613, Apr 2005.
[76] H. Ravn, "Origin and occurrence. In: Amnesic Shellfish Poisoning (ASP). IOC Manual and Guides No.31," UNESCO, Paris, 1995.
[77] G. J. Doucette, K. L. King, A. E. Thessen, and Q. Dortch, "The effect of salinity on domoic acid production by the diatom Pseudo-nitzschia multiseries," *Nova Hedwigia,* pp. 31-46, 2008.
[78] P. McCarron, S. Burrell, and P. Hess, "Effect of addition of antibiotics and an antioxidant on the stability of tissue reference materials for domoic acid, the amnesic shellfish poison," *Analytical and Bioanalytical Chemistry,* vol. 387, pp. 2495-2502, Apr 2007.
[79] S. F. Qiu, C. W. Pak, and M. C. Curras-Collazo, "Sequential involvement of distinct glutamate receptors in domoic acid-induced neurotoxicity in rat mixed cortical cultures: Effect of multiple dose/duration paradigms, chronological age, and repeated exposure," *Toxicological Sciences,* vol. 89, pp. 243-256, Jan 2006.
[80] R. Duran, M. C. Arufe, B. Arias, and M. Alfonso, "Effect of Domoic Acid on Brain Amino-Acid Levels," *Revista Espanola De Fisiologia,* vol. 51, pp. 23-27, Mar 1995.
[81] B. Arias, M. Arufe, M. Alfonso, and R. Duran, "Effect of Domoic Acid on Metabolism of 5-Hydroxytryptamine in Rat-Brain," *Neurochemical Research,* vol. 20, pp. 401-404, Apr 1995.
[82] G. Debonnel, L. Beauchesne, and C. Demontigny, "Domoic Acid, the Alleged Mussel Toxin, Might Produce Its Neurotoxic Effect through Kainate Receptor Activation - an Electrophysiological Study in the Rat Dorsal Hippocampus," *Canadian Journal of Physiology and Pharmacology,* vol. 67, pp. 29-33, Jan 1989.

[83] J. L. C. Wright, R. K. Boyd, A. S. W. Defreitas, M. Falk, R. A. Foxall, W. D. Jamieson, M. V. Laycock, A. W. Mcculloch, A. G. Mcinnes, P. Odense, V. P. Pathak, M. A. Quilliam, M. A. Ragan, P. G. Sim, P. Thibault, J. A. Walter, M. Gilgan, D. J. A. Richard, and D. Dewar, "Identification of Domoic Acid, a Neuroexcitatory Amino-Acid, in Toxic Mussels from Eastern Prince-Edward-Island," *Canadian Journal of Chemistry-Revue Canadienne De Chimie,* vol. 67, pp. 481-490, Mar 1989.

[84] T. M. Perl, L. Bedard, T. Kosatsky, J. C. Hockin, E. C. D. Todd, and R. S. Remis, "An Outbreak of Toxic Encephalopathy Caused by Eating Mussels Contaminated with Domoic Acid," *New England Journal of Medicine,* vol. 322, pp. 1775-1780, Jun 21 1990.

[85] FAO/IOC/WHO, "Report of the Joint FAO/IOC/WHO ad hoc Expert Consultation on Biotoxins in Bivalve Molluscs," FAO, IOC, WHO, Oslo, Norway, Report 26-30 Sep 2004.

[86] L. Rhodes, D. White, M. Syhre, and M. Atkinson, "Pseudo-nitzschia species isolated from New Zealand coastal waters: Domoic acid production in vitro and links with shellfish toxicity," in *Harmful and Toxic Algal Blooms*, UNESCO, Ed., pp. 155-158, 1996.

[87] M. A. Quilliam, "Phycotoxins," *Journal of Aoac International,* vol. 82, pp. 773-781, May-Jun 1999.

[88] D. L. Park, S. E. Guzman-Perez, and R. Lopez-Garcia, "Aquatic biotoxins: Design and implementation of seafood safety monitoring programs," *Reviews of Environmental Contamination and Toxicology* vol. 161, pp. 157-200, 1999.

[89] D. L. Park, "Surveillance Programs for Managing Risks from Naturally-Occurring Toxicants," *Food Additives and Contaminants,* vol. 12, pp. 361-371, May-Jun 1995.

[90] H. P. van Egmond, T. Aune, P. Lassus, G. J. A. Speijers, and M. Waldock, "Paralytic and Diarrhoeic Shellfish Poisons: Occurrence in Europe, Toxicity, Analysis and Regulation," *Journal of Natural Toxins 2,* pp. 41–83, 1993.

[91] N. Lagos, "Microalgal blooms: A global issue with negative impact in Chile," *Biological Research,* vol. 31, pp. 375-386, 1998.

[92] Y. Shimizu, "Microalgal metabolites: A new perspective," *Annual Review of Microbiology,* vol. 50, pp. 431-465, 1996.

[93] E. V. Morse, "Paralytic Shellfish Poisoning - Review," *Journal of the American Veterinary Medical Association,* vol. 171, pp. 1178-1180, 1977.

[94] AOAC., "Official Method 959.08' in Official Methods Of Analysis," *AOAC International*, Gaithersburg, MD. 1995.

[95] L. S. Ettre, "Nomenclature for Chromatography," *International Union of Pure and Applied Chemistry (IUPAC)*, Department of Chemical Engineering, Yale University, New Haven, USA, pp. 819-872, 1993.

[96] M. A. Quilliam, "The role of chromatography in the hunt for red tide toxins," *Journal of Chromatography A,* vol. 1000, pp. 527-548, Jun 6 2003.

[97] AOAC, "Domoic Acid in Mussels," *AOAC*, Gaithersburg Official Method 991.26, 2005.

[98] P. Hess, S. Gallacher, L. A. Bates, N. Brown, and M. A. Quilliam, "Determination and confirmation of the amnesic shellfish poisoning toxin, domoic acid, in shellfish from Scotland by liquid chromatography and mass spectrometry," *Journal of Aoac International,* vol. 84, pp. 1657-1667, Sep-Oct 2001.

[99] J. F. Lawrence, C. F. Charbonneau, and C. Menard, "Liquid-Chromatographic Determination of Domoic Acid in Mussels, Using Aoac Paralytic Shellfish Poison Extraction Procedure - Collaborative Study," *Journal of the Association of Official Analytical Chemists,* vol. 74, pp. 68-72, Jan-Feb 1991.

[100] H. Kodamatani, K. Saito, N. Niina, S. Yamazaki, A. Muromatsu, and I. Sakurada, "Sensitive determination of domoic acid using high-performance liquid chromatography with electrogenerated tris(2,2 '-bipyridine)ruthenium(III) chemiluminescence detection," *Analytical Sciences,* vol. 20, pp. 1065-1068, Jul 2004.

[101] C. Hummert, M. Reichelt, and B. Luckas, "Automatic HPLC-UV determination of domoic acid in mussels and algae," *Chromatographia,* vol. 45, pp. 284-288, 1997.

[102] M. A. Quilliam, "Liquid Chromatography–Mass Spectrometry of Seafood Toxins.," *In: D. Barcelo, Editor, Applications of LC–MS in Environmental Chemistry, Elsevier. Amsterdam,* pp. 415–444, 1996.

[103] M. A. Quilliam, "Liquid Chromatography–Mass Spectrometry: a Universal Method for the Analysis of Toxins?," *In: B. Reguera, J. Blanco, M.L. Fernandez and T. Wyatt, Editors, Harmful Algae. Xunta de Galicia and IOC/UNESCO, Vigo* pp. 509–514, 1998.

[104] M. A. Quilliam, P. G. Sim, A. W. Mcculloch, and A. G. Mcinnes, "High-Performance Liquid-Chromatography of Domoic Acid, a Marine Neurotoxin, with Application to Shellfish and Plankton," *International Journal of Environmental Analytical Chemistry,* vol. 36, pp. 139-154, 1989.

[105] J. F. Lawrence, C. F. Charbonneau, C. Menard, M. A. Quilliam, and P. G. Sim, "Liquid-Chromatographic Determination of Domoic Acid in Shellfish Products Using the Paralytic Shellfish Poison Extraction Procedure of the Association of Official Analytical Chemists," *Journal of Chromatography,* vol. 462, pp. 349-356, Jan 13 1989.

[106] R. Pocklington, J. E. Milley, S. S. Bates, C. J. Bird, A. S. W. Defreitas, and M. A. Quilliam, "Trace Determination of Domoic Acid in Seawater and Phytoplankton by High-Performance Liquid-Chromatography of the Fluorenylmethoxycarbonyl (Fmoc) Derivative," *International Journal of Environmental Analytical Chemistry,* vol. 38, pp. 351-368, 1990.

[107] R. B. M. Schasfoort and A. J. Tudos, "Handbook of Surface Plasmon Resonance," University of Twente, Enschede, The Netherlands: The Royal Society of Chemistry, RSC 2008.

[108] I. M. Traynor, L. Plumpton, T. L. Fodey, C. Higgins, and C. T. Elliott, "Immunobiosensor detection of domoic acid as a screening test in bivalve molluscs: Comparison with liquid chromatography-based analysis," *Journal of Aoac International,* vol. 89, pp. 868-872, May-Jun 2006.

[109] Q. M. Yu, S. F. Chen, A. D. Taylor, J. Homola, B. Hock, and S. Y. Jiang, "Detection of low-molecular-weight domoic acid using surface plasmon resonance sensor," *Sensors and Actuators B-Chemical,* vol. 107, pp. 193-201, May 27 2005.

[110] R. C. Stevens, S. D. Soelberg, B. T. L. Eberhart, S. Spencer, J. C. Wekell, T. M. Chinowsky, V. L. Trainer, and C. E. Furlong, "Detection of the toxin domoic acid from clam extracts using a portable surface plasmon resonance biosensor," *Harmful Algae,* vol. 6, pp. 166-174, Feb 2007.

[111] B. R. Hesp, J. C. Harrison, A. I. Selwood, P. T. Holland, and D. S. Kerr, "Detection of domoic acid in rat serum and brain by direct competitive enzyme-linked immunosorbent assay (cELISA)," *Analytical and Bioanalytical Chemistry,* vol. 383, pp. 783-786, Nov 2005.

[112] M. Kania and B. Hock, "Development of monoclonal antibodies to domoic acid for the detection of domoic acid in blue mussel (mytilus edulis) tissue by ELISA," *Analytical Letters,* vol. 35, pp. 855-868, 2002.

[113] I. Garthwaite, K. M. Ross, C. O. Miles, L. R. Briggs, N. R. Towers, T. Borrell, and P. Busby, "Integrated enzyme-linked immunosorbent assay screening system for amnesic, neurotoxic, diarrhetic, and paralytic shellfish poisoning toxins found in New Zealand," *Journal of Aoac International,* vol. 84, pp. 1643-1648, Sep-Oct 2001.

[114] Z. Tsao, Y. Liao, B. Liu, C. Su, and F. Yu, "Development of a Monoclonal Antibody against Domoic Acid and Its Application in Enzyme-Linked Immunosorbent Assay and Colloidal Gold Immunostrip," *Journal of Agriculture and Food Chemistry,* vol. 55, pp. 4921-4927, 2007.

Publications

Journals

1. A. R. Mohd Syaifudin, K. P. Jayasundera and S. C. Mukhopadhyay. "A Low Cost Novel Sensing System for Detection of Dangerous Marine Biotoxins in Seafood," Elsevier - Sensors and Actuators B: Chemical. Volume 137, Issue 1, 28 March 2009, Pages 67-75. doi:10.1016/j.snb.2008.12.053.

2. A. R. Mohd Syaifudin, K. P. Jayasundera, and S. C. Mukhopadhyay, "Initial Investigation of Using Planar Interdigital Sensors for Assessment of Quality in Seafood," *Journal of Sensors*, vol. 2008, Article ID 150874, 9 pages, 2008. doi:10.1155/2008/150874.

Proceeding and Conference Paper

1. A. R. Mohd Syaifudin, K. P. Jayasundera and S. C. Mukhopadhyay. "Electromagnetic Interaction of Planar Interdigital Sensors with Chemicals Contaminated in Seafood. International Conference on Sensing Technology (ICST) 2008, Tainan Taiwan, pp 620-625, Nov 30 – Dec 3, 2008.

Seminar

1. A. R. Mohd Syaifudin. Sea-food Inspection Using Novel Interdigital Sensor. IEEE Post Graduate Presentations. 28th August 2008. Victoria University. Wellington. New Zealand.

2. A. R. Mohd Syaifudin. "A Low Cost Novel Sensing System for Detection of Contaminated Acid in Seafood," Electronics, Information and Communication System (EICS) Seminar, 30th July 2008. Massey University, New Zealand.

Others

1. A. R. Mohd Syaifudin, V. Kasturi and S.C.Mukhopadhyay. "Smart Sensing System for Health and Environmental," 2008 Digital Signal Processing Creative Design Contest. 29th November 2008. Southern Taiwan University, Taiwan.